Doctor of Engineering Thesis

Study on Operational Optimization of a Combined Energy System with Photovoltaic Power Generation

By

Abeer Galal El-Sayed Saad

Supervised By

Professor Shin'ya OBARA

Department of Electrical and Electronic Engineering

March, 2011

Kitami Institute of Technology,

Graduate School of Engineering,

165 Koen-cho, Kitami, Hokkaido, 090-8507,

Japan.

Study on Operational Optimization of a Combined Energy System with Photovoltaic Power Generation

Approved by Supervisory Committee

Dr. Shin'ya OBARA
Professor
Electrical and Electronic Engineering Department
Committee Chair and Thesis Supervisor

Dr. Junji Tamura
Professor
Electrical and Electronic Engineering
Member of the Supervisory Committee

Dr. Takao Ueda
Associate Professor
Electrical and Electronic Engineering
Member of the Supervisory Committee

Dr. Hirayama Koichi
Professor
Electrical and Electronic Engineering
Member of the Supervisory Committee

Dr. Yamada Takanobu
Associate Professor
Mechanical Engineering
Member of the Supervisory Committee

Kitami Institute of Technology,
Graduate School of Engineering,
Japan

CONTENTS

Nomenclature

$H_{D,t}$: Direct solar radiation intensity [W/m^2]

$H_{S,t}$: Sky solar radiation intensity [W/m^2]

$I_{D,t}$: Direct solar radiation intensity [W/m^2]

$I_{H,t}$: Global solar radiation intensity [W/m^2]

I_j^n : Input of neuron *j* in layer *n*

$I_{S,t}$: Horizontal sky solar radiation [W/m^2]

i, j, k : Number of a neuron

N, n : Layer number

O_j^N : Estimated power value [W]

$P_{S,t}$: Photovoltaic output power [W]

R_T : Temperature coefficient [/K]

S_S : Area of the solar cell [m^2]

$T_{C,t}$: Temperature of the solar cell [K]

T_o : Reference temperature [K]

t: Sample time

$w_{j,k}^{n,n-1}$: Weight of neuron *k* layer *n-1*

$w_{j,k}^{n,n-1}$: Corrected weighted

$w_{j,k}^{-n,n-1}$: Weight before modification

$\Delta w_{j,k}^{n,n-1}$: Amount of modification

Greek Symbols

α : Latitude of the setting point

β : Angle of the gradient of the acceptance surface

δ : Solar celestial declination

η_R : Reformer efficiency [%]

η_S : Photovoltaic generation efficiency at T_o [%]

θ : Incident angle to the acceptance surface of the sunlight

λ : Reflection factor

φ : Hour angle

Subscripts

C/O : CO oxidation unit

C/U: Condenser unit

C/P : Compressor

HEX: Heat exchanger

LNG: Liquid nature gas

MSE : Mean squared error

PV : Photovoltaic system

NN : Neural network

PEFC : Proton-exchange membrane fuel cell

R/M: Reformer

SOFC : Solid-oxide fuel cell

S/U: Shift unit

Abstract

This thesis optimizes the operation planning of a photovoltaic system with a diesel engine generator or a combined fuel cell. The proposal systems allow for the construction of a power supply system with low environmental impact that uses renewable energy. The production of electricity from the photovoltaic system (PV) continues to attract interest as a power source for distributed energy generation. It is important to be able to estimate a photovoltaic power to optimize system energy management. The neural network has been proposed as suitable for statistical approaches for classifications and prediction problems. A layered neural network is made to learn and teach based on the weather data of amount of solar radiation and outside air temperature. Fuel cell power generation is another attractive option for providing power for electric utilities and commercial buildings because of its high efficiency and environmentally benign feature. The fuel cells have recently been the focus of great interest as a distributed generation technology. The solid-oxide fuel cell (SOFC) and a proton-exchange membrane fuel cell (PEFC) are two types of fuel cells and particularly suitable for distributed power generation and cogeneration systems. Moreover, energy supply characteristics of a PV and a diesel engine generator combined system are studied. Two operating cases are examined in this system: one with and one without a power storage facility. The operation of the

diesel engine generator is based on the fluctuation of the load in the operation of Case 1, and a battery is not used. Therefore, because the engine is operated over a wide area from a low to a high load, the average engine operation efficiency is low. On the other hand, in the operation of Case 2, a battery is used to supply the demand when the PV power generation is less than the demand, and the diesel engine generator operates at 25% or less of the battery residual quantity to work in safety mode in the proposed system. Furthermore, operation of the engine generator is based on the charge or discharge of the battery, with maximum engine efficiency at maximum output power. Comparisons are presented of the results from the two cases with respect to the actual calculations of output power and the predicted electricity production from the photovoltaic system. Energy is supplied to a demand side of three households in Sapporo city, Japan from the proposed system, and no external sources are used. The analysis error of the operation prediction is considered.

A photovoltaic and SOFC-PEFC combined system is developed in this study. The proposed system consists of a SOFC-PEFC combined system and a PV as the energy supply to a micro-grid of 30 residences in Sapporo, Japan. The operation plan of the system has three cases: without solar power, with 50% and with 100% of solar output power. Furthermore, three types of system operation of using the SOFC independent operation, PEFC independent operation and SOFC-PEFC combined system are used to supply the demand side. A comparative study between the types of system operation is presented. The power generation efficiency is investigated for

different load patterns: average load pattern, compressed load pattern and extended load pattern.

The operation results the PV and the diesel engine combined system shows that, when the NN production-of-electricity prediction is introduced, the engine generator operating time is reduced by 12.5% in December and 16.7% for March and September. The engine generator operation time is shortened by introducing a NN prediction algorithm. Furthermore, the operation results of the PV and SOFC-PEFC combined system show that, the difference between the SOFC independent system and the PEFC independent system is small. The fuel consumption of the SOFC-PEFC combined system is reduced 10 to 35% compared with the SOFC or PEFC systems independently. The power generation efficiency of the SOFC-PEFC combined system considering the three load patterns of the proposed system is 27% to 48%. When photovoltaic generation is not introduced into the SOFC-PEFC combined system, the change in the power generation efficiency is small.

Considering all the results of this thesis, it is found that the optimized operation of an energy system with a PV power generation reduced the time operation of the diesel engine generator and the energy cost of the proposal systems. In addition, the proposed energy systems with a PV power generation are proved to be effective to achieve the purpose supplying energy to a micro-grid with good performance without any external source.

1 Introduction

1.1 Background

Energy is a vital element in human life. A secure, sufficient and accessible supply of energy is very crucial for the modern societies. Energy plays an indispensable role in modern society. We all depend on a constant and reliable supply of energy - for our homes, businesses and for transport. The demand for the provision of energy is increasing rapidly worldwide and the trend is likely to continue in future. Electricity producing systems presently in use across the world can be classified into three main categories: fossil fuels, nuclear power and renewable. Fossil fuels in their crude form, i.e. wood, coal and oil have traditionally been an extensive used energy resource. Nuclear power due to a number of reasons is not accessible to the vast majority of the world and has found its application only within developed countries [1-5]. Renewable energy resources are easily accessible to mankind around the world. Renewable energy is not only available in a wide range, but are also abundant in nature. Renewable energy sector is meeting at present 13.5% of the global energy demand [3-5]. Renewable energy sector is now growing faster than the growth in overall energy market. Some long-term scenarios postulate a rapidly increasing share of renewable technologies (made up of solar, wind, geothermal, modern biomass, as

well as the more traditional source i.e. hydro). In the future, the amount and proportion of renewable energy generated is set to rise, largely because of scarce supplies of gas and oil and also because of government policy and programs to support renewable energy generation. Under these scenarios, renewable could meet up to 50% of the total energy demand by mid-21st century with appropriate policies and new technology developments [2-5]. The increasing consumption of conventional fuels coupled with environmental degradation has led to the development of renewable energy sources. Generating electricity, particularly by making use of renewable resources, allows the attainment of notable reductions of environmental pollution. Electricity generated from sunlight is called solar electricity and the process of converting solar light into electricity is known as the photovoltaic process. There has been growing interest in utilizing a photovoltaic generation systems as a renewable source. Photovoltaic technology enables direct conversion of sunlight into electricity through semi-conductor devices called solar cells. Solar cells are interconnected and hermetically sealed to constitute a photovoltaic module. The photovoltaic modules are integrated with other components such as storage batteries to constitute photovoltaic systems and power plants. Photovoltaic systems and power plants are highly reliable and modular in nature [5-9]. Photovoltaic systems can be successfully utilized for world poverty reduction.

1.2 Historical Overview

In this paper, some term are mentioned such as a photovoltaic system (PV), a diesel engine power generator, a SOFC and PEFC fuel cells, a neural network algorithm and a micro-grid. Here, introducing historical overview for each one.

1.2.1 Photovoltaic system (PV)

Photovoltaic systems are solar energy systems that produce electricity directly from sunlight. Photovoltaic (PV) systems produce clean, reliable energy without consuming fossil fuels and can be used in a wide variety of applications. Many utilities have recently installed large photovoltaic arrays to provide consumers with solar-generated electricity, or as backup systems for critical equipment. Research into photovoltaic technology began over one hundred years ago. In 1880, Charles Fritts developed the first selenium-based solar electric cell. Broader acceptance of photovoltaic as a power source didn't occur until 1905, when Albert Einstein offered his explanation of the photoelectric effect. In the early 1950's, Bell scientists discovered that silicon [5-9], the second most abundant element on earth, was sensitive to light and, when treated with certain impurities, generated a substantial voltage. By the early 1960s, PV systems were being installed on most satellites and spacecraft. Today, solar modules contribute power to 175,000 villages in over 140 countries worldwide, producing thousands of jobs and creating sustainable economic

opportunities. The applications include communications, utility power, and other residential and commercial applications. The intense interest generated by current photovoltaic applications provides promise for this rapidly developing technology.

Due to the growing demand for renewable energy sources, the manufacture of solar cells and photovoltaic system has advanced dramatically in recent years [10-13]. Today, the majority of PV modules use silicon as their major component.

PV consists of multiple components, including cells, mechanical and electrical connection. Solar cells produce direct current electricity from sun light, which can be used to power equipment or to recharge a battery. The first practical application of photovoltaics was to power orbiting satellites and other spacecraft, but today the majority of photovoltaic modules are used for grid connected power generation. In this case an inverter is required to convert the DC to AC.

The PV offer substantial advantages over conventional power sources as follows:

• Electricity produced by solar cells is clean and silent. Because they do not use fuel other than sunshine, PV systems do not release any harmful air or water pollution into the environment.

• Reliability. Even in harsh conditions, photovoltaic systems have proven their reliability.

• Reduced sound pollution. Photovoltaic systems operate silently and with minimal movement. Photovoltaic systems are quiet and visually unobtrusive.

• Small-scale solar plants can take advantage of unused space.

• Solar energy is a locally available renewable resource.

• Photovoltaic Modularity. A PV system can be constructed to any size based on energy requirements.

• Safety. PV systems are very safe when properly designed and installed.

• Independence. Many residential PV users cite energy independence from utilities.

PV has some disadvantages when compared to conventional power systems. The disadvantages of PV systems are:

• Initial cost. Each PV installation must be evaluated from an economic perspective and compared to existing alternatives.

• Solar power is a variable energy source, with energy production dependent on the sun. Solar electricity is not available at night and is less available in cloudy weather conditions.

• Solar cells produce DC which must be converted to AC (using an inverter) when used in current existing distribution grids. This incurs an energy loss of 4-12%

Therefore, there is some disadvantage of using solar cell, electricity produced from photovoltaic is much safer and more environmentally benign than conventional sources of energy production. However, there are environmental, safety, and health issues associated with manufacturing, using, and disposing of photovoltaic

equipment. Photovoltaic systems can be configured in many ways. For example, many residential systems use battery storage to power appliances during the night [14-16]. In contrast, water pumping systems often operate only during the day and require no storage device. A large commercial system would likely have an inverter to power AC appliances. Some systems are linked to the utility grid, while others operate independently. To date, there has been considerable research concerning the operation plan of a hybrid system, combining a photovoltaic system and a diesel power plant [17-26]. These research show that a reduction in energy cost can be realized by both electricity production of a photovoltaic system and the power load being predicated.

In this thesis, a study on operation optimization of a combined energy system with a photovoltaic power generation is developed. Furthermore, the photovoltaic electricity production for every sample time is predicated using the NWI (numerical weather information). The amount of solar radiation and outside air temperature can be obtained from the NWI which is available from the Internet. The amount of solar radiation and outside air temperature are used to calculate and predicate the photovoltaic power generation from a solar module. Optimizing the operation planning of a photovoltaic system with a diesel engine generator or a combined fuel cell is developed in this study.

Table 1-1 Generator specifications

Generator type	Single-phase synchronized
Rated output	5 kVA
Rated voltage	100V
Rated electric current	50A
Frequency	50 Hz
Number of revolution	3000 rpm
Size	200 X 221 X 359 mm
	Automatic voltage regulator

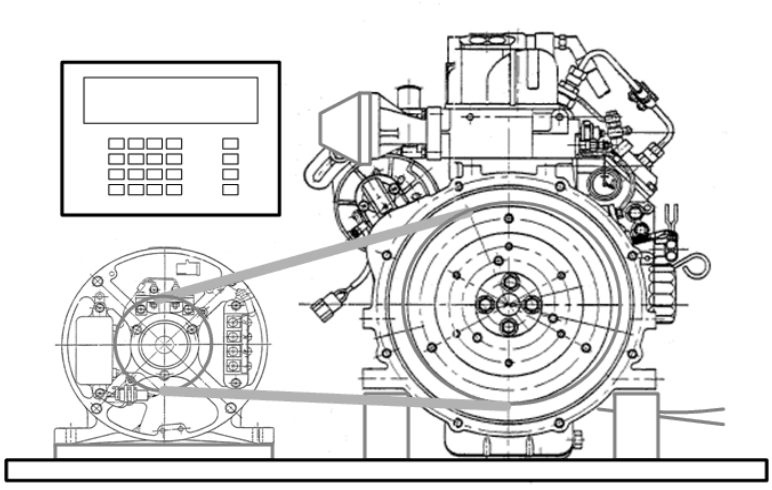

Fig. 1-1 Test diesel engine generator

1.2.2 Diesel engine power generator

A diesel engine power generator is the combination of a diesel engine with an electrical generator to generate electric energy. Diesel generating sets are used in places without connection to the power grid or as emergency power-supply if the grid fails. The diesel engine power generator has different capacities from small to large according to the used application. Set sizes range from 8 to 30 kVA for homes, small shops & offices with the larger industrial generators up to 2,000 kVA used for large office complexes, factories. Sizes up to about 5 MW are used for small power stations and these may use from one to 20 units. In these larger sizes the engine and generator are brought to site separately and assembled along with ancillary equipment. In isolated areas, electrical energy is often produced with the help of diesel engine generators.

Diesel engines have several advantages over other internal combustion engines:

- They burn less fuel than other types of engines performing the same work.
- They have no high-tension electrical ignition system to attend to, resulting in high reliability and easy adaptation to damp environments.
- They can deliver much more power of their rated power on a continuous basis.
- The life of a diesel engine is generally about twice as long as that of petrol engine due to the increased strength of parts used.

- They generate less waste heat in cooling and exhaust.

The diesel engine power generator owes its roots to mainly two inventors. One of these is the creator of the first generator Michael Faraday [27-29] and the other is the creator of the diesel engine Rudolph Diesel [27-29]. The first of these two has contributed greatly to life as we know it today with all his discoveries in electricity. Power generation using reciprocating engines was not as common three decades ago as it is today [30], [31].

The main application for the diesel engine generator derived power was in small backup plants for hospitals, airports, hotels and industry that needed to ensure a reliable power supply at all times. Engine based power production today represents some 10–15% of the total installed capacity all over the world [32], [33]. This is the result of its high efficiency, power concentration and reliability that have been improved considerably during the last decade. Reducing engine emissions to legally acceptable levels has been a challenge for large Diesel engine manufacturers [30-35].

The test equipment of a small -scale diesel engine is shown in Fig. 1-1 [34-36]. The analysis of this thesis uses the experimental results obtained by the operation of the test equipment of Fig. 1-1. The generator specifications used in Fig.1-1 are shown in table 1-1. The fuel of a diesel engine is kerosene and the engine has two cylinders with four cycles. The output characteristics results of a test diesel engine

generator are shown in Figs. 1-2 and 1-3 [34-36]. This result is the relation among the calorific heat of the kerosene fuel supplied to the diesel engine generator, the engine - cooling - water heating value and the exhaust gas heating value, and the production of electricity as shown in Fig. 1-2. A power generator is of a single – phase synchronous type, and power is transmitted through a belt from the power shaft to the diesel engine. If the amount of kerosene fuel is increased, the production of electricity and exhaust gas heating value increase, but the engine - cooling water heating value decreases. The maximum power generation output is 3kW.

Figure 1-3 shows the production of electricity of the diesel engine generator and the relation of power generation efficiency obtained by a test. Although the power generation efficiency changes with the number of engine rotation, since this difference is small. The approximated curves shown in Figs. 1-2 and 1-3 are used in the analysis of this study. The approximated curves in Fig. 1-2 are used to calculate the output power and exhaust heat from diesel engine generator. Furthermore, the approximated curve and equation in Fig. 1-3 are used to calculate the diesel engine generator efficiency at different output power from the diesel engine generator. For example at a certain output power from the diesel engine generator, the output exhaust heat output from the diesel engine generator can be calculated by using the curves in Fig. 1-2, in addition the efficiency of the diesel engine generator can be calculated by using the formula in Fig. 1-3.

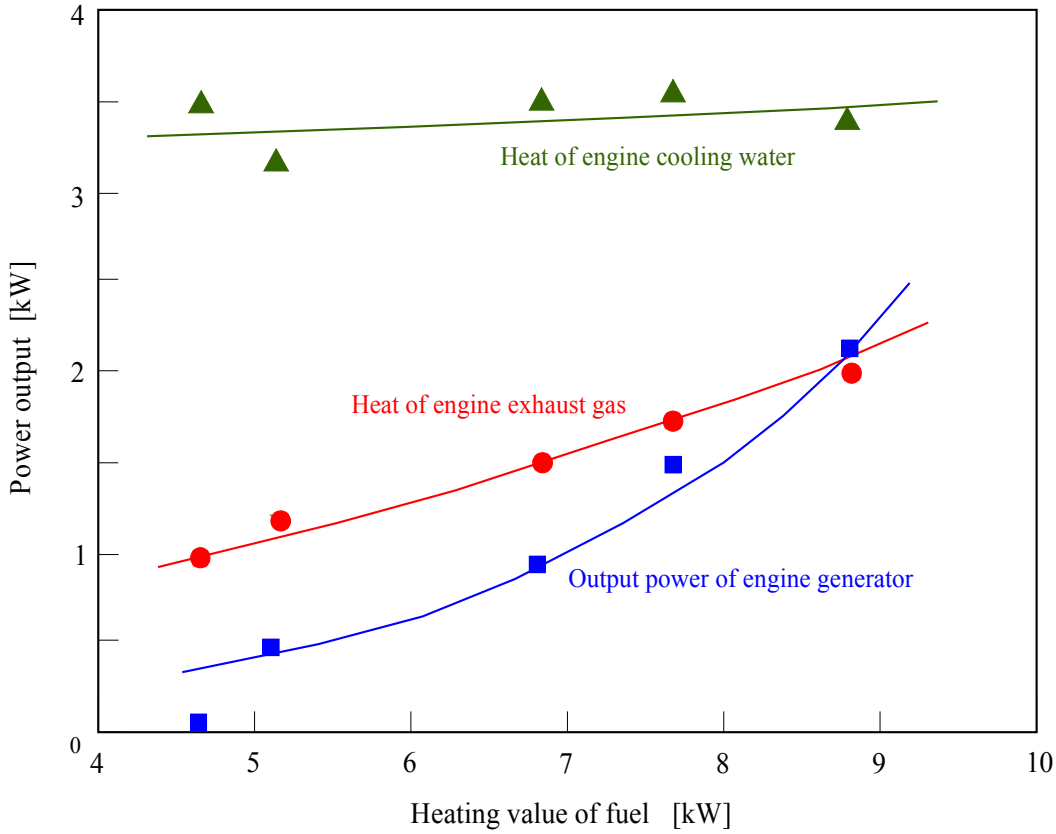

Fig. 1-2 Characteristics of the diesel engine generator output at engine number of revolutions is 1600 rpm

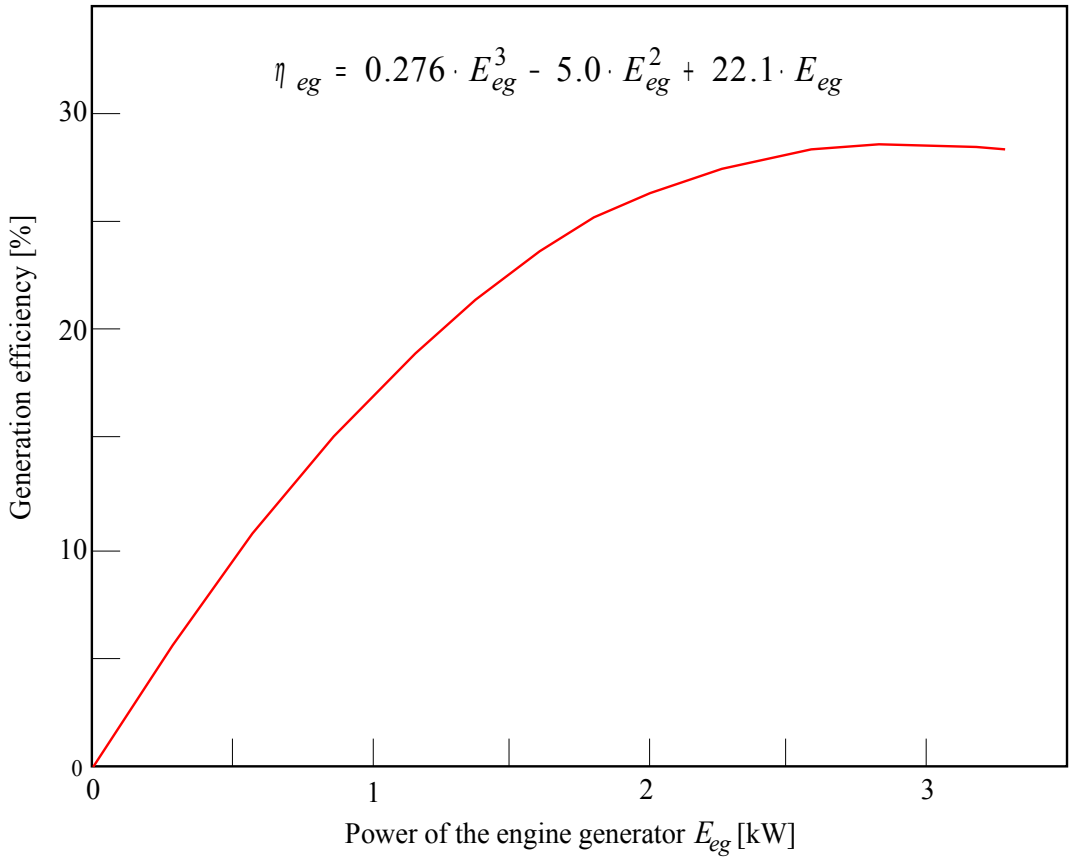

Fig. 1-3 Diesel engine generator efficiency

1.2.3 Solid oxide fuel cell (SOFC) and proton-exchange membrane fuel cell (PEFC) fuel cells

Fuel cells are electrochemical devices that convert the chemical energy of a fuel directly into electrical energy. Fuel cells are a clean, quiet and efficient energy conversion technology and have been considered to be an advanced alternative to conventional combustion technologies for power generation. Fuel cells also may have high efficiencies even in small size units and are easy to site. Because of these features, fuel cells have recently been the focus of great interest as a distributed generation technology [37–46]. Fuel cell power generation is another attractive option for providing power for electric utilities and commercial buildings because of its high efficiency and environmentally benign feature. This type of power production is especially economical (i) where potential users are faced with high cost in electric power generation from coal or oil, (ii) where environmental constraints are stringent, or (iii) where load constraints of transmission and distribution systems are so tight that their new installations are not possible.

The fuel cell concept was developed in 1839 by Sir William Grove, a Welsh judge and gentleman scientist [37]. The invention did not take off, partly due to the success of the internal combustion motor. The revival occurred when the first fuel cell was used in the Gemini space program during the 1960s [37-42]. Based on the alkaline

system, the fuel cell generated electricity and produced the astronauts drinking water. Commercial application of this power source was prohibitive at that time because of high material costs. Improvements in the stack design during the 1990's led to reduce costs and increase power densities [37-46].

Solid oxide fuel cell (SOFC) is one type of fuel cell and use ceramic materials as their electrodes and electrolyte. This allows SOFC to work at high temperatures. Because of their high operating temperature, SOFC is capable of incorporating internal fuel reformation, which allows multiple fuel options. SOFC systems also exhibit stable performance with a varying load. SOFC is a promising technology for decentralized power generation and co-generation [43]. In addition, the proton-exchange membrane fuel cell (PEFC) deliver high power density and offer the advantages of low weight and volume compared with other fuel cells [44], [45]. Though higher temperatures are required with SOFC in comparison with PEFC, the power generation efficiency is high and the uses for exhaust heat are wide. These features make SOFC and PEFC particularly suitable for distributed power generation and co-generation systems [46-51]. The SOFC and PEFC have been developed as fuel cells for houses [49-51]. In order to utilize the hot exhaust heat of SOFC effectively, the SOFC and gas turbine (GT) compound system was develop [52-57]. Although high thermal efficiency is achieved in the SOFC-GT compound system, maintenance of the high thermal efficiency is difficult. Moreover, because the partial

load quality of GT is bad, it is difficult to maintain the power generation efficiency of the whole system. In this system, it is necessary to perform synchronous operation the exhaust heat output from the SOFC and the driving of GT. Consideration of the load characteristic of the demand side is indispensable to investigate the power generation efficiency. Moreover, an operation plan with high power generation efficiency by a high load factor is required.

In this study, the exhaust heat of SOFC is used for the steam reforming of bio-ethanol fuel. The reformed gas is stored in a cylinder; this reformed gas is supplied to the PEFC. In other words, time shift utilization of the exhaust heat of the SOFC is installed. When using this time shift utilization of the exhaust heat of the SOFC, the operation of the system can be planned so that a load peak is cut [58].

1.2.4 Neural network algorithm

A Neural networks are a form of multiprocessor computer system with simple processing elements, a high degree of interconnection and simple scalar messages. A neural network (NN), which can perform pattern-matching task, has a large number of highly interconnected processing elements (nodes) that demonstrate the ability to learn and generalize from training patterns. Neural network has the shortcoming of implicit knowledge. NN are inspired by biological nervous systems and they were first introduced as early 1960. Nowadays studies of NN are growing rapidly for

many reasons:

• NN work pattern recognition at large.

• NN have a high degree of robustness and ability to learn.

• NN are prepared to work with incomplete and unforeseen input data.

• NN have high speed and fault tolerance due to massive parallelism.

• NN can be trained rather than programmed, hence their performance may improve with experience.

• NN is capable of high-level function such as adaptation or learning with or without supervision.

A neural network consists of many simple processing element neurons. The connections between neurons have a weighted links *wi* over which signals can pass. The back propagation algorithm gives a prescription for the weights in any feed forward network to learn training set input/output pair. The back propagation algorithm is central to much current work on learning in neural networks [59-62]. Bryson and Ho in 1969, Werbos 1974, Parker 1985 [60-62] and Rumelhart, Hinton and Williams in 1986 [63] invented it independently several times. A closely related approach by Le Chun in 1985. The back propagation algorithm works very well by adjusting the weights, which are connected in successive layers of multi-layer perception [56-64]. The back propagation algorithm is created by generalizing the learning rule to multiple layer networks and nonlinear differentiable transfer

functions. Input vectors and corresponding target vectors are used to train a network until it can approximate a function. Networks with biases, a sigmoid layer and a linear output layer are capable of approximating any function with a finite number of discontinuities. Properly trained NN tend to give reasonable answers when presented with inputs that they have never seen, Typically, a new input leads to an output similar to the correct output for input vectors used in training that are similar to the new input being presented.

1.2.4.1 Simple neuron

Figure 1-4 shows a simple model of a neuron characterized by a number of inputs, the weights and an output. As shown in this figure a simple neuron representation with inputs I_1, I_2, ... I_n , the node receives its inputs through a set of weighted links w_1, w_2, ... w_n. These inputs may come from other nodes or from outside sources. Sum of all weighted inputs represents the node activation and the node output is determined by output function, which responds to this activation. The transfer function may be the sigmoid threshold function, linear threshold function The ramp threshold function, or the step threshold function. The transfer function used by individual neurons to translate the input to an output response is three-step process:

1. The neuron computes the weighted sum of its inputs.

2. Net input is converted into an activation level. This can be accomplished in several way, but typically we using sigmoid function or s-shaped function.

3. The process converts the activation level into an output signal.

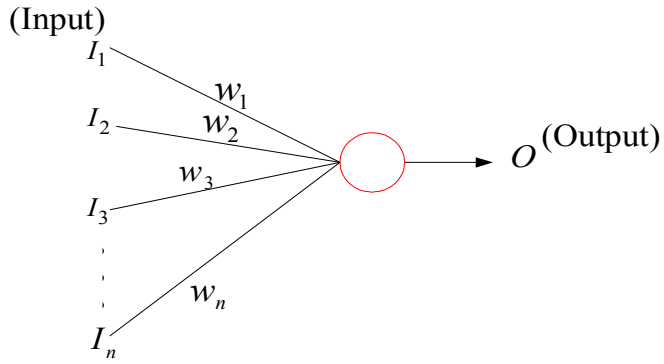

Fig. 1-4 The illustration of the processing node (neuron)

1.2.4.2 Neural network architectures

Neural network are capable of finding internal representations of interrelations within raw data. Neural network are considered to be intuitive because they learn by example rather than by following programmed rules[56-73]. Two or more of the neurons described before can be combined in a layer, and a particular network could

contain one or more such layers. Figure 1-5 shows a layered neural network. In this figure, the network consists of three layers input layer, hidden layer and the output layer. Furthermore, a set of N input units (I_n, $n=1,2,3...N$), a set hidden units and a set of output units are shown.

The ability to learn is one of the key aspects of neural network. This typical characteristic, together with the simplicity of building and training neural network, has encouraged their application to task of prediction. Because of their inherent non-linearity, neural network are abled to identify the complex interactions between independent variables without the need for complex functional models to describe the relationships between dependent and independent variable. Thus, neural networks are proposed as a substitute for classifications and prediction problems. In this thesis, an operation prediction program using a layered neural network is proposed to predict the photovoltaic output power with sufficient accuracy.

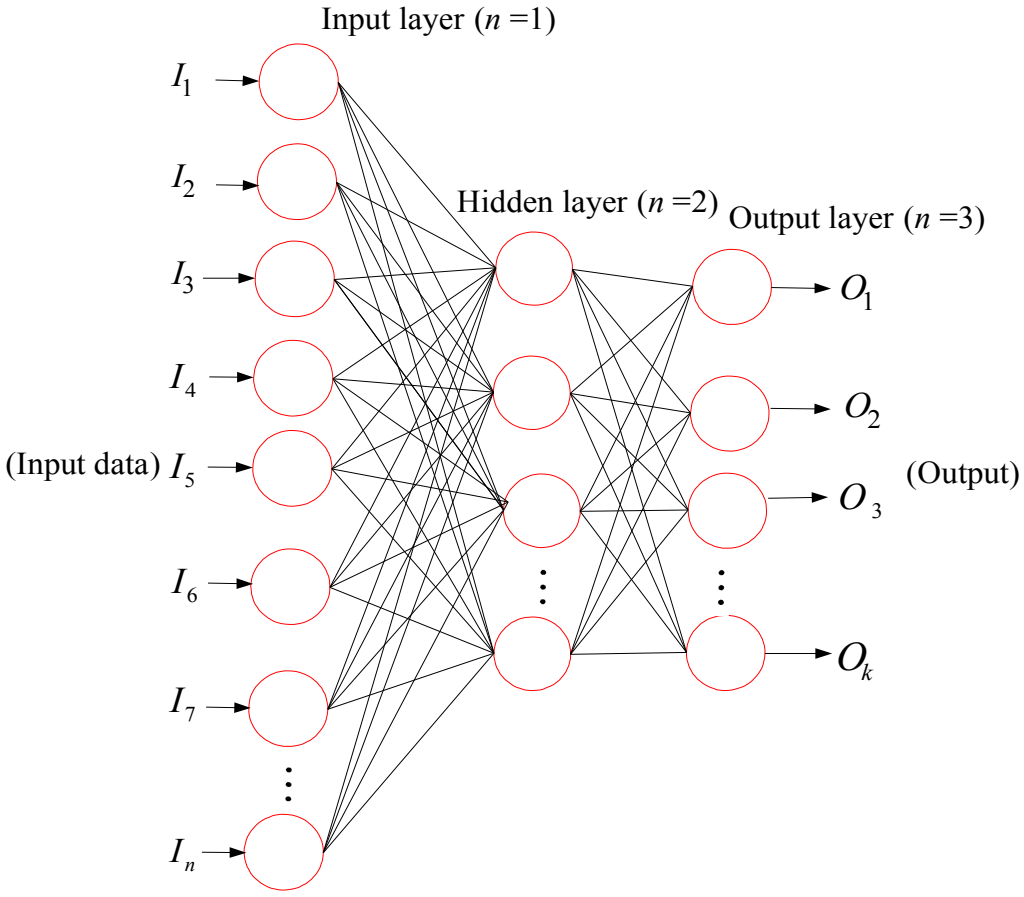

Fig. 1- 5 Three layered neural network algorithm

1.2.5 Micro-gird

An independent micro-gird system supplies electric power and heat without interconnecting with other power systems realizes the advantages of a distributed power source. Application of micro-gird technology provides a backup power supply in an emergency, peak cut of an electric power plant and effective use of exhaust heat [74-76]. Although, the energy transport distance of a micro-gird is short, effective use of exhaust heat is possible. Therefore, Overall efficiency is improved compared with conventional power generation systems.

Micro-grid technology with the capacity for sustainable energy operation has been widely discussed recently from the point of view reducing the environmental impact of society [73-75]. In these setups, the operation optimization program installed in the controller of a combined system is the most aspect of the technology for determining the performance of the system [76]. However, a micro-grid is required for the rapid dynamic characteristic that follow changes in power load compared with a grid interconnected for other systems [77]. Since, the independent micro-gird realizes maximum distributed energy, there are issues to tackle such as the stability of the dynamic characteristics of power and development of an optimal design method [78].

When a building linked to a grid is a house, in a micro-gird, both load fluctuation and demand fluctuation are expected to be large. In a large scale power plant, since

power is supplied to various demands, demand fluctuation is smoothed. In a micro-gird with big load fluctuation, if no electricity storage system is installed, the operating point of the power generator will change significantly. Load fluctuation can be leveled by installing a battery in a micro-gird [79]. In independent micro-gird that does not have a battery installed, the power generator connected to the grid is expected to have frequent partial-load operations with low efficiency [80].

In this study, a micro-grid with little environmental impact is developed by introducing a photovoltaic and a SOFC- PEFC combined system for supplying energy to 30 houses in Sapporo city, Japan. The schematic figure of an independent micro-gird is shown in Fig. 1-6. In this figure, a power system model of a micro-gird with 30 houses is shown. This micro-gird is installed into a residential area, energy is supplied by introducing a photovoltaic and a SOFC- PEFC combined system.

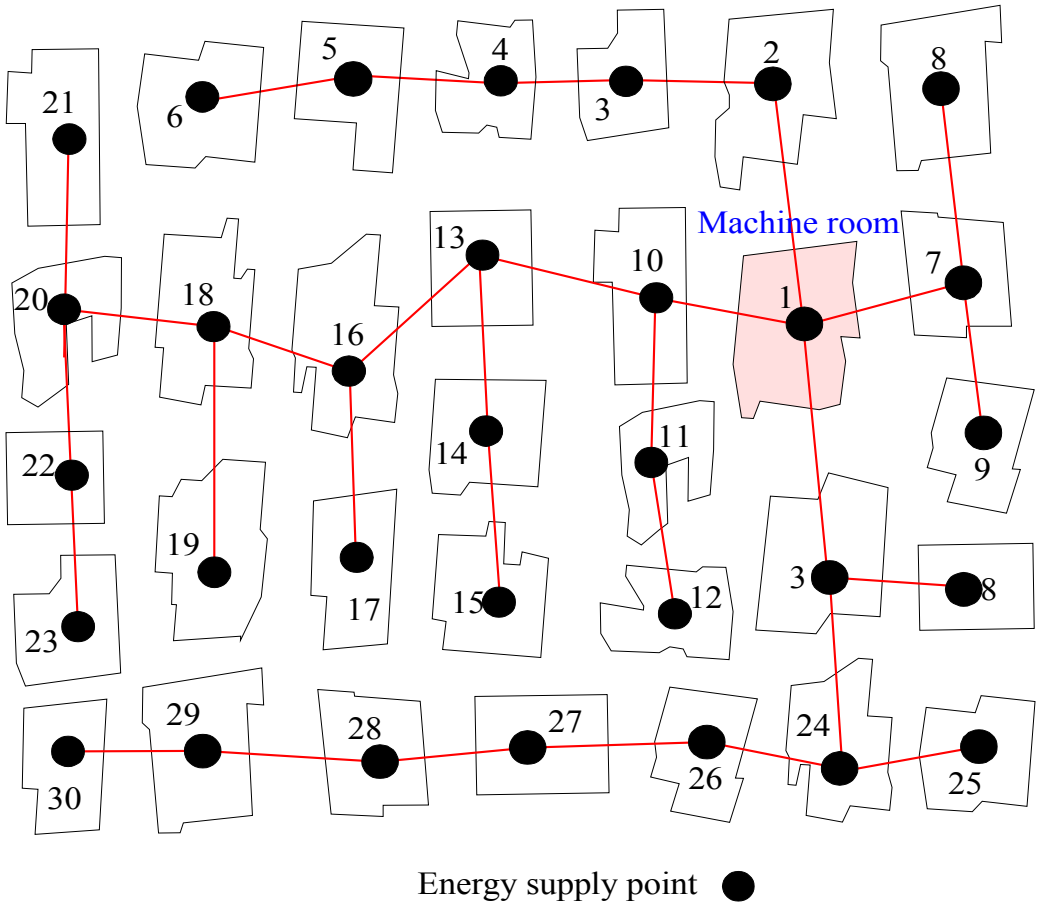

Fig. 1-6 Micro-grid model concerning a power system

1.3 The Purpose of This Research

The optimization of the operation planning of a micro-grid with diesel engine generator or a combined fuel cell with the photovoltaic power generation is proposed. Energy supply characteristics of a photovoltaic and a diesel engine generator combined system are studied. The objective of this study involves developing an algorithm based on neural network to predict the power output from the photovoltaic system and optimizing the operation planning of combining a photovoltaic and a diesel engine generator system. The analysis error of the operation prediction is also considered. Energy is supplied to the demand side from the proposed system, and no external sources are used.

Furthermore, a photovoltaic and a SOFC- PEFC combined system is proposed. In this system, the SOFC-PEFC combined system with a time shifting of the reformed gas is proposed to supply energy to a micro-grid consisting of 30 residences in Sapporo city, Japan. Three cases are proposed for the operation plan of the SOFC-PEFC combined system: without a photovoltaic system and with 50% and 100% solar power. In addition, three types of system operation of using the SOFC independent operation, PEFC independent operation and SOFC-PEFC combined system are used to supply the demand side A comparative study between the types of system operation is illustrated. The power generation efficiency is investigated for different load patterns.

1.4 The Structure of This Paper

The proposal system schemes, the operating methods, the results and discussions of this thesis are illustrated. This thesis is organized as follows:

In **Chapter 2**, the proposed system of a photovoltaic and diesel engine generator combined system is proposed to supply energy to three houses in Sapporo, Japan. In addition, configuration and the analysis method are explained. The operation planning of this system is clarified. In this chapter, the proposed neural network algorithm to predict the power output from the photovoltaic is present. Furthermore, the operating methods of the cases study are explained. The results and discussion of the proposed system are presented. The proposal system is examined using the neural network prediction algorithm. The average values for the prediction error of electricity production from the photovoltaic is shown. The diesel engine operations characteristics are described, and a back-up boiler operation plan is developed. Comparing results from using the actual calculations of the output power with the prediction of electricity production from the photovoltaic is illustrated.

In **Chapter 3**, the system configuration of a photovoltaic and a SOFC – PEFC combined system is proposed. This system is used to supply energy to 30 houses in Sapporo city, Japan. Moreover, three types of system operation of using the SOFC independent operation, PEFC independent operation and SOFC-PEFC combined system are used to supply the demand side. The operation planning of this system is

explained. In addition, the analysis procedure of the proposed system is clarified. The results and discussion of the proposed system at three cases: without solar power, with 50% and with 100% of solar output power are modified. A comparative study between the types of system operation is presented. The power generation efficiency is calculated for different load patterns: average load pattern, compressed load pattern and extended load pattern.

In **Chapter 4**, the conclusion obtained from the work carried out in this thesis will be summarized. In addition, the suggestion for the future work is illustrated.

The results show that when introducing the NN prediction algorithm in the photovoltaic and the diesel engine generator combined system, the operating period of the engine generator is shortened for the energy supplied to the demand side. The average values for the prediction error of electricity production from the PV are 25%, 29%, 19% and 26% for December, March, June and September, respectively. Furthermore, when photovoltaic generation is not introduced into the SOFC-PEFC combined system, the change in the power generation efficiency is small. However, the load factor of the proposal system falls when the amount of PV power increases. The fuel consumption of the SOFC-PEFC combined system is reduced 10 to 35% compared with the SOFC or PEFC systems independently. The power generation efficiencies of the proposed system of the PV and the SOFC-PEFC combined system with consideration of the load patterns are 27% to 48%.

2 Photovoltaic and Diesel Engine Generator Combined System

2.1 System Configuration

The block diagram of the photovoltaic system and diesel engine generator combined system is shown in Fig. 2-1. As shown in the figure, the proposed system consists of a photovoltaic system (PV), a diesel engine generator, a battery, a heat storage tank, a back-up boiler and a system controller. As shown in the figure, the proposed PV system consists of a solar cell, DC-DC converter and DC-AC converter. The power output from the solar cell can be supplied to the power demand through a DC-AC converter and inverter, which also charges the battery. The power output from the inverter is supplied to a power grid or sold off to utilities through an interconnection device. Table 2-1 shows the specifications of the solar cell, battery, engine and generator. A nickel hydrogen type battery is used [81]. The battery capacity introduced into this system shall be 4kWh, which corresponds to about 170 minutes of an average household's power load (0.4kW x 170 minutes = 4 kWh). The optimal capacity of the solar cell and the battery should be discussed and determined for the dynamic operation plan. The maximum power generation efficiency of the diesel engine generator is 3kW [82].

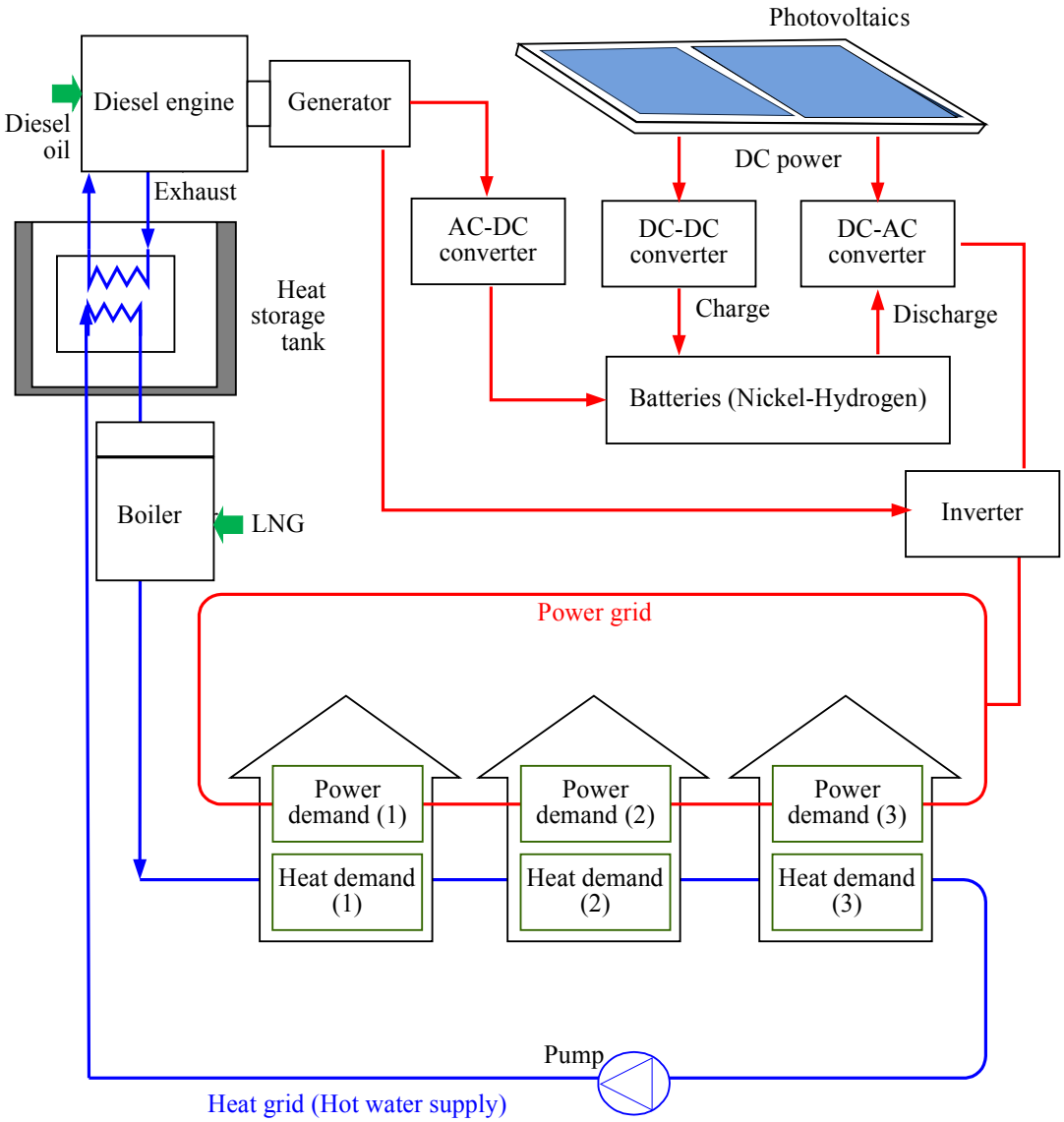

Fig. 2-1 System scheme

The engine generator consists of a kerosene diesel – engine and a synchronous power generator (as described before in Chapter 1, Section 1.2.2). The exhaust heat outputted with the engine generator is engine – cooling water and exhausts gas, and this heat is stored in a heat storage tank through a heat exchanger. Furthermore, the heat – transfer – medium heat exchanger for supplying heat to the houses is installed in the heat storage tank. After exchanging this heat transfer medium for exhaust heat in the heat storage tank, it is supplied to a back up boiler. When there is a large amount of exhaust heat compared with the heat load, the excess exhaust heat is stored in the heat storage tank. The approximated curves shown in Figs. 1-2 and 1-3 are used in the analysis of this study. In addition, the approximated equation in Fig. 1-3 is used to calculate the engine generator efficiency in this proposed system. This system supplies power and heat to three household's in Sapporo city in Japan and no external sources are used. The proposal system is used to supply the energy to only three household's because only one engine generator is used in this system with maximum output power of 3 kW to apply the demand patterns. If this system is used to supply energy to more than three household's, more diesel engine generator must be installed to apply the more demand patterns. The operating time of the diesel engine generator is illustrated. Furthermore, the diesel engine heat characteristics are described, and a back-up boiler operation plan is developed.

Table 2-1 System apparatus specifications

Apparatus	Specifications
Solar cell type Area and generation efficiency Temperature coefficient of a solar cell	Multi crystalline silicon 72 m^2, 14% 0.4%/K
Battery type Battery efficiency, Battery capacity	Nickel – Hydrogen 95%, 4 kWh
Engine type Number of cylinders Total stroke volume, Rated shaft output Combustion type Compression ratio, Fuel Size, Dry weight	Vertical straight 4 cycle diesel, 2 cylinders 451 cc, 8.6 kW Special swirl chamber 24.5, Kerosene 369 X 385 X 485 mm, 60 kgf
Generator type Rated out, Rated voltage Frequency, Number of revolution Size	Single phase synchronized 5kVA, 100 V 50 Hz, 300 rpm 200 X 221 X 359 mm

2.2 Analysis Method

In this section, the analysis operation method is illustrated:

2.2.1 Examination of system

Two operating cases are used in this system Case 1 and Case 2. The battery is not introduced into the proposed system in the operation of Case 1. In addition, when the photovoltaic power generation is less than the power demand, the diesel engine generator operates according to the load fluctuation, and the surplus power from the photovoltaic power generation is sold off as shown in the flow chart of Fig. 2-2.

In this figure, the proposal system in the operation of Case 1 has the following steps from 1 to 5:

(1) The PV power generation and the power demand are determined (as will describe in the following sections 2.2.2 and 2.2.3).

(2) The PV power generation and the power demand are compared at every sample time.

(3) The surplus PV power generation (the large amount of PV power than the power demand) is determined

(4) The surplus PV power generation is sold to utilities.

(5) On the other hand, when PV power is insufficient compared with the power demand, the diesel engine generator is operated and supply the demand side. As

described before in Chapter 1 in Section 1.2.2, a test diesel engine generator is used in this proposal system with the output power generation shown in Fig. 1-2. The operation of the diesel engine generator is according to the load fluctuation with different output power and the diesel engine generator efficiency is calculated according to the efficiency curve in Fig. 1-3 with using the formula shown in this figure.

(6) On the other hand, in the operation of Case 2, the proposal system has same steps from 1 to 3, but the the surplus power from the photovoltaic is used to charge a battery in the operation of Case 2 as shown in the flow chart in Fig. 2-3.

(7) The battery supplies the load when the photovoltaic output power is less than the demand.

(8) The battery capacity is measured for every sampling period.

(9) If the battery capacity drops to 25% or less in the safety operation mode, the engine generator operates and supplies the demand side. The engine generator operates at a fixed load (3 kW output power) for maximum efficiency.

When the diesel engine generator is operated in the two operating cases, exhaust heat is supplied to the heat storage tank. Figure 1-2 (in Chapter 1, Section 1.2.2), has the values of the exhaust heat (it is included exhaust gas and cooling water). When the heat demand is higher than the heat storage in the heat storage tank, a back -up boiler is operated and supplies the demand side. So the heat from the engine and boiler is used to supply the heat demand. Furthermore, Energy supply characteristic

of the photovoltaic and the diesel engine generator combined system is studied.

Two methods are used to examine the two operating cases. In Method 1, the system operation plan depends on actual calculations of the photovoltaic power generation (as will describe in section 2.2.3). On the other hand, the production of electricity from the solar cell using a NN prediction algorithm is introduced in Method 2, and the system operation plan is based on the NN predicted output results for the photovoltaic power generation (as will describe in section 2.2.4). In this study, the operation plan of the engine generator is investigated using the results of Method 1 and Method 2. Moreover, a comparative study between the results of the two methods is presented.

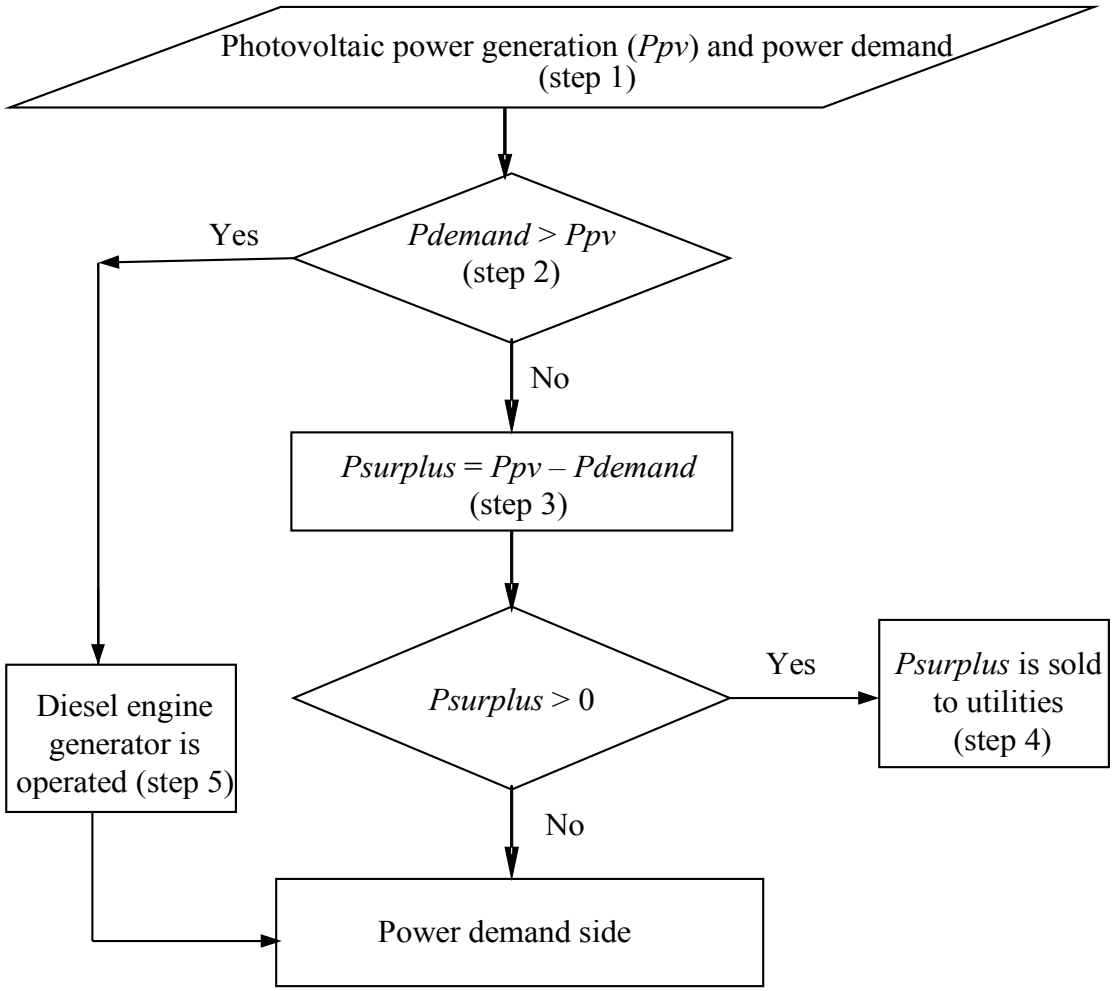

Fig. 2-2 Flow chart of proposal system in the operation of Case 1

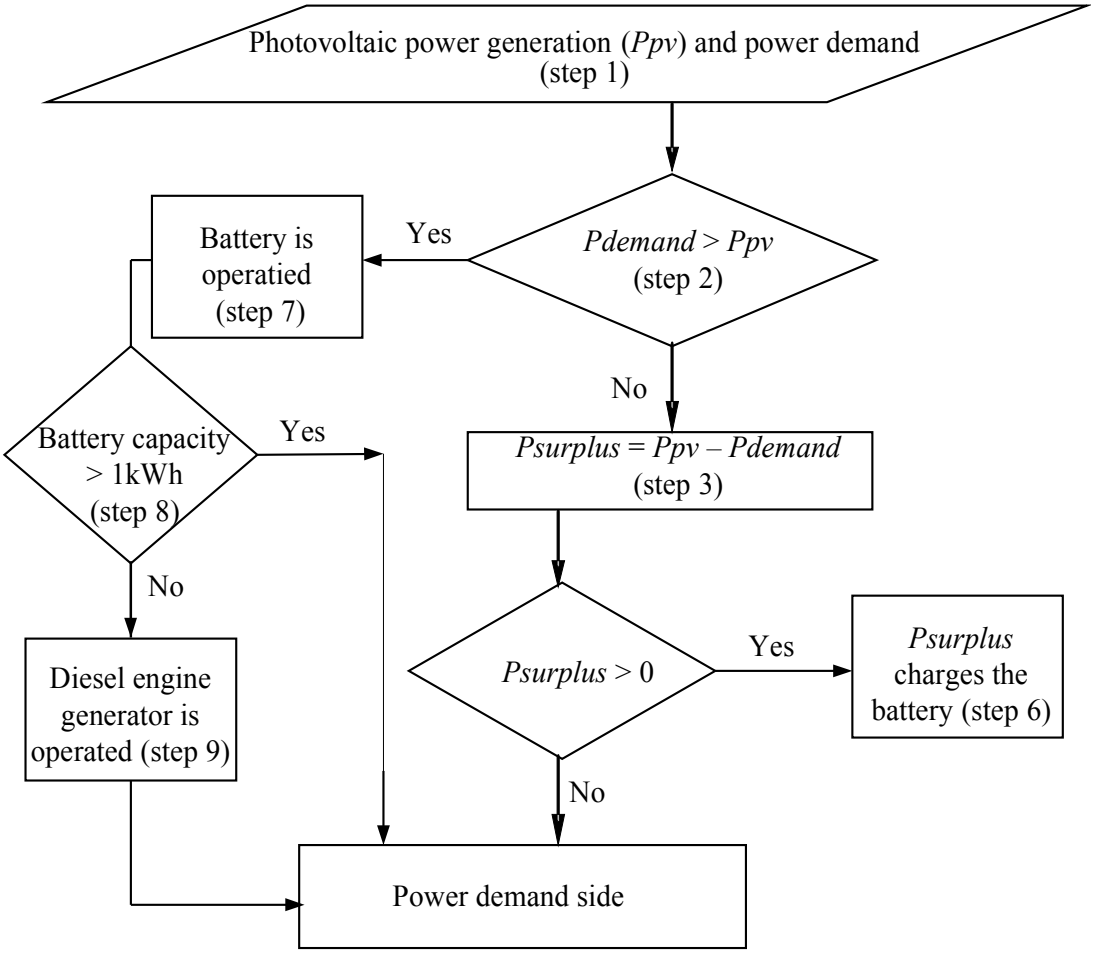

Fig. 2-3 Flow chart of the proposal system in the operation of Case 2

2.2.2 Energy demand pattern

The power and heat demand patterns of a typical household in Sapporo city, Japan, are shown in Fig. 2-4 [82], [83]. In this figure, the average power and heat demand of one household for months March, June, September and December are shown. In addition, the power demand pattern does not change significantly each month, this is because there is no cooling load in the summer in Sapporo. The electricity demand includes household appliances and electric lighting. For this reason, the difference in every month in the figure is small. Heat demand comes from heating, hot water supply and baths. The exhaust heat and heat of the back-up boiler are supplied to the houses assuming the heat load of winter. The exhaust heat from the diesel engine generator is obtained from the curve shown in Chapter 1, Section 1.2.2. This value of the exhaust heat is different according to the operation of the diesel engine. In the operation of Case 2, the diesel engine operated with maximum power with maximum efficiency so the exhaust heat output from the diesel engine generator is constant value according to the constant output power from the diesel engine generator of 3kW maximum output power.

Power and heat are supplied from the proposal system to three households in Sapporo city, Japan. The operating system are introduced into three apartments with the load and heat patterns shown in Fig. 2-4, multiplied by three.

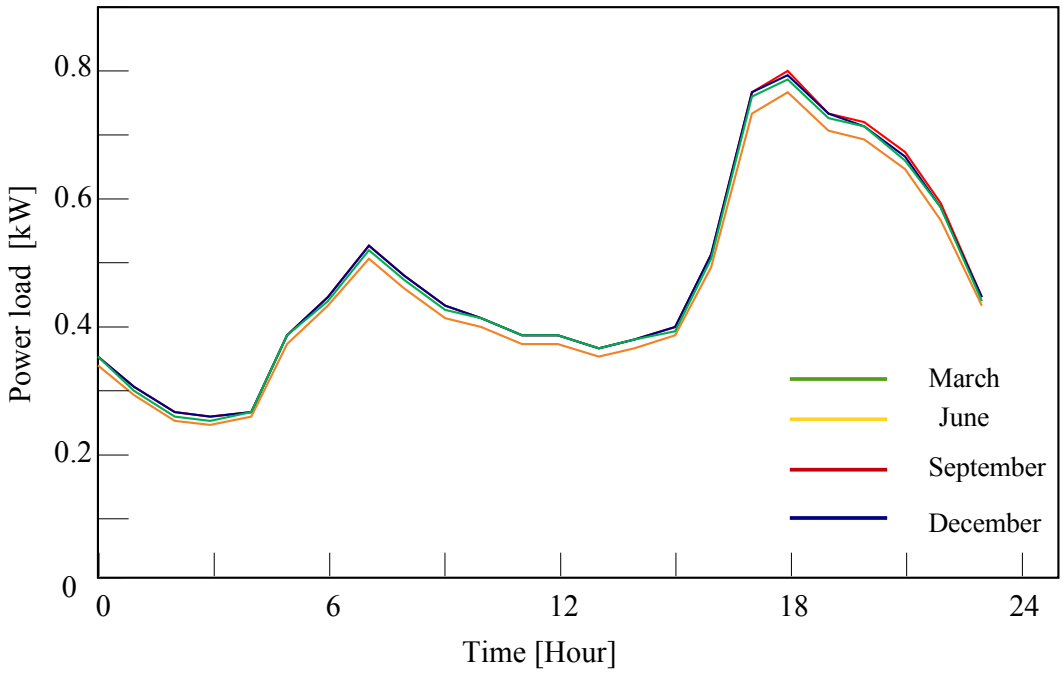

(a) Power demand

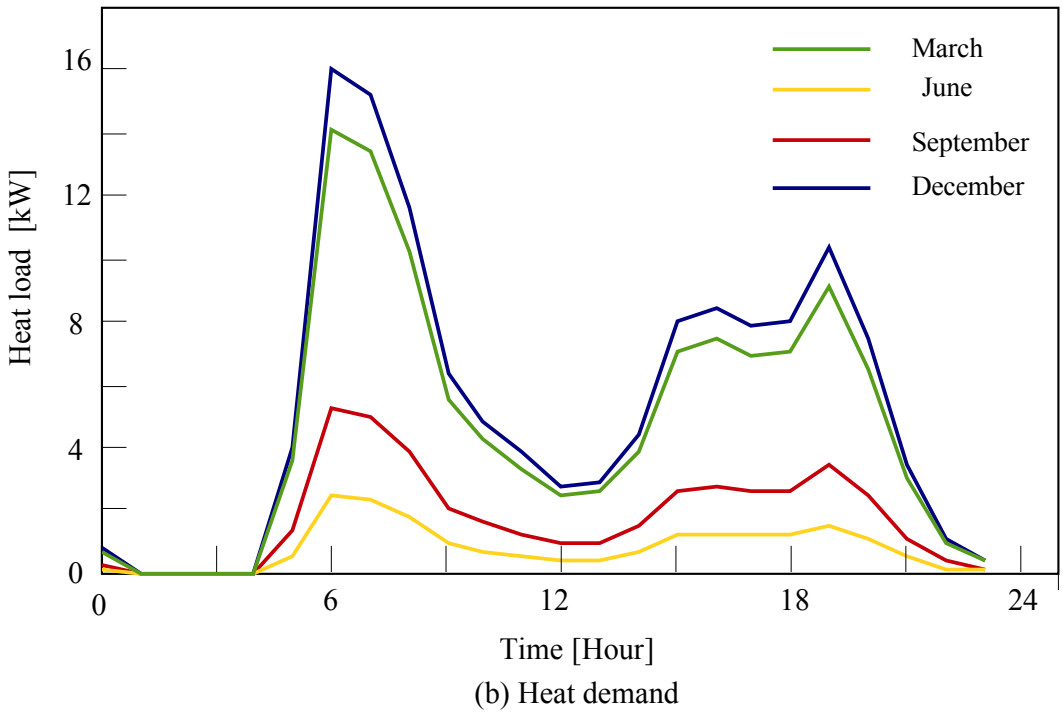

(b) Heat demand

Fig. 2-4 Power load and heat load of one household in Sapporo in Japan

2.2.3 Amount of slope–face solar radiation and photovoltaic power generation

Direct solar radiation intensity $H_{D,t}$ and sky solar radiation intensity $H_{S,t}$ are used to calculate the amount of slope-face solar radiation and the photovoltaic power generation. The global-solar-radiation intensity ($I_{H,t}$), horizontal sky solar radiation intensity ($I_{S,t}$) and direct solar radiation intensity ($I_{D,t}$) at time t (t =0, 1, 2, 3,....., 23) can be determined from the numerical weather information (NWI) [84-87]. The formulas for direct solar radiation and the sky solar radiation are calculated using the following equations:

$$H_{D,t} = I_{D,t} \cdot cos\theta \tag{2-1}$$

$$\sin\theta = \cos\alpha \cdot \sin\delta - \sin\alpha \cdot \cos\varphi \cdot \cos\delta \tag{2-2}$$

$$H_{S,t} = 0.5 \cdot I_{S,t} \cdot (1 + \cos\beta) + 0.5 \cdot \lambda \cdot I_{H,t} \cdot (1 - \cos\beta) \tag{2-3}$$

$$\cos\beta = \cos\alpha \cdot \cot\varphi + \sin\alpha \cdot \operatorname{cosec}\varphi \cdot \tan\delta \tag{2-4}$$

Equations (2-1) to (2-4) are used to calculate the slope-face solar radiation, the calculation results are shown in Fig 2-5. In this figure, the average values of slope-face solar radiation are calculated for months March, June, September and

December.

The amount of solar radiation and the outside air temperature for every sampling time can be obtained by the numerical weather information (NWI). Moreover, the output of photovoltaic power can be obtained by introducing the installation angles of the solar cell to Eqs. (2-1) to (2-5) and the following equation is used to calculate the photovoltaic power generation $P_{s,t}$ [88], [89]:

$$P_{s,t} = S_S \cdot \eta_S \cdot (H_D + H_S) \cdot \{1 - (T_C - T_O) \cdot (R_T / 100)\} \tag{2-5}$$

Where $P_{s,t}$ is the output power from the solar cell (photovoltaic power), $T_{C,t}$ is the temperature of the solar cell, S_S is the area of the solar cell (72 m^2), η_S is the generation efficiency (14%), R_T is the temperature coefficient (0.4%/K), and T_O is the reference temperature (298K). Equation (2-5) is used to calculate the photovoltaic power generation, the calculation results are shown in Fig. 2-6. As shown in this figure, the average values of the photovoltaic power generation are calculated for months March, June, September and December.

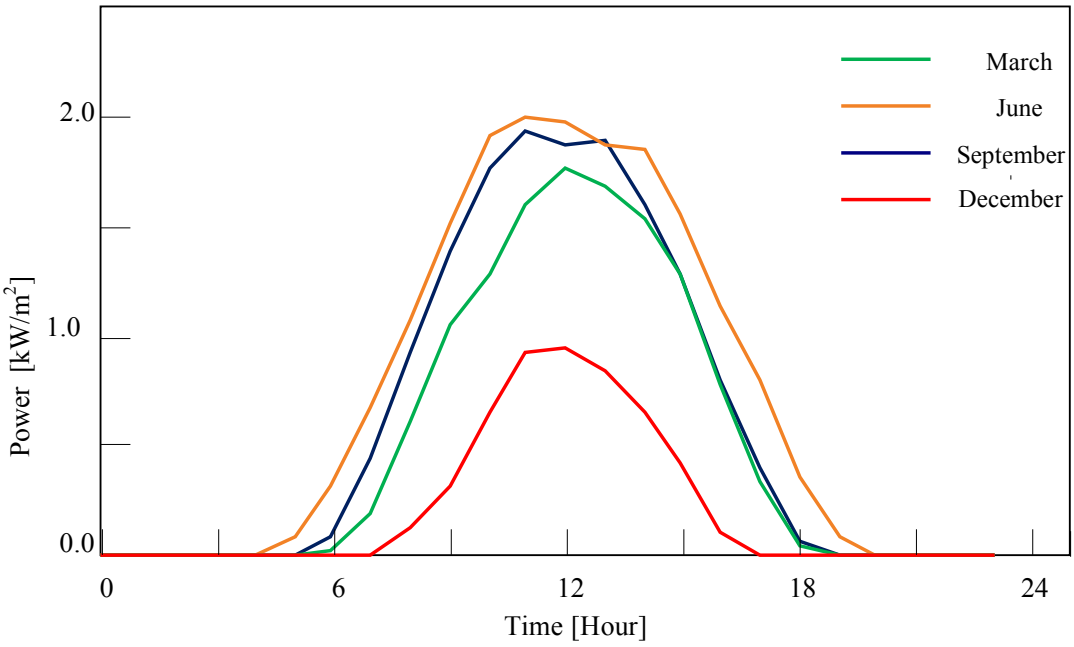

Fig. 2-5 Slope-face solar radiation

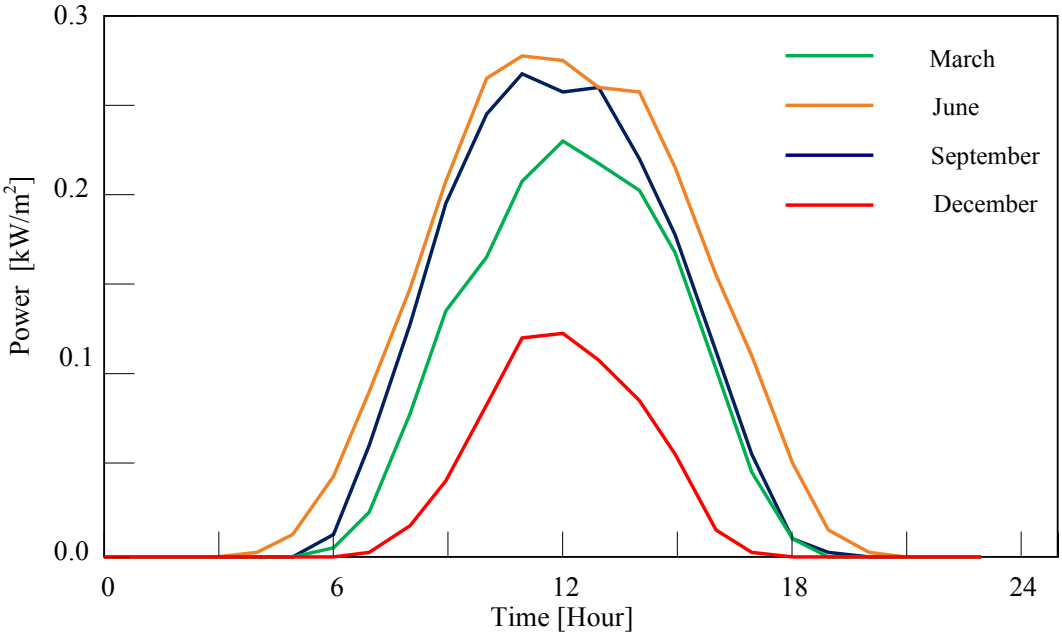

Fig. 2-6 Photovoltaic power generation

2.2.4 Power and heat balance

Equation (2-6) is a power balance equation. $P_{DE,t}$, $P_{pv,t}$ and $P_{bt,t}$ on the left-hand-side in the equation are the diesel engine generator power, photovoltaic power, and battery power, respectively. $P_{need,t}$, $P_{btc,t}$, and $P_{loss,t}$ on the right-hand-side in the equation represent power demand, the amount of battery charge, and loss of power, respectively. Charge-and-discharge loss of a battery is included in the power loss $P_{loss,t}$.

$$P_{DE,t} + P_{pv,t} + P_{bt,t} = P_{need,t} + P_{btc,t} + P_{loss,t} \quad (2\text{-}6)$$

Equation (2-6) is applied in the operation of Case 2 where there is a battery. But in the operation of Case 1, there is not a battery so the following Eq. (2-7) is applied for a power balance:

$$P_{DE,t} + P_{pv,t} = P_{need,t} + P_{loss,t} \quad (2\text{-}7)$$

On the other hand, Eq. (2-8) is a heat balance equation. $H_{DE,t}$, $H_{bl,t}$ and $H_{st,t}$ on the left-hand-side in the equation are the exhaust heat output from the diesel engine generator, a boiler, and a heat storage tank, respectively. $H_{need,t}$, $H_{sts,t}$ and $H_{loss,t}$ on the right-hand-side of the equation are heat demand, the amount of heat storage, and the

heat loss, respectively. Heat storage loss is included in the heat loss $H_{loss,t}$ on the right-hand-side of the equation.

$$H_{DE,t} + H_{bl,t} + H_{st,t} = H_{need,t} + H_{sts,t} + H_{loss,t} \quad (2\text{-}8)$$

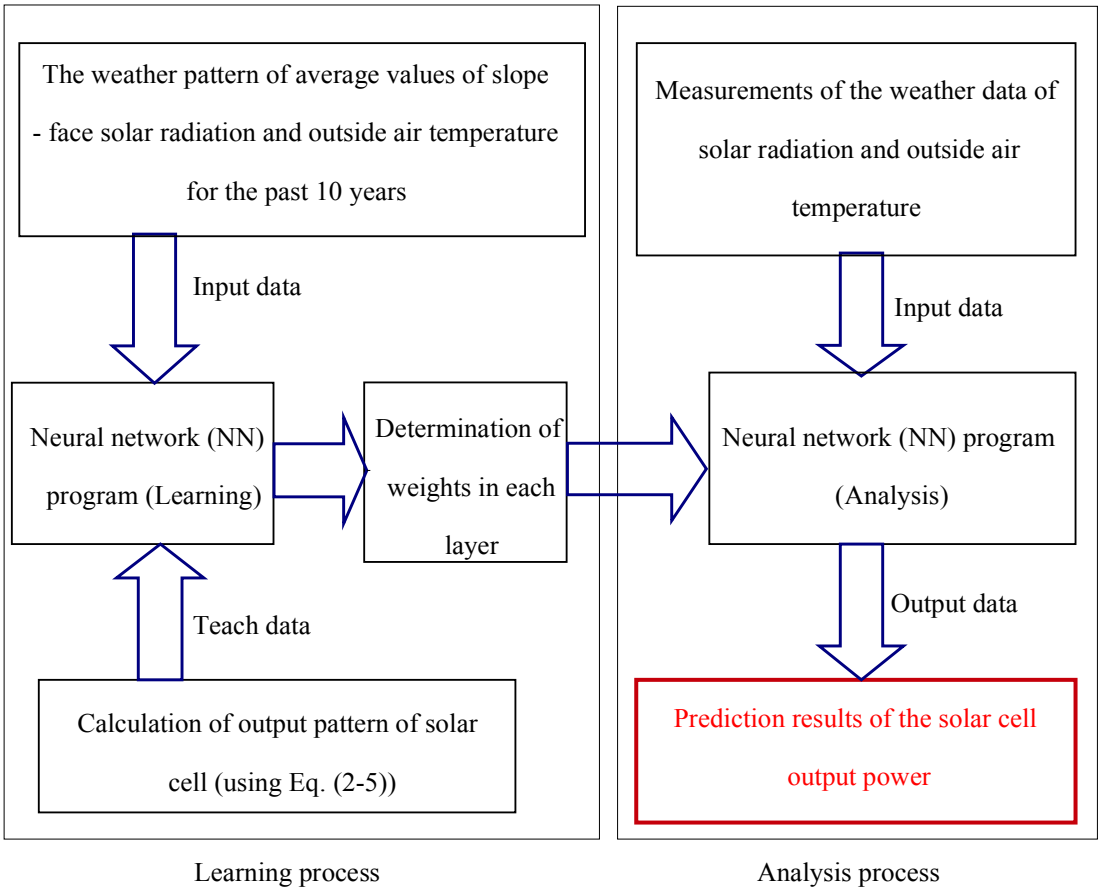

Fig. 2-7 Prediction algorithm of the photovoltaic power generation

2.2.5 Proposed neural network algorithm

The NN is suitable to predict the power output from the photovoltaic system because of its speed, simplicity and high prediction performance [90]. The prediction algorithm of the output power from the photovoltaic uses a layered NN, as shown in the block diagram in Fig. 2-7. The structure of the layered NN is shown in Fig. 2-8, it consists of three layers: the input layer, the hidden layer and the output layer. The successful implementation of a NN depends on the training (learning) process. In the learning process, the connection weights between layers are determined following the total minimum error.

First, all weights are chosen randomly, and the past weather pattern of a slope-face solar radiation and outside air temperature are used as input signals to the NN. The photovoltaic power production teaching data from the solar cell are input into the output layer. During the learning process, the learning rate is specified as 0.1, and the sigmoid function is utilized for the input-output characteristics of the neurons. For each neuron, the teaching data is the calculation of output photovoltaic power by using Eq. (2-5), the output of neuron *j* in the *n* layer is given as:

$$O_j^n = \frac{1}{1+e^{-I_j^n}} \tag{2-9}$$

The term I_j^n in Eq. (2-9) is the input of neuron *j* in layer *n*. It is calculated using the output O_k^{n-1} and weight $w_{j,k}^{n,n-1}$ of neuron *k* layer *n-1*, as follows:

$$I_j^n = \sum_{k=1}^{L_{n-1}} w_{j,k}^{n,n-1} \cdot O_k^{n-1} \tag{2-10}$$

Where $j = 1,\ldots, L_n$, and $k = 1,\ldots\ldots, L_{n-1}$

2.2.5.1 Learning process

First, all weights in the NN is determined randomly. When the random initial values are input into the proposed NN, the outputs agree with the correct answer with high precision. The past weather patterns, amount of slope face solar radiation and outside temperature are given to the NN, and the learning data is the actual output photovoltaic power. The mean squared errors (*MSE*) equation is described as:

$$MSE_N = 0.5 \cdot \sum_{j=1}^{L_n} (t_j - O_j^N)^2 \tag{2-11}$$

Where t_j is the output target actual power, and O_j^N is the estimated power

value. In this study, the NN modifies the weights so that the *MSE* approaches 0.0055%.

2.2.5.2 Weight modification

Equation (2-12) is used to calculate the corrected weighted $w_{j,k}^{n,n-1}$ by using the weight before modification $w_{j,k}^{-n,n-1}$ and the amount of modification $\Delta w_{j,k}^{n,n-1}$. The amount of modification in Eq. (2-13) is expressed in Eq. (2-14). The partial differential of Eq. (2-13) is calculated using Eqs. (2-14) and (2-15) [91].

$$\Delta w_{j,k}^{n,n-1} = w^{new} - w^{old} = w_{j,k}^{n,n-1} - w_{j,k}^{-n,n-1} \tag{2-12}$$

$$\Delta w_{j,k}^{n,n-1} = -\eta \frac{\partial MSE_N}{\partial w_{j,k}^{n,n-1}} = -\eta \frac{\partial MSE_N}{\partial I_j^n} \cdot O_j^{n-1} \tag{2-13}$$

when $n=N$

$$\frac{\partial MSE_N}{\partial I_j^n} = -(t_j - I_j^N) \cdot O_j^N \cdot (1 - O_j^N) \tag{2-14}$$

when $n < N$

$$\frac{\partial MSE_N}{\partial I_j^n} = \left\{ \sum_{L=1}^{L_n} \frac{\partial MSE_N}{\partial I_j^{n+1}} \cdot w_{L,j}^{n+1,n} \right\} \cdot O_j^n \cdot (1 - O_j^n) \tag{2-15}$$

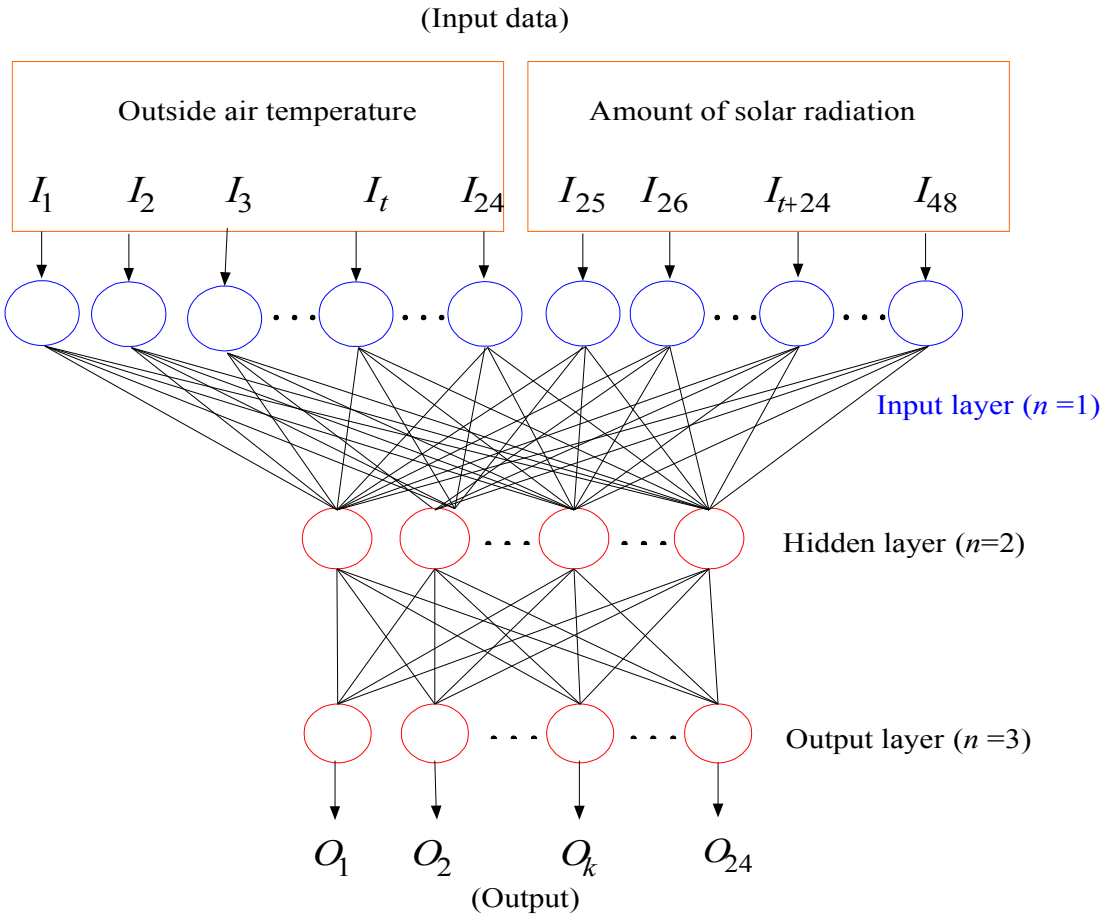

Fig. 2-8 The layered neural network of the prediction algorithm

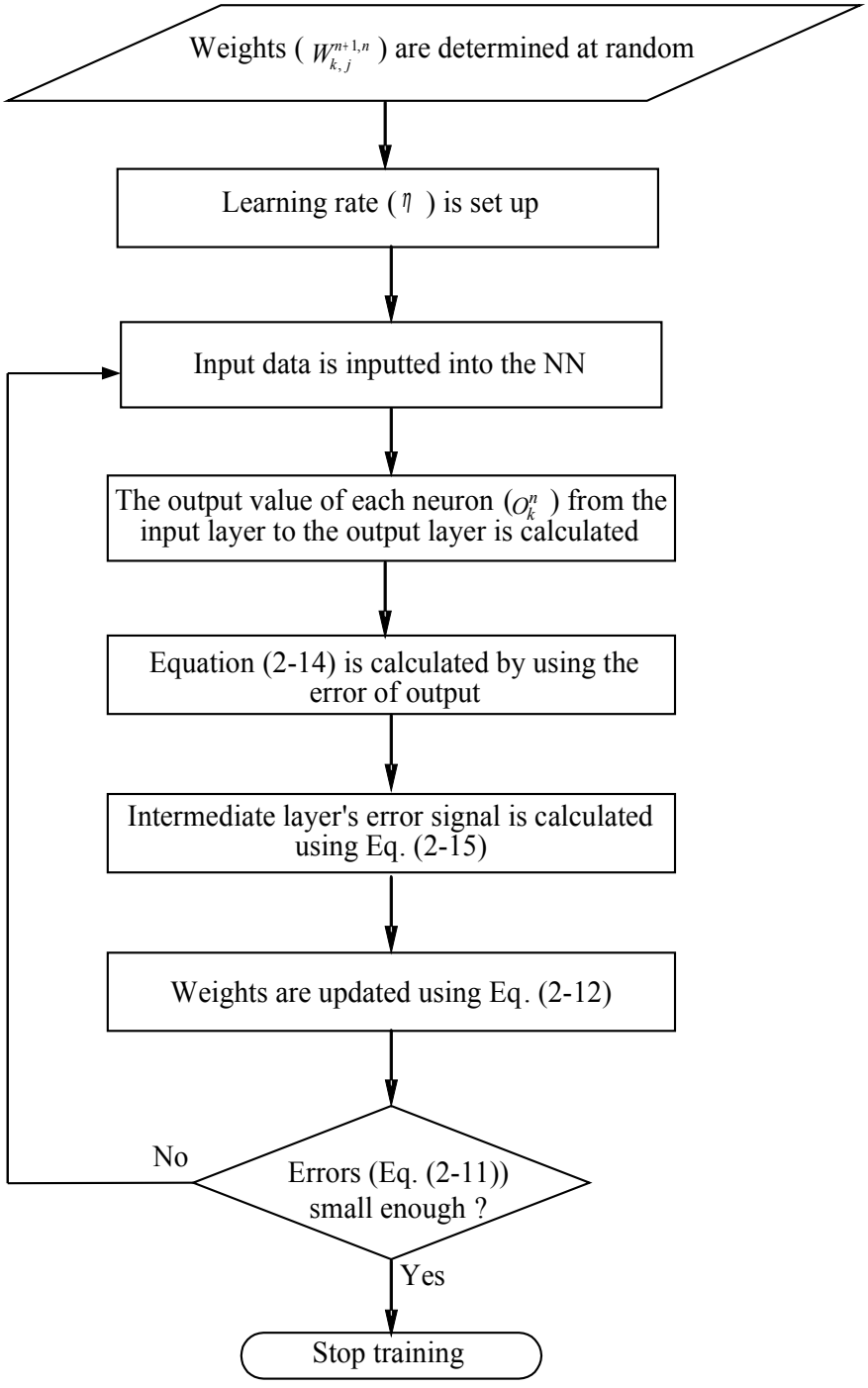

Fig. 2-9 The NN algorithm learning process calculation flow

2.2.5.3 Analysis flow of the learning process

Figure 2-9 shows the proposed NN algorithm learning process analysis flow. All weights $w_{j,k}^{n,n-1}$ are determined randomly, and the learning rate η in Eq. (2-13) is given to the program. The input data I_j^n and teaching data t_j are input into the program. The input and output data of each neuron are calculated. Equation (2-14) is calculated using O_j^n and t_j, as well as Eq. (2-15). These results are used in Eq. (2-13), and $\Delta w_{j,k}^{n,n-1}$ is calculated. This value is given to Eq. (2-12) and the weight of each neuron is updated. The analysis error is calculated using Eq. (2-11). When the analysis error is smaller than the previously defined value, the training process stops. On the other hand, if it is larger than the threshold value, the process is returns and calculates repeatedly.

2.2.5.4 Relation between the input data and analysis error

In this section, the relation between input data and analysis error is illustrated. Equation (2-11) is used to calculate the analysis error. The analysis error is calculated by using this equation and the calculation will finish if this value is smaller than the value set up previously. On the other hand, when the analysis error is larger than the value set up previously, as shown in Fig. 2-9 , the process is returned and calculated repeatedly as explained before in the last sections.

The relation between the kind of input data of the proposal NN shown in Fig. 2.8

and the analysis result of the photovoltaic power generating is clarified in this section. The result of each input data of the proposed NN and analysis error is shown in Fig. 2-10. In this figure, the relation between the input data and analysis error is graphed for three cases: the input includes all outside temperature data and solar radiation data that are the average daily values, ±10% of random fluctuation is given to solar radiation; and ±20% random fluctuation is given to solar radiation. As shown in Fig. 2-10, the variation of solar radiation influences the analysis. The biggest influence occurs in case3.This means that the input data (outside air temperature and solar radiation) to the proposed NN algorithm have influence on the analysis procedure.

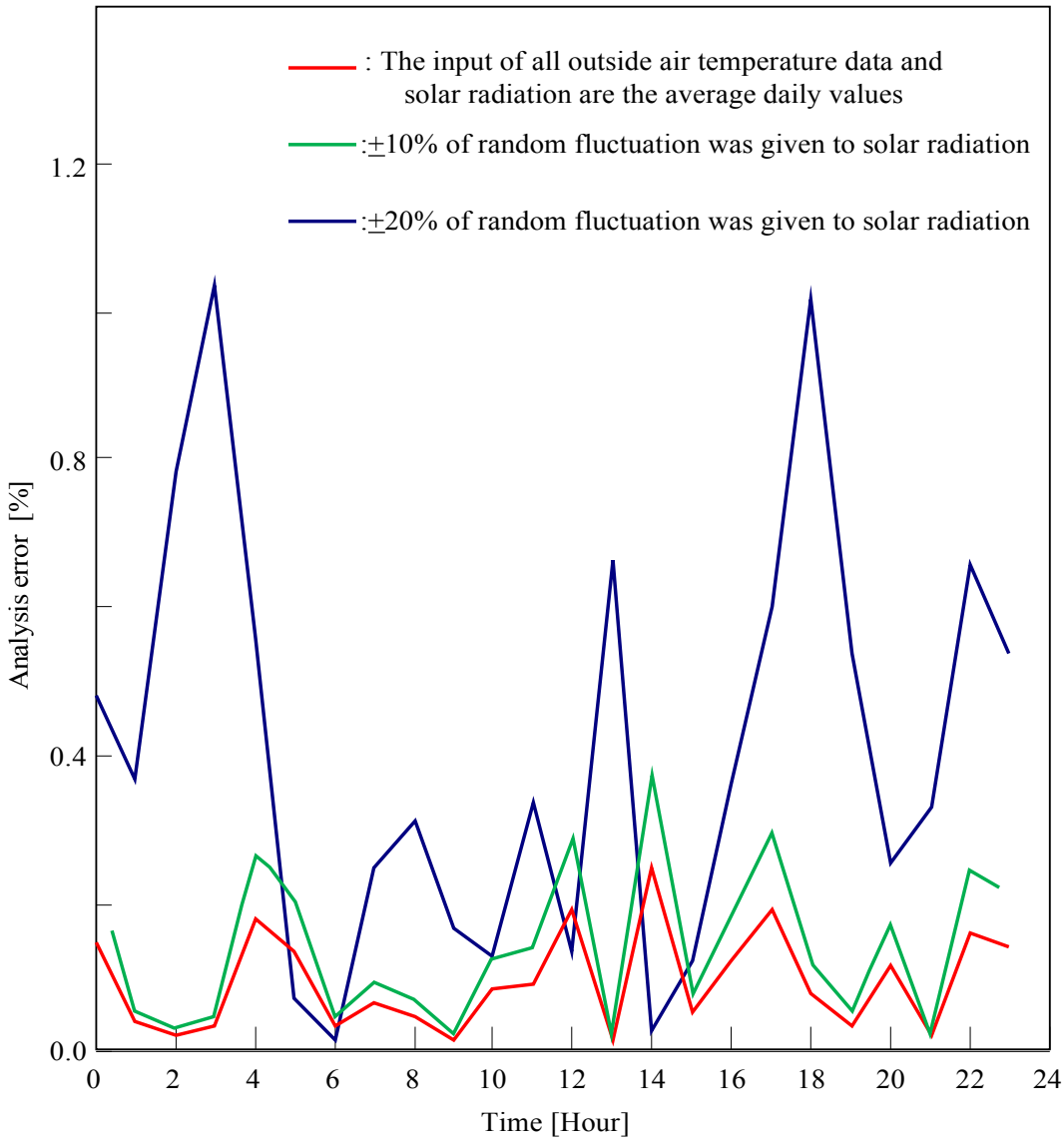

Fig. 2-10 Relation between input data and analysis error in March

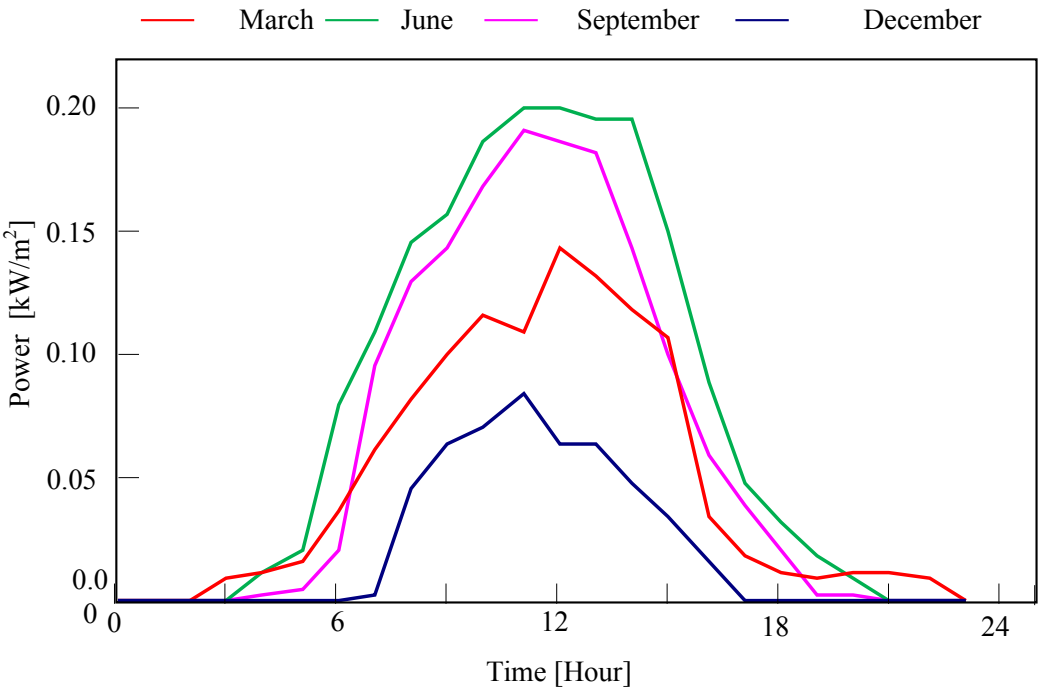

Fig. 2-11 Predictive values of the solar cell electricity

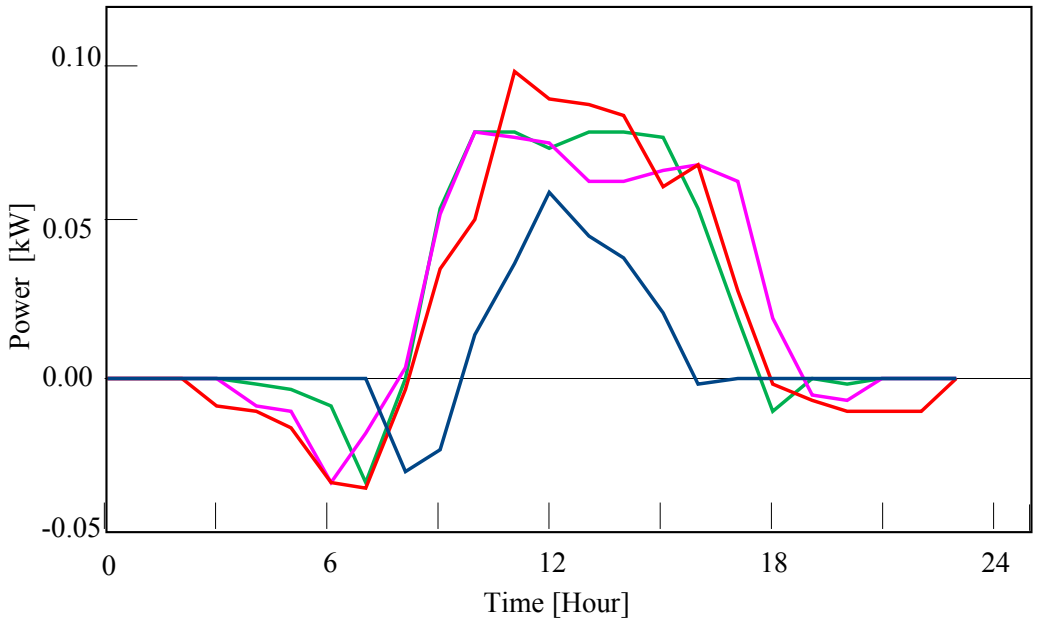

Fig. 2-12 Error in power generation prediction

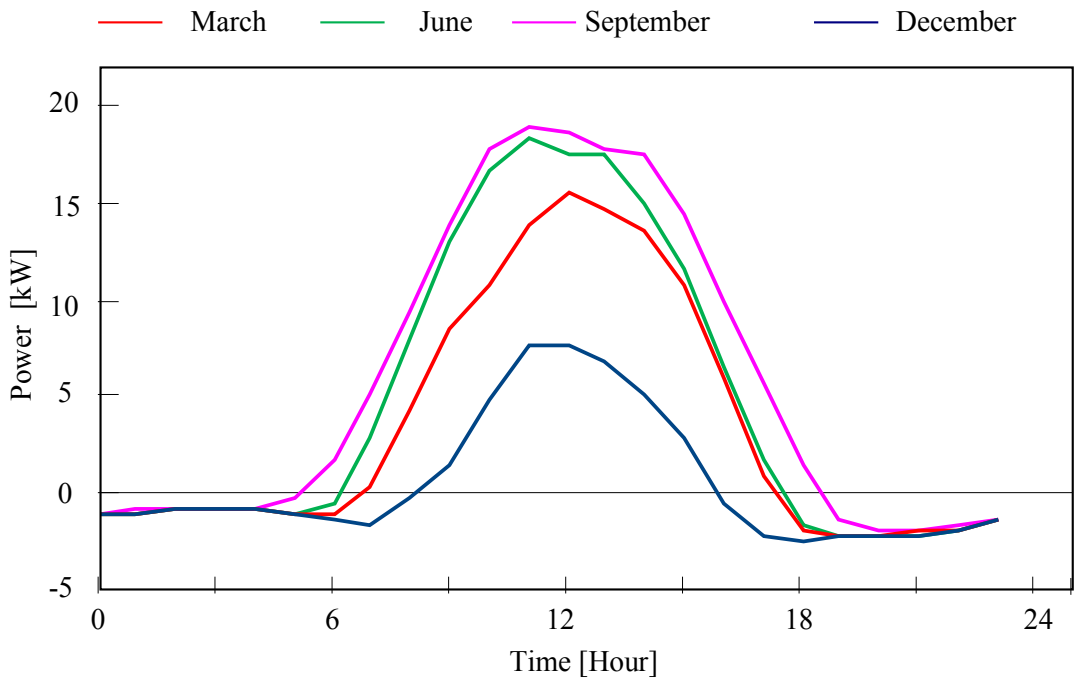

(a) Using actual output power (Method 1)

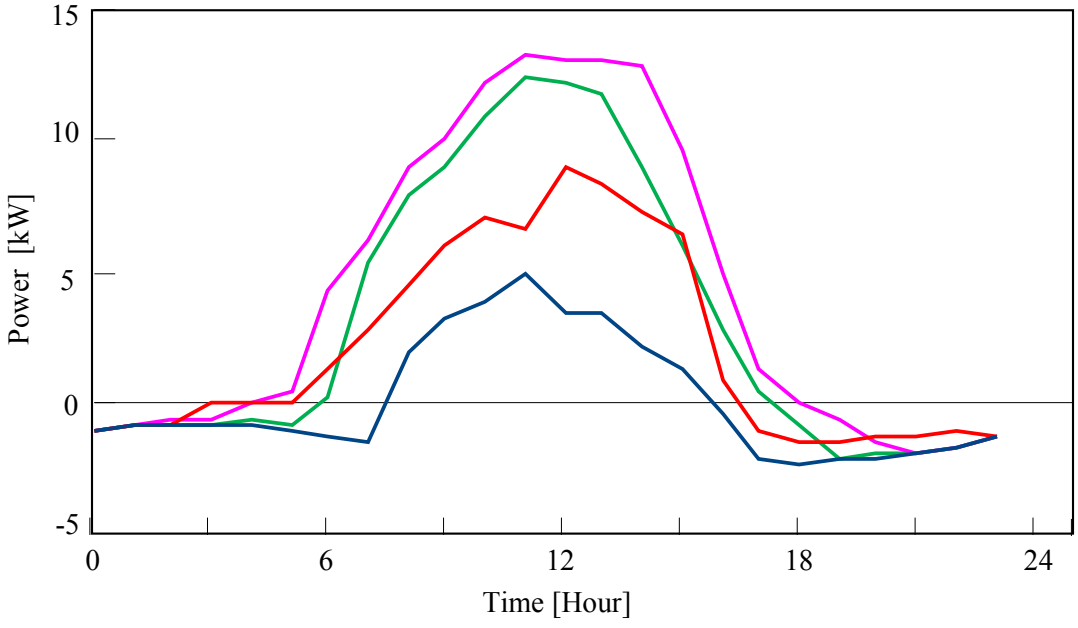

(b) Using NN prediction power (Method 2)

Fig. 2-13 Power results generated by subtracting the power demand from the solar cell output power

2.3 Results and Discussion of the Proposed System

In this section, the operation results and discussion of the proposed system are presented depending on the analysis procedure as discussed before. The NN algorithm is used to predict the power output from the photovoltaic system. The predicted average values for the photovoltaic power generation using NN prediction algorithm are shown in Fig. 2-11. Figure 2-12 presents the average power generation prediction error values of the predicated photovoltaic power generation, this figure is obtained by subtracting Fig. 2-11 from Fig. 2-6. In Fig. 2-12, the average error percentages are 29%, 19%, 26% and 25%, for March, June and September and December respectively. These values are different because of the differences in slope-face solar radiation and outside air temperature for each month.

The output power generated by subtracting the photovoltaic power generation and the demand power is shown in Fig. 2-13 for the two methods, using actual output power (Method 1) and using NN predicated power (Method 2). Figure 2-13(a) is obtained by subtracting the power demand of three houses from the photovoltaic power generation (multiplying Fig. 2-4 by 72 m^2 to transfer values from kW/m^2 to kW). Furthermore, Fig. 2-13(b) is obtained by subtracting the power demand from the NN predictive values of photovoltaic power generation for three houses. The energy supply characteristic of the photovoltaic and diesel engine generator combined system is proposed in the two methods for two operating cases.

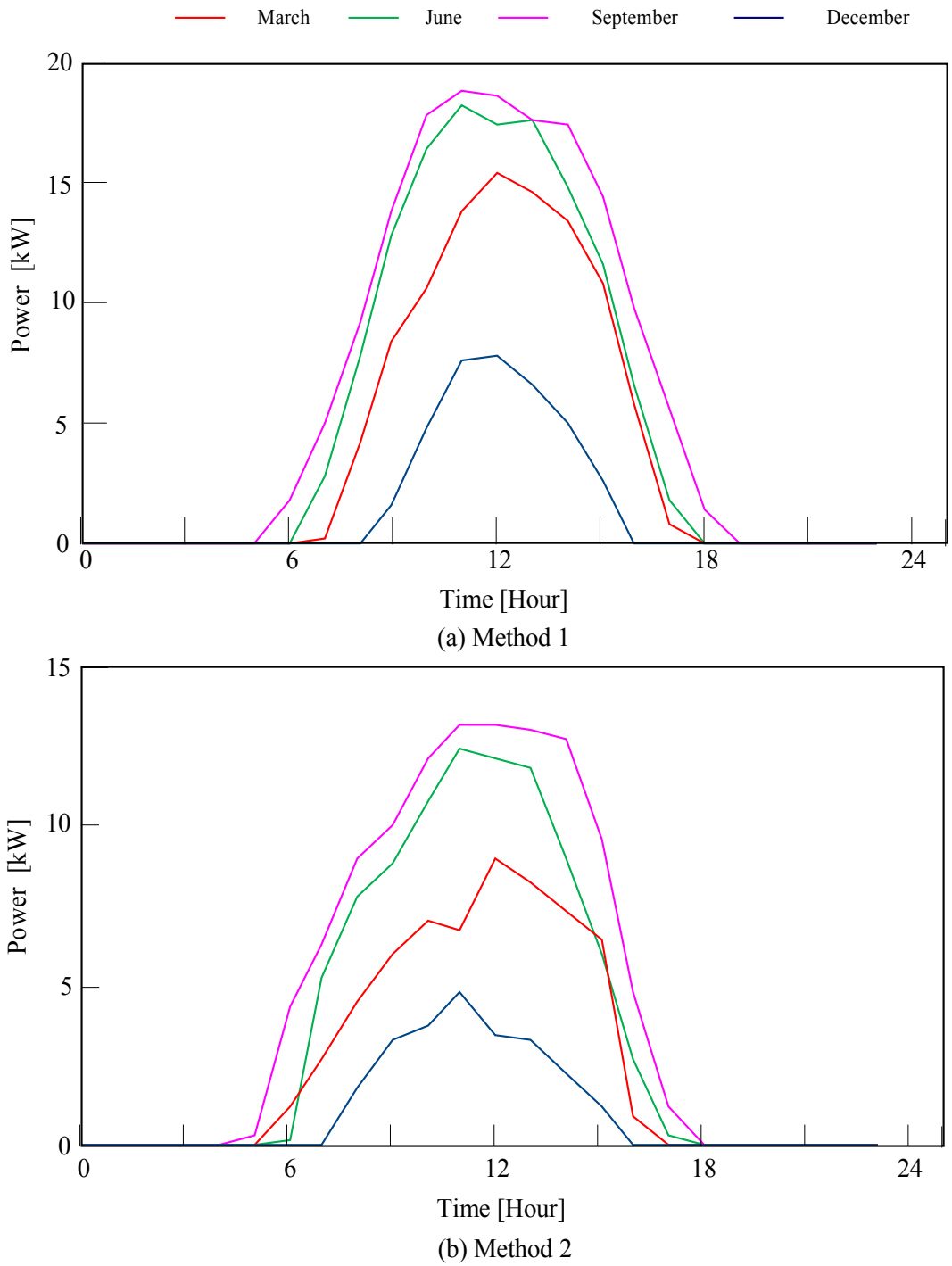

Fig. 2-14 Electricity sales to utilities in the operation of Case 1

2.3.1 Case 1 result

The proposed system is operated without battery in the operation of Case 1, the surplus photovoltaic power is sold off and the operation of the diesel engine generator is accordance to the load fluctuation. The surplus power of the photovoltaic output power is sold as shown in Fig. 2-14. When the power output from the photovoltaic system is insufficient compared with the power demand, the engine generator operates and supplies the demand, as shown in Figs. 2-15 and 2-16. The engine generator exhaust heat (heat of the cooling water and the heat of engine exhaust gas) is shown in Fig. 2-15. Furthermore, the engine generator efficiency for the two methods in each month is shown in Fig. 2-16. The peak values of engine heat exhaust are shown in Table 2. As shown in this table, the peak values of heat exhaust are reduced by 3.3%, 7.5%, 1.1% and 2.7% by introducing the NN algorithm for each month. In addition, the peak value of engine generator efficiency is 28.1 for the two methods. The engine generator operates with low efficiency because it operates according to load fluctuation.

When the engine heat exhaust is less than the demand, the back-up boiler supplies the demand side, as shown in Fig. 2-17. In this figure, the peak heat values from the back-up boiler in case of Method 1 are 156 and 26 MJ at 6:00 am. for September and June, respectively, and also 145 and 54 MJ at 7:00 am. for March and September, respectively. Moreover, in Method 2, the peak heat values from the back-up boiler

are 155, 153, 26 and 57 MJ for each month at 6:00 in the morning. In the system operation of Case 1, the power is sold to the utilities, so the overall system efficiency is good.

Table 2.2 Peak values of exhaust heat from the engine generator in MJ

Month	Method 1	Method 2	Time
December	20.97	20.27	06:00:00 PM
March	20.3	18.77	07:00:00 PM
June	19.6	19.39	09:00:00 PM
September	20.21	19.67	07:00:00 PM

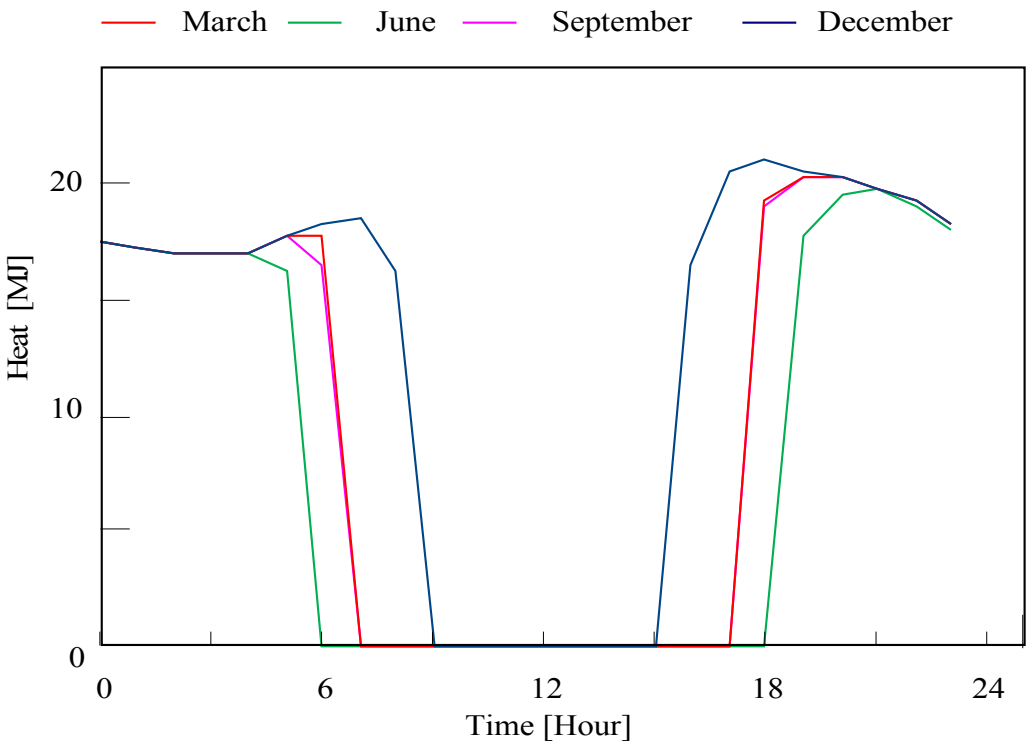

(a) Method 1

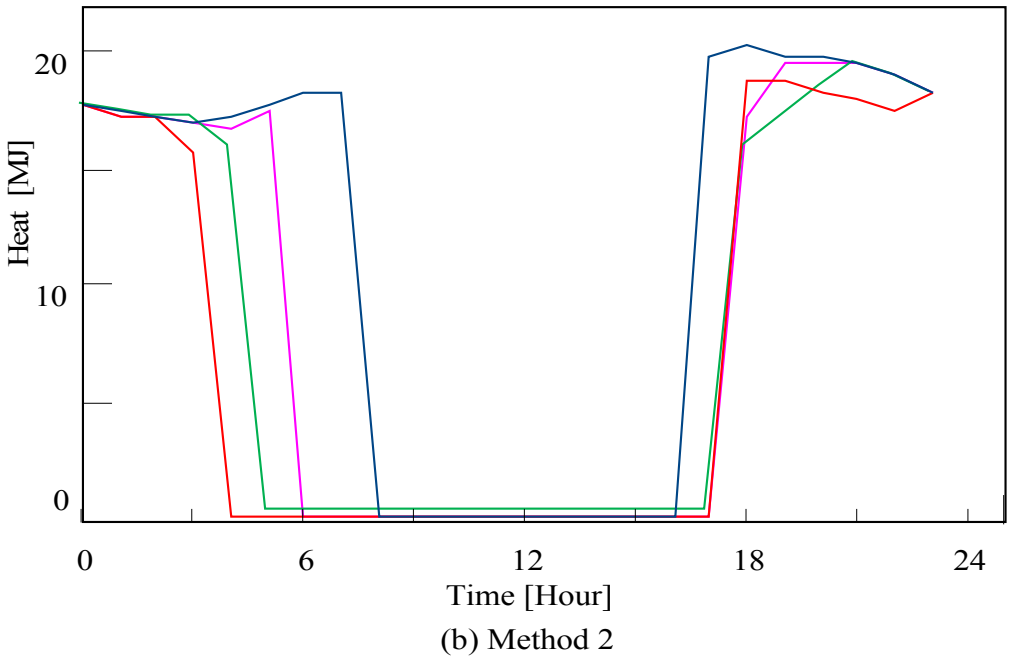

(b) Method 2

Fig. 2-15 Engine generator heat exhaust

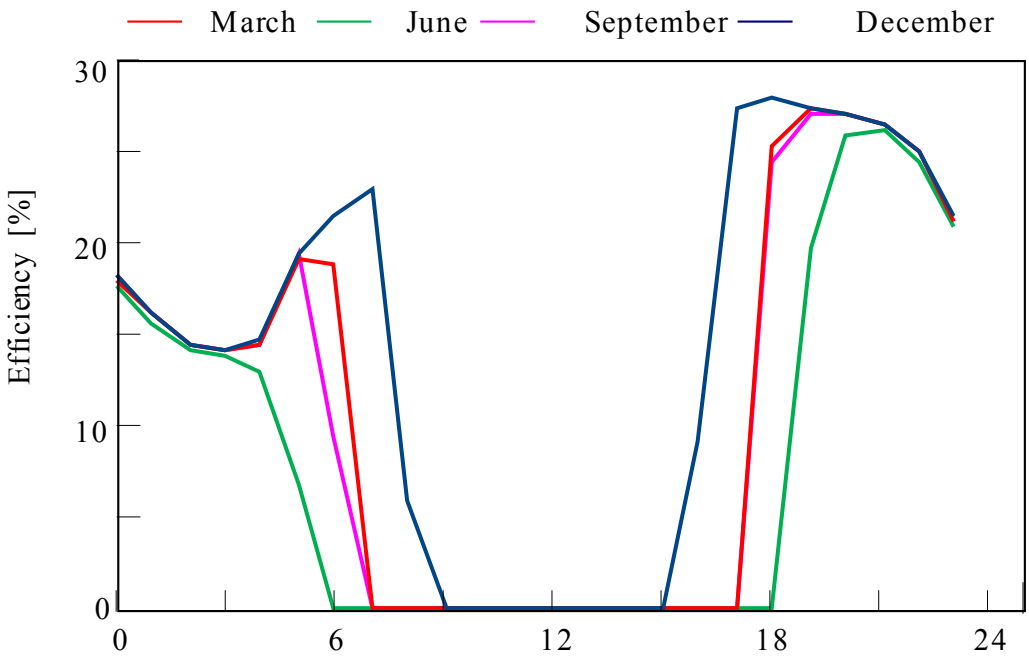

(a) Method 1

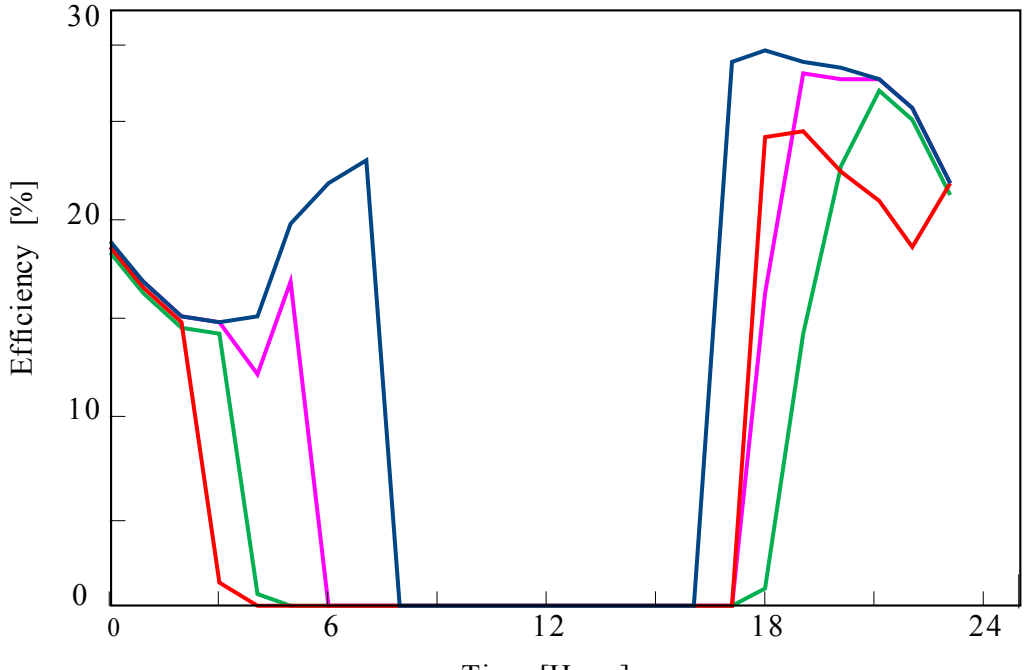

(b) Method 2

Fig. 2-16 Engine generator efficiency

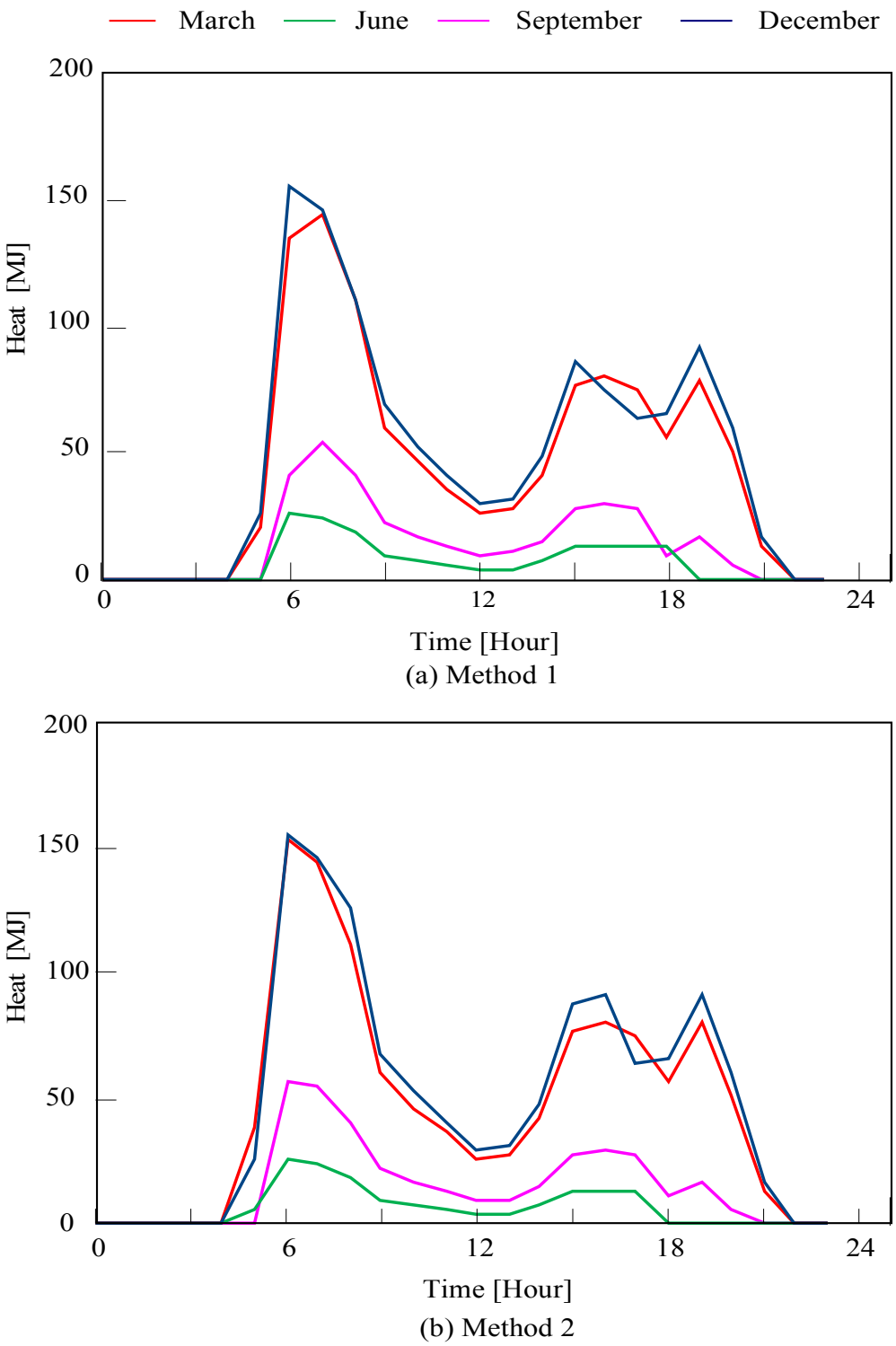

Fig. 2-17 Heat from the back-up boiler in the operation of Case 1

2.3.2 Case 2 result

The engine generator operates at fixed load with maximum efficiency in the operation of Case 2. In addition, the power demand is supplied by the battery electric discharge when the photovoltaic output power less than the power demand. When the photovoltaic output power exceeds the power demand, surplus power is charged the battery. Figure 2-18 shows the battery operation plan . In this figure, the battery is used to supply the demand side when the photovoltaic output power is lower than the demand. As shown in this figure, the maximum output power from the battery is 4 kWh and it is supplied the demand power at there is insufficient photovoltaic power compared to the power demand.

The surplus power from the photovoltaic power generation is used to charge the battery. The diesel engine generator operates according to the charge or discharge of the battery, as shown in Fig. 2-19. The diesel engine generator is operated with maximum output power of 3kW and maximum efficiency as described before in Chapter 2, Section 1.2.2 with output characteristic shown in Figs. 1-2 1nd 1-3. Thus, in Fig. 2-19, each point means that the diesel engine generator output power is 3 kW and it is operated in this period to supply the demand side at the battery capacity drops to 1 kWh or less. In Fig. 2-19, the engine generator operates an average of 8, 6, 4, and 6 hours in Method 1 and 7, 5, 4, and 5 hours in Method 2 for each month, respectively. During these engine generator operating hours, the heat is supplied to

the demand side. When comparing Fig. 2-19(a) with Fig. 2-19(b), the operating period of the engine generator is shortened by introducing the NN prediction algorithm. The engine operating time is reduced by 12.5% in December and 16.7% for March and September.

The back-up boiler is operated when there are insufficient heat in the heat storage tank compared to the heat demand. The operation plan of the back-up boiler is shown in Fig. 2-20. In this figure, the peak values of heat from the back-up boiler are 8.6, 8.5, 8.3, 8.6 MJ for each month at 18:00 in Method 1. In addition, for Method 2, the peak values are 8.6, 8.3 and 8.6 MJ for December, June and September at 18:00, respectively, and 8.2 MJ for March at 17:00. The average total engine heat is 51, 39, 26 and 38 MJ; furthermore, the back-up boiler provides 77, 89, 97 and 90 MJ in Method 1 for each month. Moreover, for Method 2, The average values of total engine heat is 39, 32, 26 and 32 MJ, respectively, and the average heat from the back-up boiler is 87, 87, 96 and 95 MJ for each month.

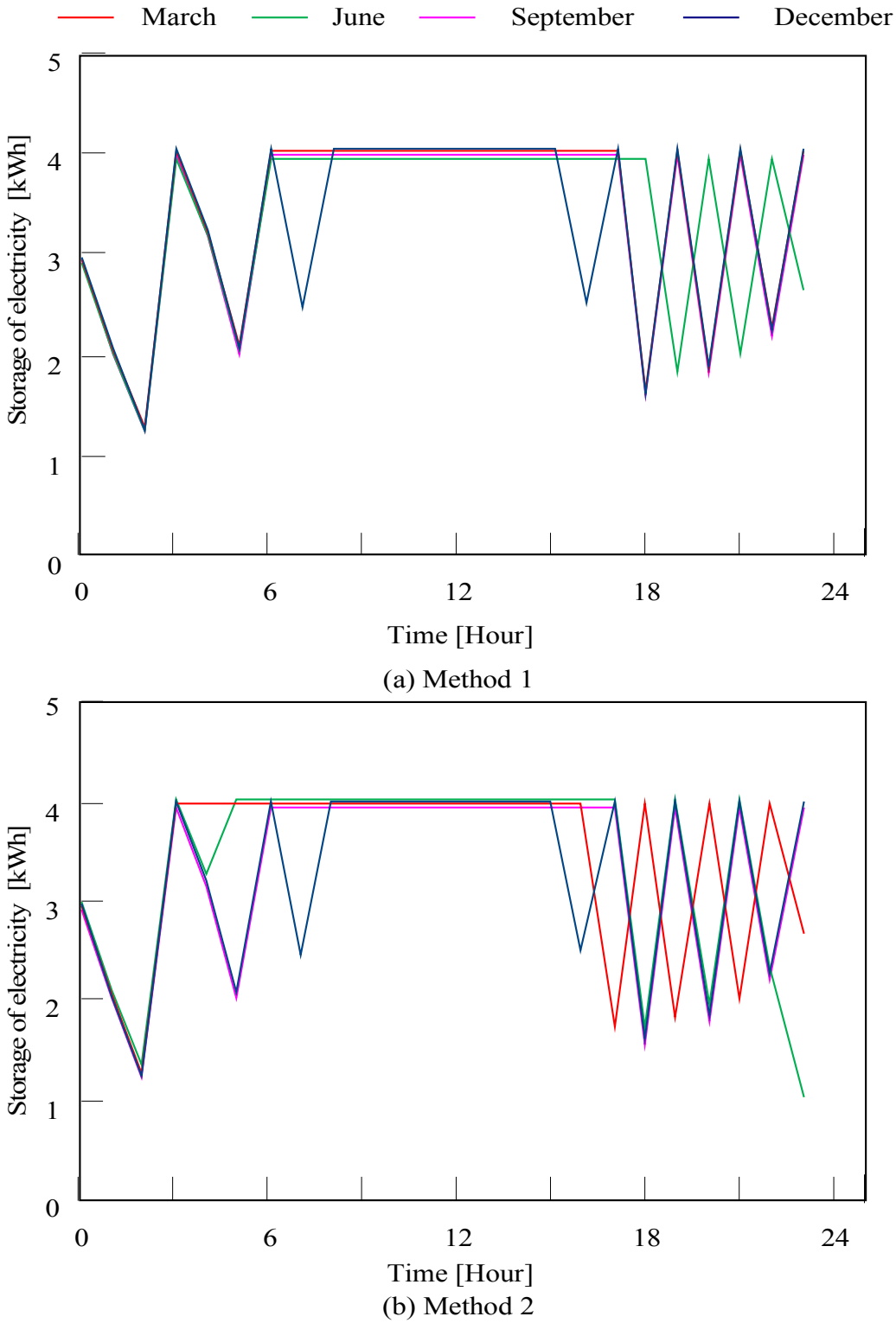

Fig. 2-18 Battery operation plan

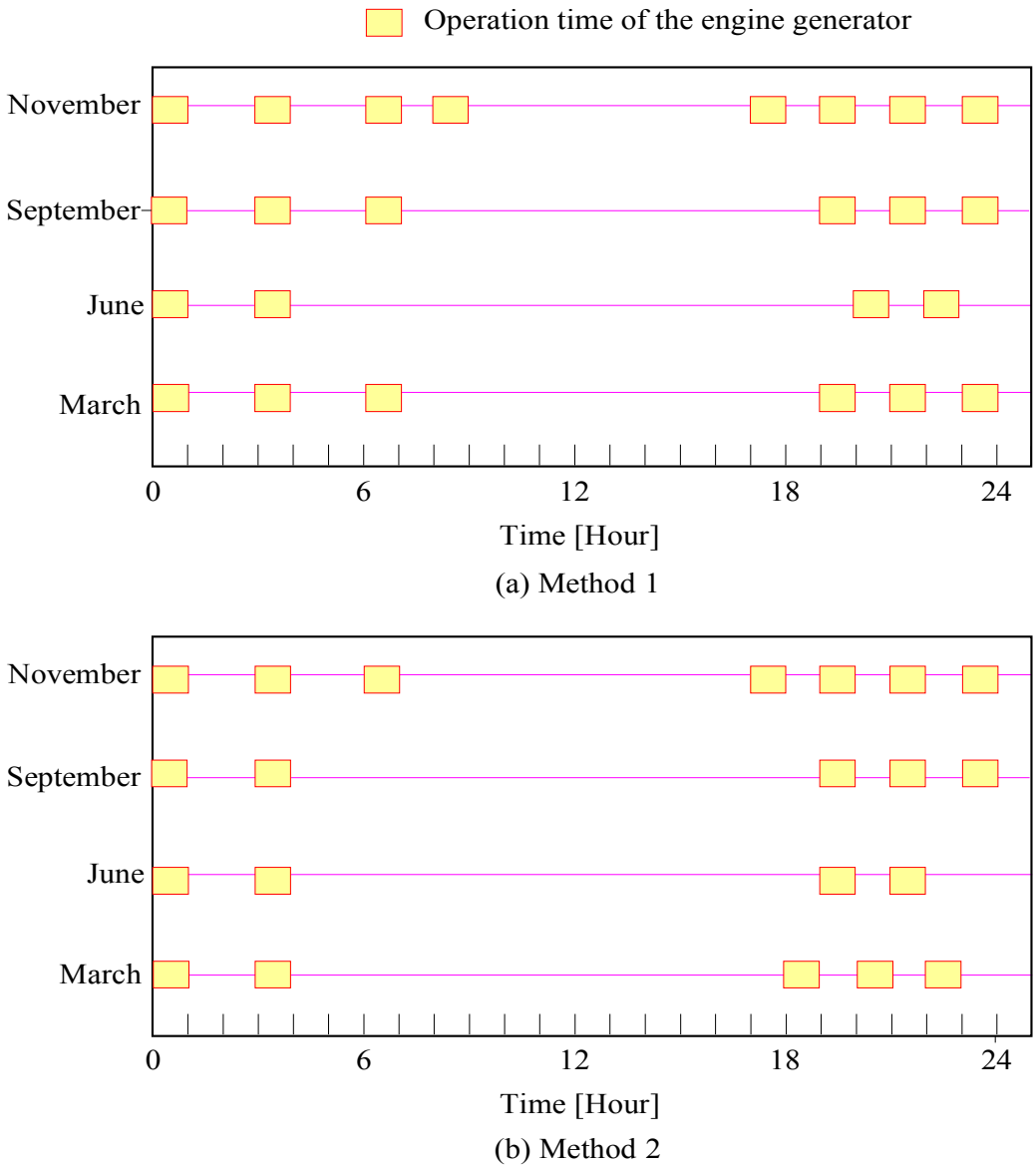

Fig. 2-19 Analysis results of the engine generator operation plan

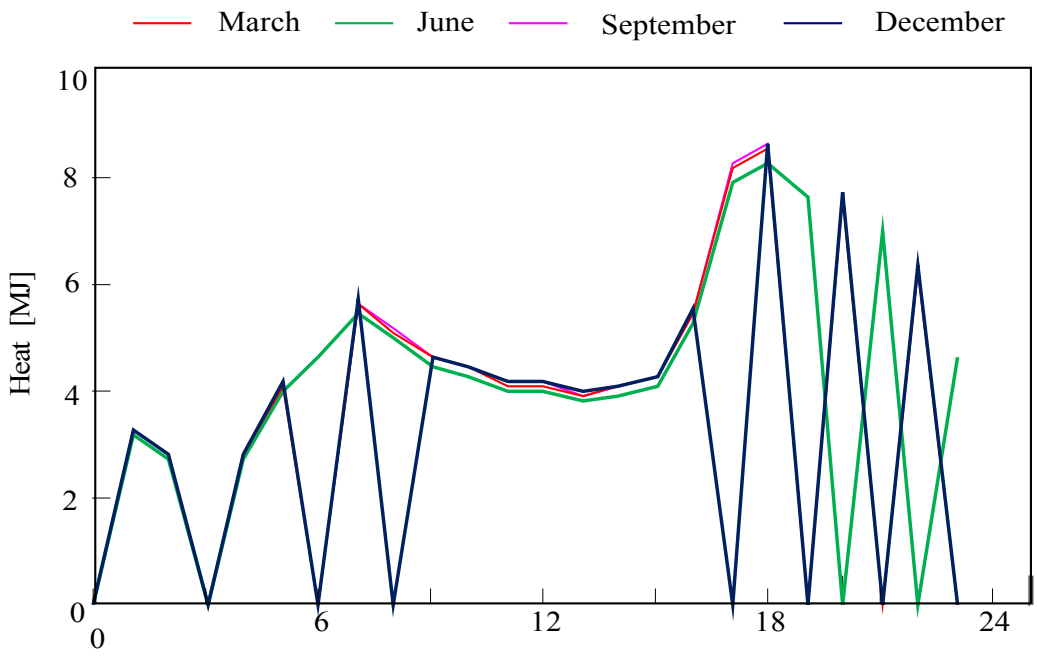

(a) Method 1

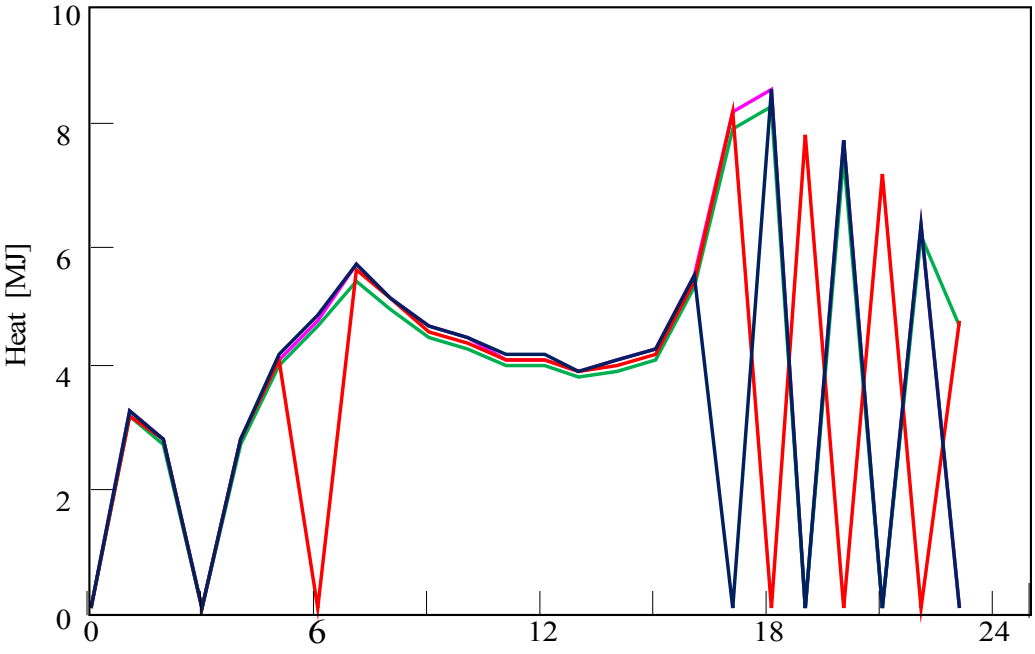

(b) Method 2

Fig. 2-20 Heat from the back-up boiler in Case 2

3 Photovoltaic and a SOFC-PEFC Combined System

3.1 System Configuration

The proposed photovoltaic system and a SOFC-PEFC combined system is shown in Fig. 3-1. The electric power and heat of the SOFC-PEFC combined system and PV system are used to supply power and heat to a grid of 30 residences in Sapporo in Japan. A schematic figure of the proposed system is shown in Fig. 3-1(a). It consists of the SOFC-PEFC combined system, PV system, power conditioning system, heat supply system and system controller. The details of each system are shown in Figs. 3-1(b) to (e). The system controller is used to operate each piece of equipment of the proposal system [92]. The photovoltaic electricity production for every sample time for each day is predicted by using NWI (the numerical weather information) obtained by the system controller, as shown in Fig. 3-1(a). The SOFC outputs high temperature exhaust heat at 750°C - 900°C . This high temperature exhaust heat is used for the steam reforming of bio-ethanol and the heating of LNG (liquid natural gas) and air supplied to the SOFC. The reformed gas is stored in a cylinder. The power load peak of the following day is cut by supplying the stored reformed gas to the PEFC. The optimal system operation is planned by the system controller.

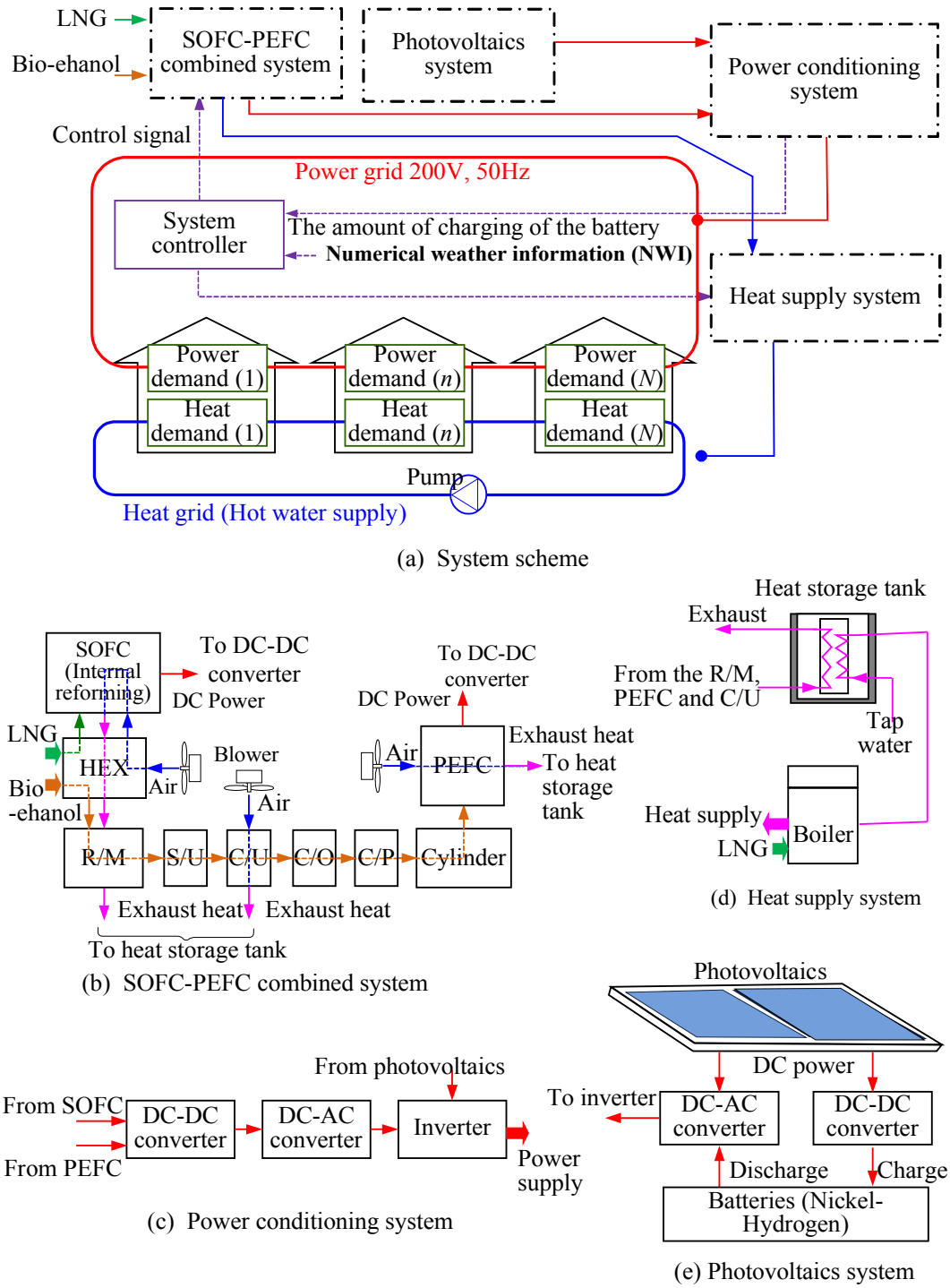

Fig. 3-1 Proposal microgrid with photovoltaics and SOFC-PEFC combined power system

In addition, load with various fluctuations added to the micro-gird is expected. Accordingly, this thesis investigates operation of the PV system and SOFC-PEFC combined system using three different load patterns (average load pattern, compressed load pattern and extended load pattern).

3.2 Operation of the SOFC-PEFC Combined System

The block diagram of the SOFC-PEFC combined system used in the proposal system is shown in Fig. 3-1(b). The SOFC that is introduced into the system has an internal reformer. As shown in this figure, the exhaust heat of SOFC heats the LNG, bio-ethanol gas and the air, which are supplied to the SOFC cathode using the heat exchanger (HEX). Supplying the exhaust heat of the SOFC to the steam reformer (R/M) with a shift unit (S/U) produces a reformed gas with a high hydrogen density [93-95]. Moisture is present in the reformed gas, so a condenser unit (C/U) for air cooling is used. A CO oxidation device (C/O) is used to remove CO from the reformed gas. After decreasing the CO, the reforming gas is stored in the cylinder by a compressor (C/P).

The electric power of the SOFC and PEFC is supplied to the DC-DC and the DC-AC converter and inverter, then to the power grid. On the other hand, in case of heat gird, the exhaust heat of the SOFC with an internal reformer is used for heating the

LNG, bio-ethanol gas and the air supplied to the SOFC cathode. The remaining exhaust heat is supplied to the steam reformer (R/M). The exhaust heat of the reforming unit, condenser unit (C/U) and PEFC is stored in the heat storage tank. The heat exchanger is installed in the heat storage tank. Heat is exchanged between the tap water and the heat medium in the heat storage tank. A boiler is operated when there is little heat storage compared with the heat demand.

The power division rate of the SOFC-PEFC combined system that is introduced to the demand side is shown in Fig. 3-2 (a) . As shown in this figure, the operation plan of the SOFC corresponds to the base load, so the SOFC is operated with maximum generation efficiency. On the other hand, the operation plan of the PEFC is in accordance to the load fluctuation. The base load is set as a larger value than the minimum value of the load fluctuation. The amount of exhaust heat from the SOFC-PEFC combined system depends on the operation plan of the SOFC, as shown in Fig. 3-2(b). Furthermore, the quantity of reformed gas produced changes with the setting of the load of the SOFC, as shown in Fig. 3-2(c). In Fig. 3-2(d), the stored reformed gas is supplied to the PEFC, and it is used in the next day.

The following equations from (3-1) to (3-7) show the steam reformation of bio-ethanol gas and the hydrogen production process, as described before. Here, (l) and (g) show the state of the liquid and gas, respectively.

$$H_2O(l) \rightarrow H_2O(l) - 0.1924kJ/(mol \cdot K) \quad (3\text{-}1)$$

$$C_2H_5OH(l) \rightarrow C_2H_5OH(l) - 0.113kJ/(mol \cdot K) \quad (3\text{-}2)$$

$$H_2O(l) \rightarrow H_2O(g) - 40.6kJ/mol \quad (3\text{-}3)$$

$$C_2H_5OH(l) \rightarrow C_2H_5OH(g) - 38.6kJ/mol \quad (3\text{-}4)$$

$$C_2H_5OH + 3H_2O \rightarrow 2CO_2 + 6H_2 - 173kJ/mol \quad (3\text{-}5)$$

$$C_2H_5OH + 3O_2 \rightarrow 2CO_2 + 3H_2O + 1369kJ/mol \quad (3\text{-}6)$$

$$H_2 + 1/2O_2 \rightarrow 3H_2O + 287kJ/mol \quad (3\text{-}7)$$

3.3 Partial Load Performance

Figure 3-3(a) shows relationship between the load factor of the SOFC and the power generation efficiency with internal reforming [96], [97]. Figure 3-3 (b) is the efficiency of the PEFC at different load factors, where the PEFC is accompanied by a steam reformer related to the power generation efficiency [98], [99]. Moreover, the relation between the output of the reforming gas and the reformer efficiency of the steam reforming using natural gas is shown in this figure.

When Fig 3-3 (a) is compared with Fig. 3-3 (b), the SOFC shows greater power generation efficiency compared with of the PEFC for a load factor of 25% or more. Furthermore, at a load factor less than 25%, the power generation efficiency of the SOFC decreases greatly. Therefore, a SOFC load factor of 25% or less is not generally assumed. The power generation efficiency of the SOFC differs by nearly 21% for load factor of 25% and 100%. On the other hand, the power generation efficiency of the PEFC differs by nearly 11% for load factors of 15% and 100%.

The performance of the R/M, S/U, and CO is dependent on the reformer efficiency. The reformer efficiency η_R in Fig. 3-3 (b) is defined by the following equation:

$$\eta_R = \frac{\text{Heating value of reformed gas}}{\text{Heating value of supply bioethanol}} \tag{3-8}$$

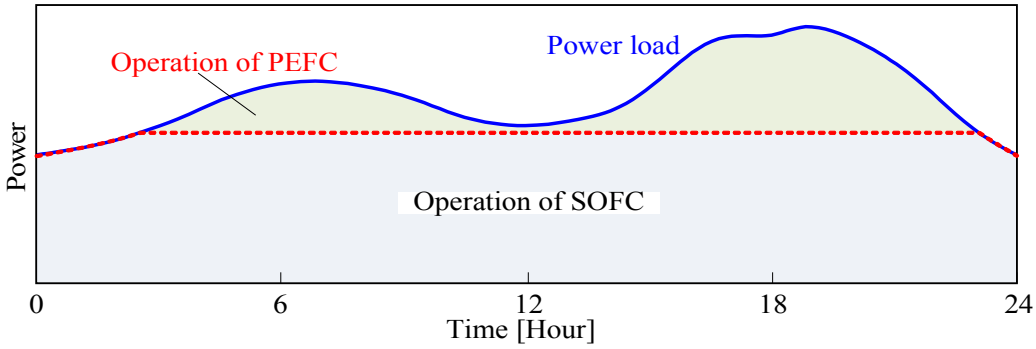

(a) Operation pattern of SOFC and PEFC

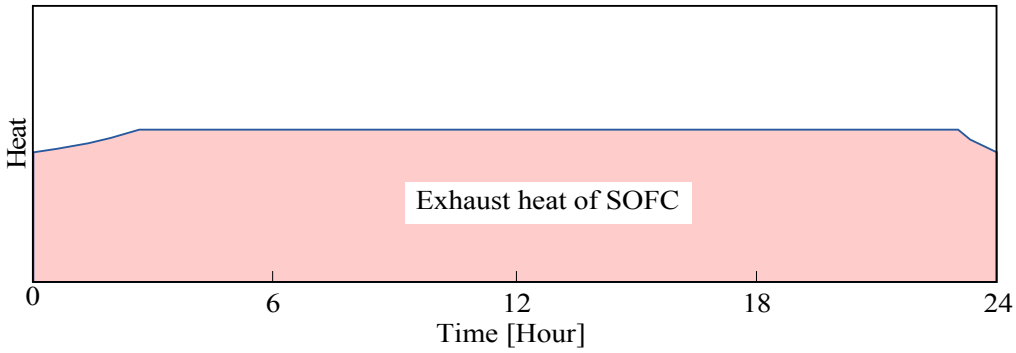

(b) Exhaust heat model of SOFC

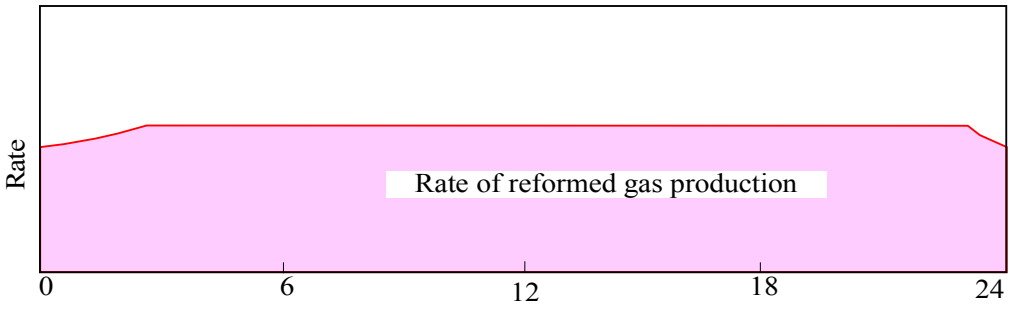

(c) Characteristics of reformed gas production

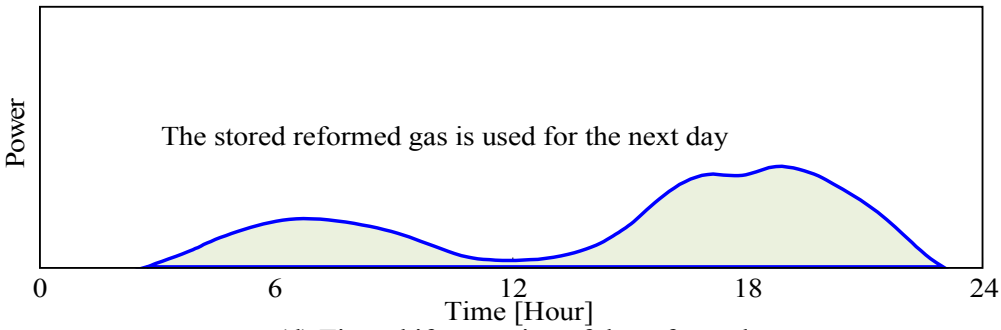

(d) Time shift operation of the reformed gas

Fig. 3-2 Power division rate of the SOFC-PEFC combined system

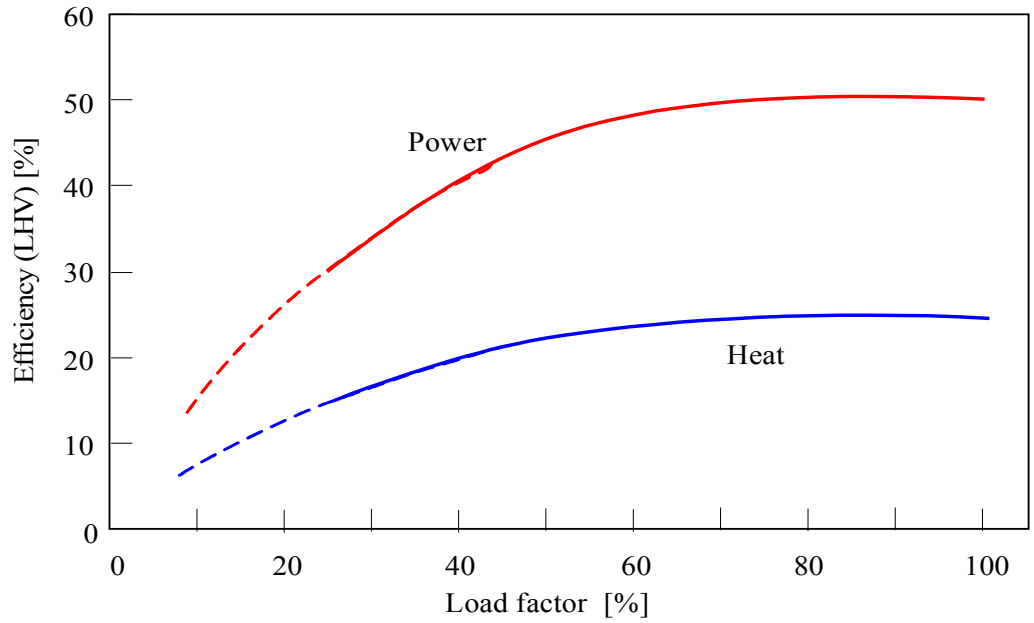

(a) SOFC with internal reforming

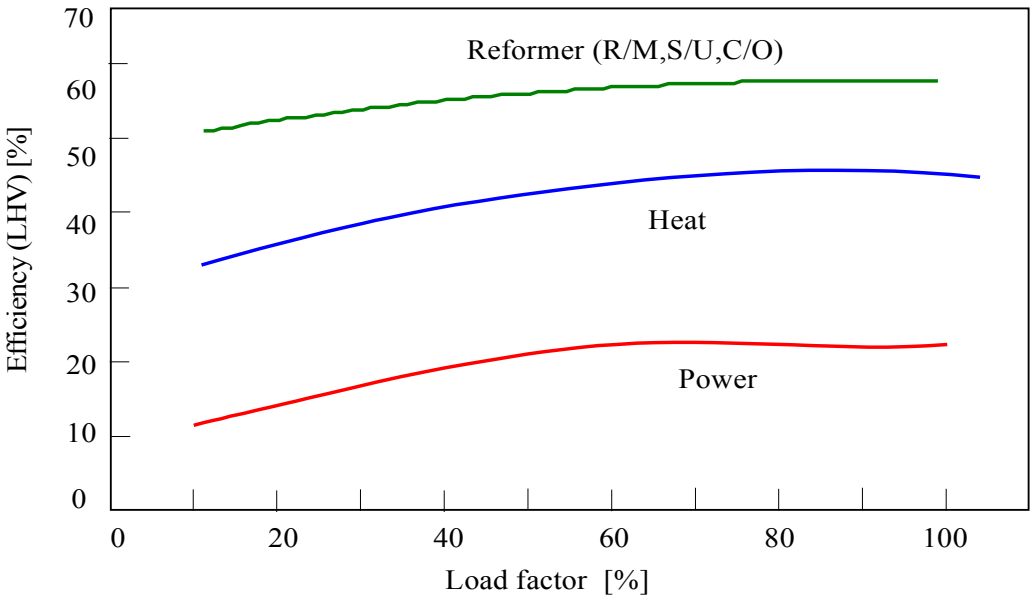

(b) PEFC with steam reformer

Fig. 3-3 Power generation efficiency of SOFC and PEFC, and reformer efficiency

3.4 Operation Plan of the Proposal PV and the SOFC-PEFC Combined System

Figure 3-4 shows the power operation method of the proposal system for three days (Day_n , Day_{n+1} and Day_{n+2}). The predicted output power from the photovoltaic system and the power demand are shown in Fig. 3-4 (a) are calculated as described before in chapter 2 section. The photovoltaic output power are predicated by using equations from (2-1) to (2-5). In this study, the maxmium efficiency and the photovoltaic temperature coefficient are 16.4% and 0.4%/K, respectively. These values are general facility values used in Japa. The solar panel is stalled with a slope of 30- degree facing south.

In Fig. 3-4(a), the operation plan of the SOFC and PEFC are shown. Moreover, the base load of the SOFC is shown and the operation of PEFC corresponds to the fluctuation load. If the SOFC is made to correspond to the base load operation, exhaust heat will be outtputted. The steam reformer of natural gas is operated using this exhaust heat and the reformed gas is produced. Figure 3-4 (b) shows the amount of production of reformed gas each day. After storing this reformed gas, it is supplied to the PEFC to use in the next day. Figure 3-4 (c) shows the operation of the PEFC using the reformed gas produced on the previous day.

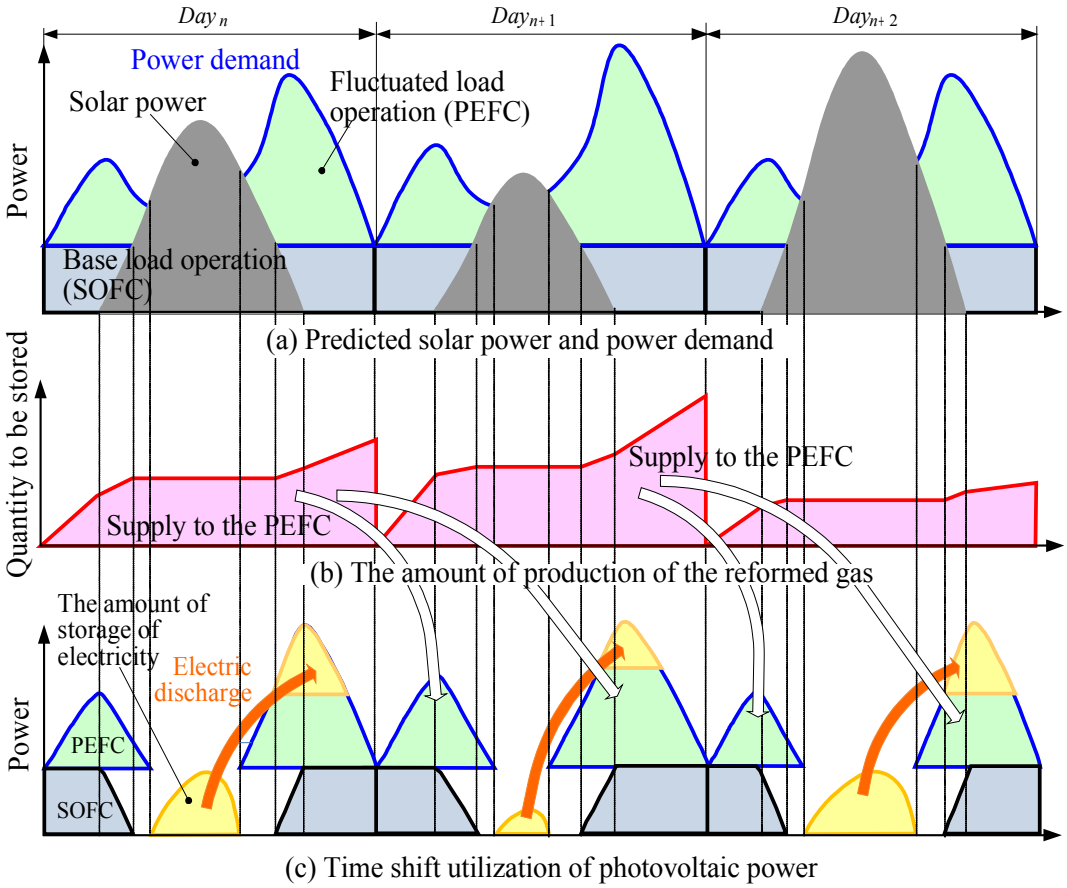

Fig. 3-4 Power operation method of the proposal microgrid

3.5 Energy Demand Pattern

Power and heat are supplied to a micro-grid of 30 residences in Sapporo in Japan from the photovoltaic system and the SOFC-PEFC combined system and no external source is used. Figures 3-5 (a) and (b) are the compressed model of the width of daily power load fluctuations (compressed load pattern) and the extended model of the width of daily load fluctuations (extended load pattern), respectively. These patterns compress and extend fluctuations of the average load of power demand on a representative day to 50% and 150%, respectively. Here the load integration value (the amount of power demand on the representative day) of both patterns is the same as the total power demand under an average load. As a result, this paper investigates the electricity demand model of the micro-grid of the three patterns, as shown in Fig. 3-6. This figure is an example of a representative day in February of 30 residences in Sapporo [100]. The electricity demand includes appliances and electric lighting. The thermal demand comes from heating, hot water supply and baths. There is no cooling load in the summer so the power load pattern on a representative day of every month does not vary significantly throughout the year. On the other hand, the magnitude of demand heat varies greatly between the summer season and the winter season. In the SOFC-PEFC combined system, the production quantity of reformed gas depends on the operation method of the SOFC, so the electric power demand pattern of the micro-grid affects the operation plan of

the proposal system. In the analysis, three load patterns, the average load pattern, the extended load pattern and the compressed load pattern, are investigated.

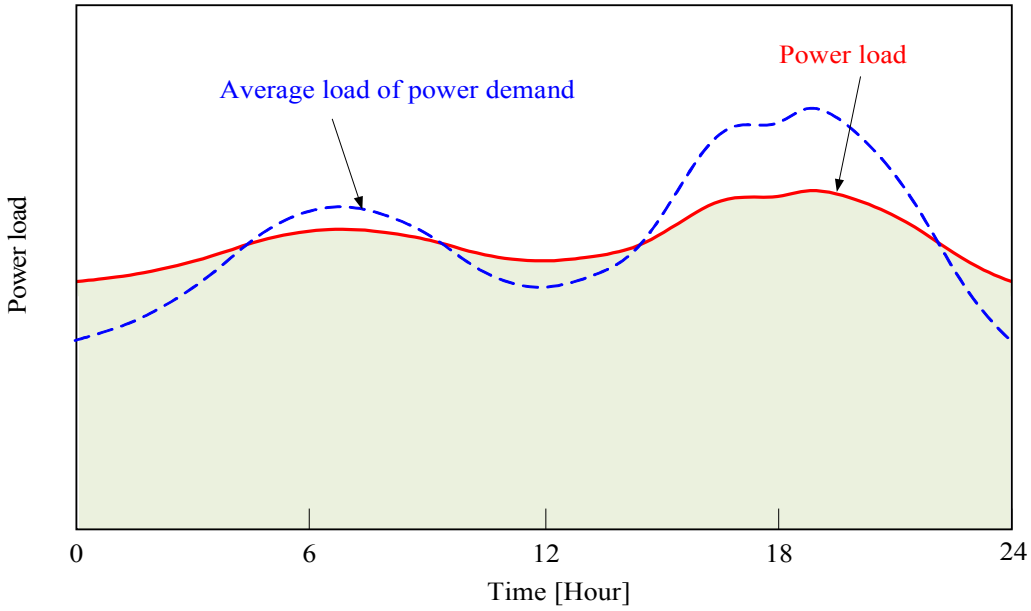

(a) Compressed load pattern

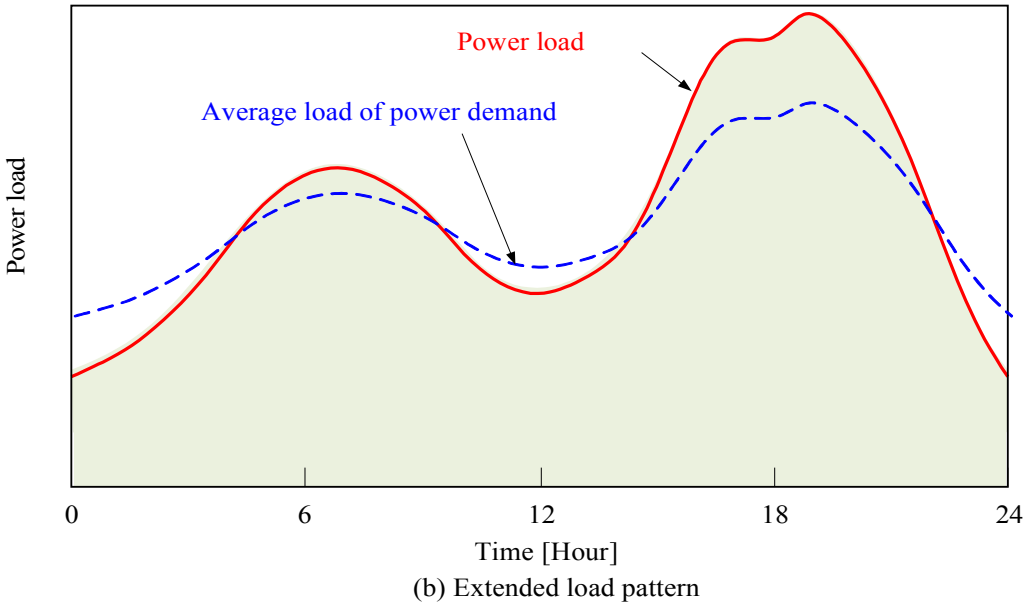

(b) Extended load pattern

Fig. 3-5 Power demand model of the microgrid

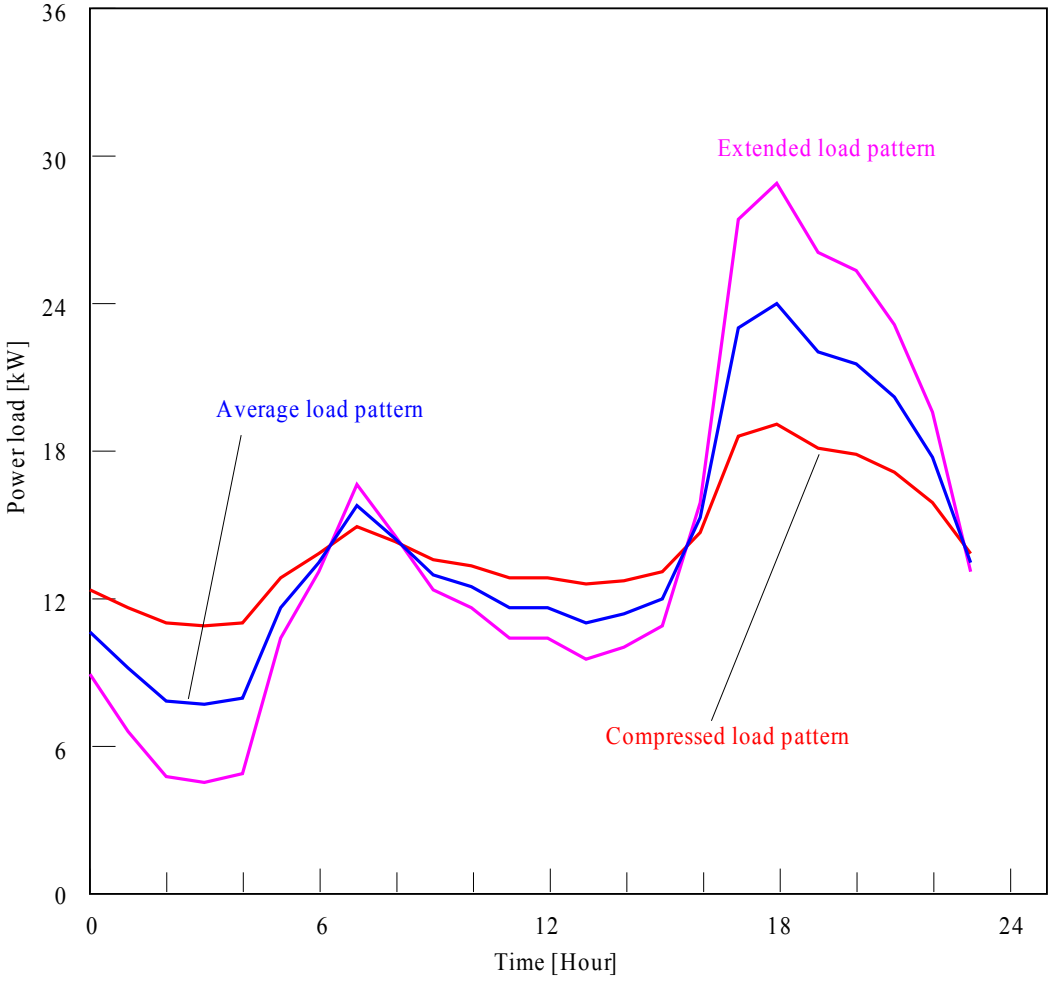

Fig. 3-6 Power demand pattern of the micro -grid (Sapporo in Japan, 30 houses, February representative day)

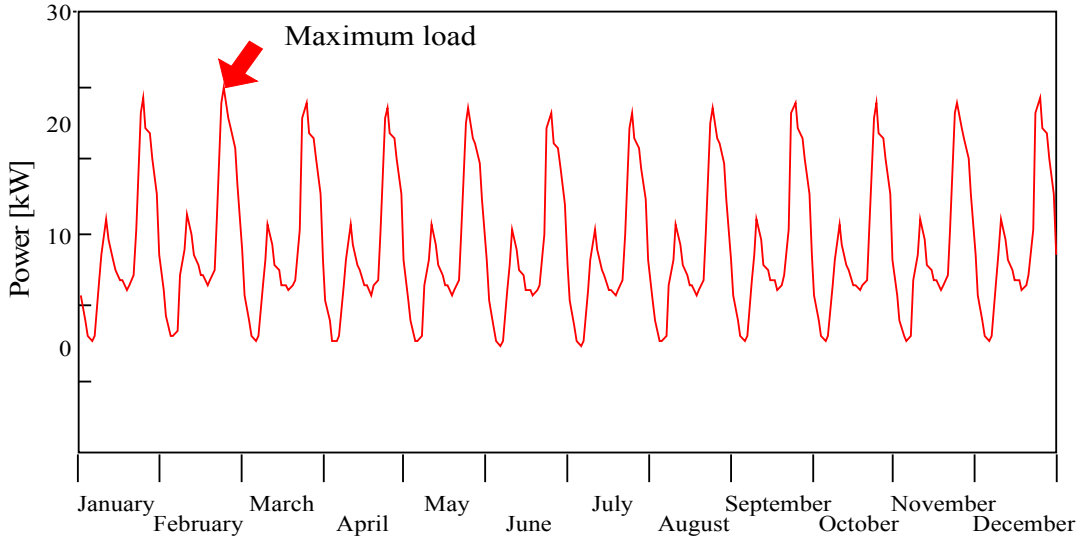

(a) Power demand model of a representative day

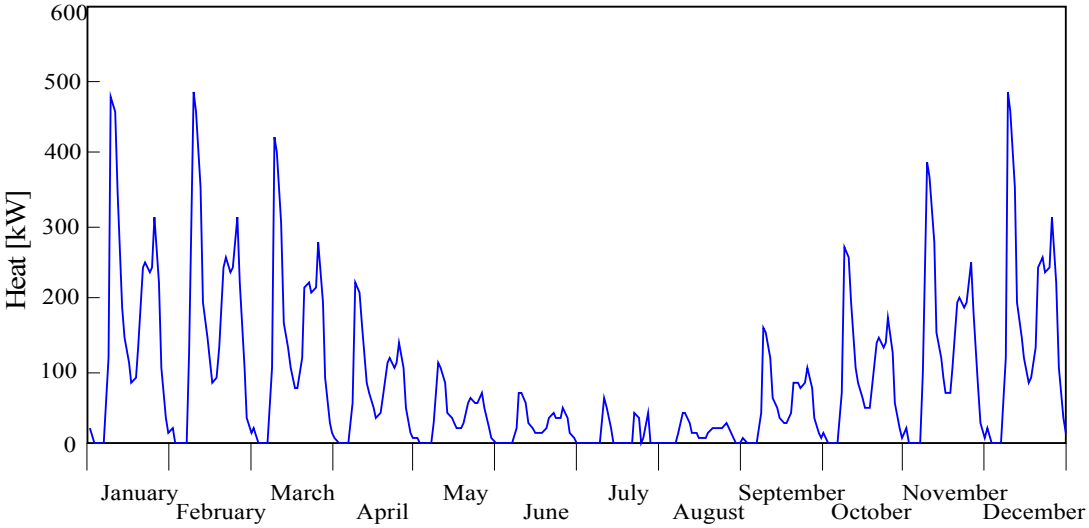

(b) Heat demand model of a representative day

Fig. 3-7 Energy demand pattern of the microgrid. Sapporo-city in Japan, 30 houses.

3.6 Analysis Procedure

The analysis procedure of the SOFC-PEFC combined system is described as follows:

(1) The power load pattern shown in Fig. 3-6 and the predictive values of and the production of electricity of the photovoltaic power in Fig. 3-4 (a) are obtained for every sampling time. The production of the electricity of the photovoltaic power is predicted using the NWI as described before in Chapter 2, Section 2.2.3. As described before, the amount of solar radiation and the outside air temperature for every sampling time can be obtained by the NWI. In addition, when the installation angles of the solar cell is introduced to Eqs. (2-1) to (2-5), the output of photovoltaic power can be indicated. In this analysis method of the power load estimation and output prediction of photovoltaic power should be considered separately.

(2) The operation of the SOFC is according to the base load and the value of the base load is shown in Fig. 3-2(a). The boundary value (i.e., capacity of the SOFC) between the base load and the load following is decided using the power demand pattern obtained by (1). This boundary value is decided using the power demand pattern of a representative day with the highest peak of the power load. In this study, the extended power load pattern of a representative day in February is used.

(3) The amount of power demand and the production of electricity from

photovoltaic power generation are compared for each sampling time. When there is a greater amount of photovoltaic power than power demand, the surplus power is charged to a battery. On the other hand, the storage power is discharged during the load peak in the evening.

(4) The SOFC operates as shown in Figs. 3-2 (a) to (c). On the other hand, the operation of the PEFC for the next day is planned by using the reformed gas. The PEFC is made to correspond to the fluctuation load operation shown in Fig. 3-2(a). The reformed gas produced by the exhaust heat of the SOFC on the previous day is used for the PEFC operation.

(5) The amount of exhaust heat of the SOFC is obtained from Fig. 3-3 (a) for every sampling time. The amount of reformed gas (namely, the amount of hydrogen) outputted from the C/O in Fig. 3-1 (b) is obtained from the amount of SOFC exhaust heat using Eqs. (3-1) to (3-7). The reformed gas is stored in a cylinder and is used in the operation of the PEFC the next day. As described in (2), the boundary value between the base load zone and the factual load zone is decided using the power load pattern of a representative day with the highest power load peak. Therefore, a shortage of the storage reformed gas used for the operation of the PEFC the following day is not assumed.

(6) The amount of exhaust heat from the R/M, C/U and PEFC shown in Fig. 3-1 (b) is obtained from the heat balance. This exhaust heat is stored in a heat storage

tank. Heat storage losses are 0.5%/hour supposing a real system. The balance of heat is calculated for every sampling time. When the amounts of heat storage run short of the heat demanded, a boiler with 90% efficiency is operated.

The fuel consumption (which is expressed with the heating value) of the SOFC is calculated in the case of the operation of the proposal system according to (1) to (6), R/M and a boiler. By the operation of the proposed system based on (1) to (6), the fuel consumption of the SOFC, R/M and the boiler is calculated. Figure (3-8) shows a flow chart of the above analysis procedure.

The ratio of the production of power to the maximum production of power is defined as the load factor. Furthermore, the power generation efficiency is the rate of the power supply of the SOFC and PEFC to the heating value of the fuel supplied to the SOFC and R/M.

3.7 Power and heat balance of the proposed system

Equation (3-9) is a power balance equation. $P_{FC,t}$, $P_{pv,t}$ and $P_{bt,t}$ on the left-hand-side in the equation are the fuel cell power, photovoltaic power, and battery power, respectively. The fuel cell output power depends on the system operation, it is the SOFC output power , PEFC output power, and output power of SOFC-PEFC combined system in case of SOFC independent operation, PEFC independent operation and a SOFC-PEFC combined system respectively. $P_{need,t}$, $P_{btc,t}$, and $P_{loss,t}$ on

the right-hand-side in the equation represent power demand, the amount of battery charge, and loss of power, respectively. Charge-and-discharge loss of a battery is included in the power loss $P_{loss,t}$.

$$P_{FC,t} + P_{pv,t} + P_{bt,t} = P_{need,t} + P_{btc,t} + P_{loss,t} \tag{3-9}$$

The heat balance is calculated by using Eq. (3-10). $H_{FC,t}$ on the left-hand-side in the equation is the exhaust heat output from the SOFC-PEFC combined system (exhaust heat from R/M, C/U and PEFC), in addition $H_{bl,t}$ and $H_{st,t}$ are the heat from the boiler, and a heat storage tank, respectively. $H_{need,t}$, $H_{sts,t}$ and $H_{loss,t}$ on the right-hand-side of the equation are heat demand, the amount of heat storage, and the heat loss, respectively. Heat storage loss is included in the heat loss $H_{loss,t}$ on the right-hand-side of the equation.

$$H_{FC,t} + H_{bl,t} + H_{st,t} = H_{need,t} + H_{sts,t} + H_{loss,t} \tag{3-10}$$

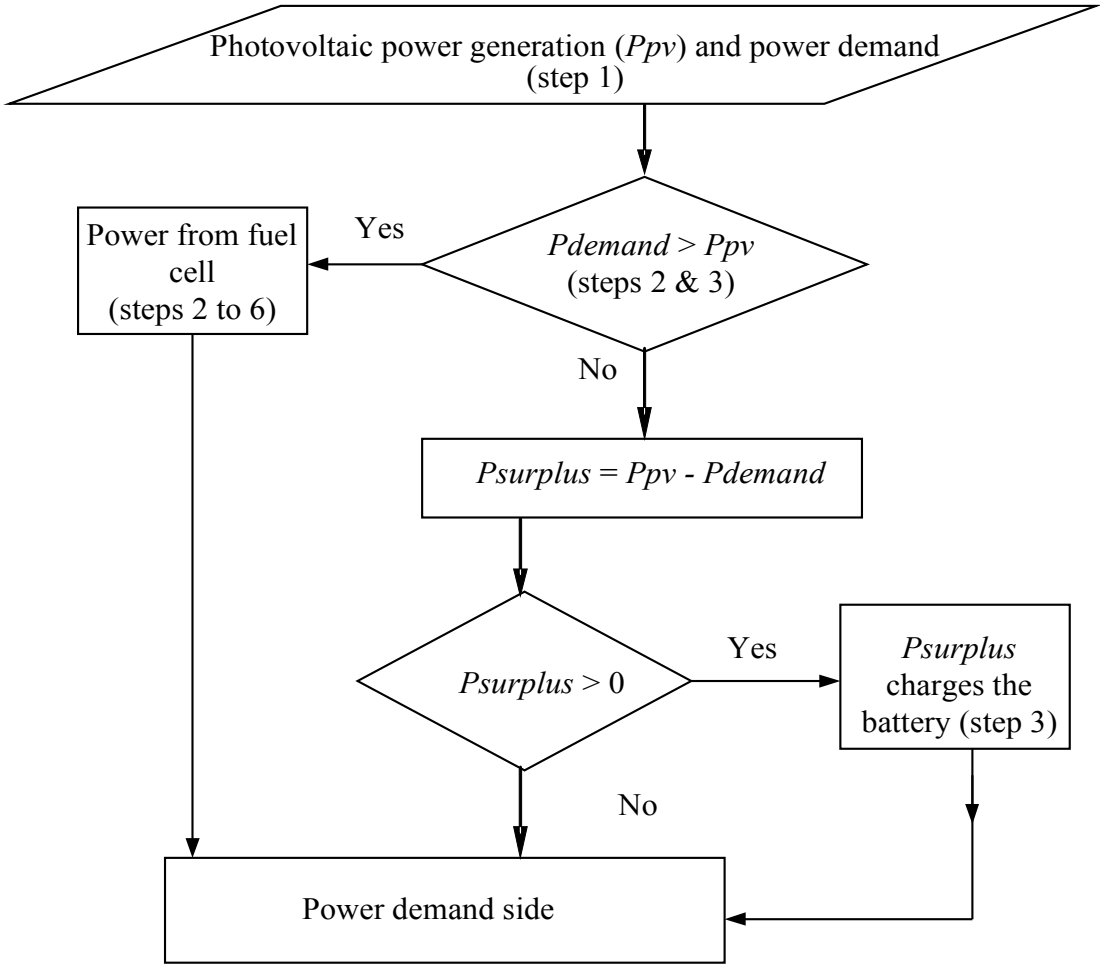

Fig. 3-8 Flow chart of the proposal system operation

3.8 Results and Discussion of the Proposed System

The maximum electrical load of the micro-grid shown in Fig. 3-7(a) appears in February. Therefore, the capacity of the SOFC or PEFC should be optimized with the extended load pattern in a representative day in February. As a result, considering the maximum power load in a representative day in February, the capacity (30 kW) is decided for the operation analysis with the independent operation of the SOFC and PEFC. In the SOFC-PEFC combined system, the total capacity of the SOFC and PEFC is 30 kW. In addition, the capacities of the SOFC and PEFC are 25.5 kW and 4.5 kW respectively.

Figure 3-9 shows the load factor of the SOFC and PEFC at different load patterns (average, compressed and extended load patterns) and at 0% (without solar power), 50% and 100% output solar power. The amount of photovoltaic power generated is calculated using the NWI and Eq. (2-1) to (2-5) as described before in Chapter 2. In this analysis, the average value in Sapporo in 1990 to 2003 is used as the NWI. The production of photovoltaic power at this time is set to 100%. In consideration of a cloudy sky etc., the case of solar power at 50% and 0% (without solar power) is also analyzed. In the analysis of this thesis, 30 kW photovoltaic power generation (145 W/m^2, efficiency of the power generation is 14%) is introduced. The load factor of each fuel cell in daytime falls by this photovoltaic power generation as shown in Fig. 3-8.

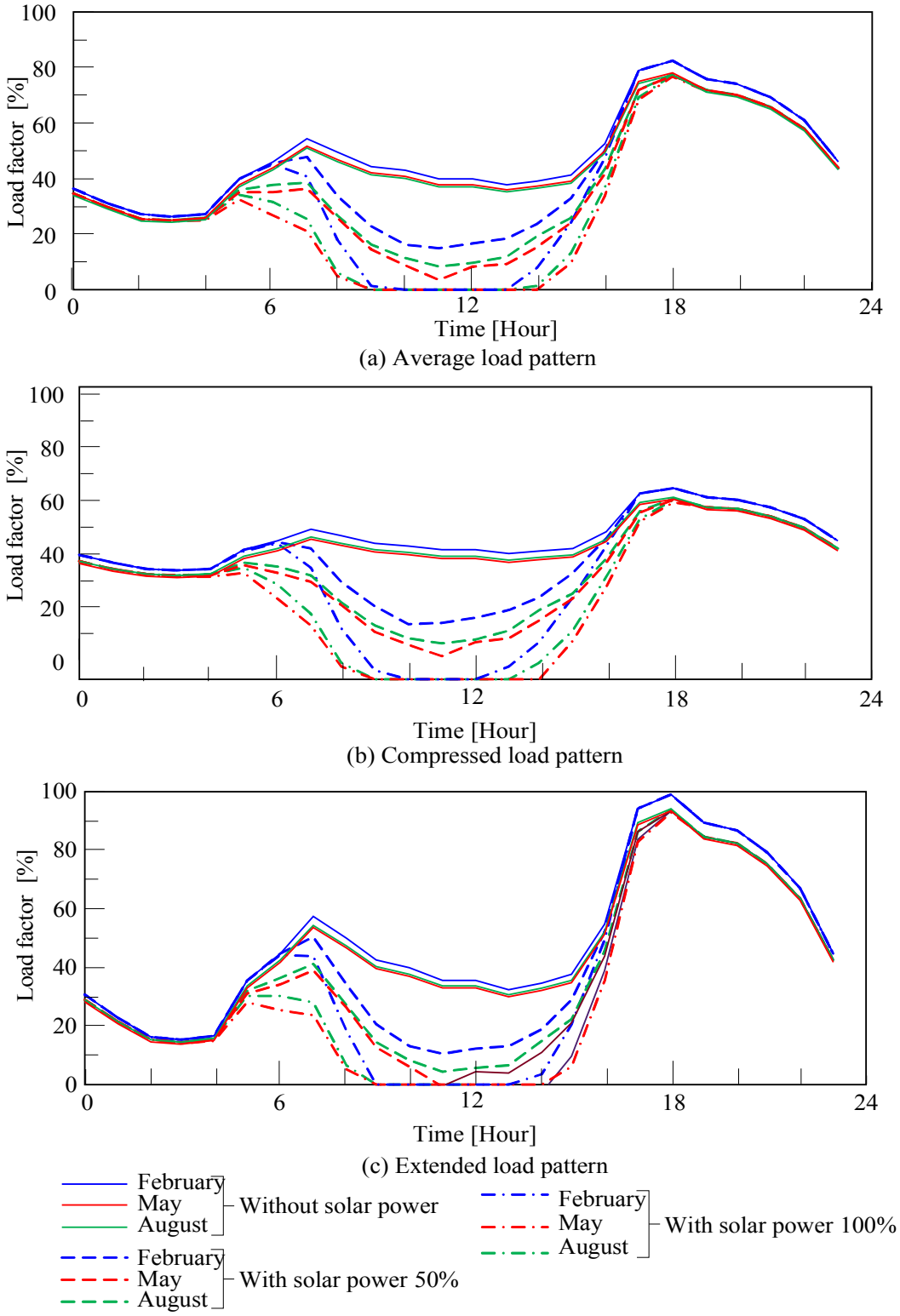

Fig. 3- 9 Load factor of the SOFC and PEFF without storage of electricity

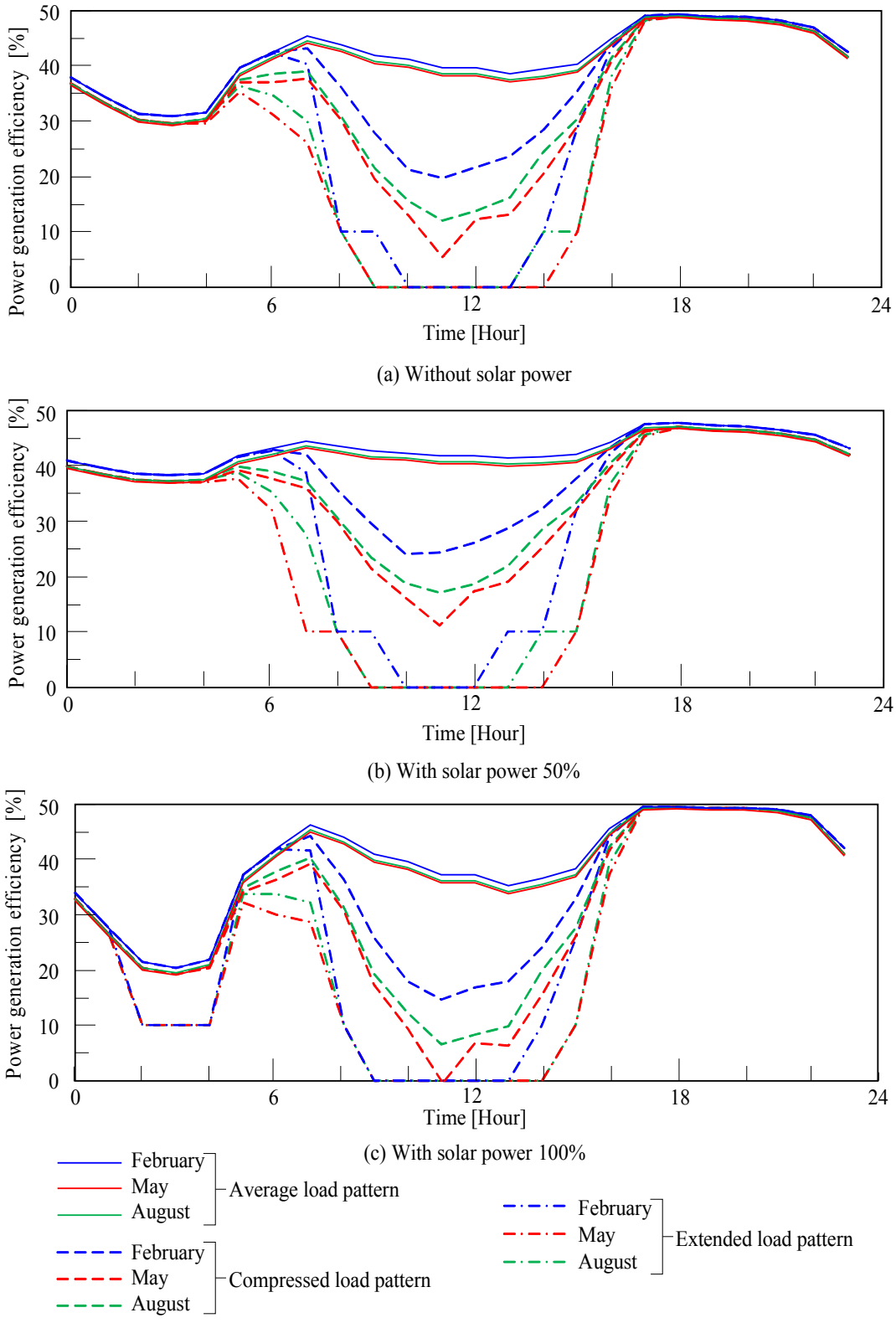

Fig. 3-10 Power generation efficiency of the SOFC

The operation plan of only the SOFC to supply the demand side is shown in Figs. 3-10 to 3-12. Moreover, the operation plan of only the PEFC to supply the demand side is shown in Figs. 3-13 to 3-15. As shown in Figs. 3-10 and 3-13, the power generation efficiency of the SOFC independent operation is large compared with the PEFC independent operation. When the amount of photovoltaic power generated increases, the load of the fuel cell falls. As a result, the power generation efficiency of the fuel cell falls. The analysis results for the fuel consumption of the SOFC and PEFC are shown in Figs. 3-11 and 3-14. When the amount of photovoltaic power generated is large, the fuel consumption of the fuel cell increases because the partial-load operation with low fuel cell efficiency occurs. On the other hand, because the amount of solar radiation fluctuates greatly, the amount of photovoltaic power generated changes. Therefore, as shown in Figs. 3-11 and 3-14, the fuel consumption of the fuel cell in the daytime has sharp changes.

Figures 3-12 and 3-15 show the analysis results of the boiler operation of the SOFC and PEFC independent systems, respectively. Because the heat load is very large compared with the power load, the difference between the SOFC independent system and the PEFC independent system is small.

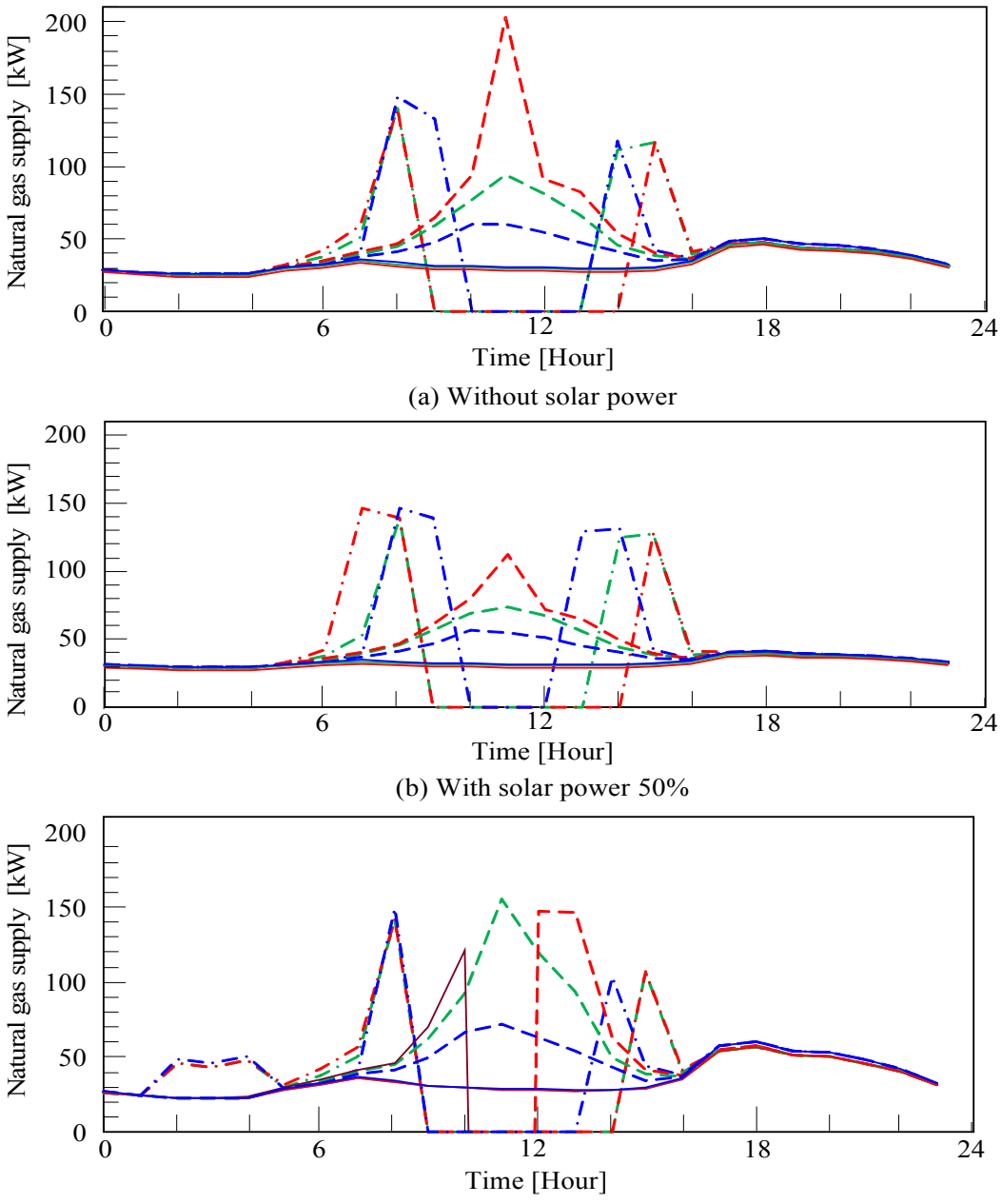

Fig. 3-11 Natural gas supply of the SOFC

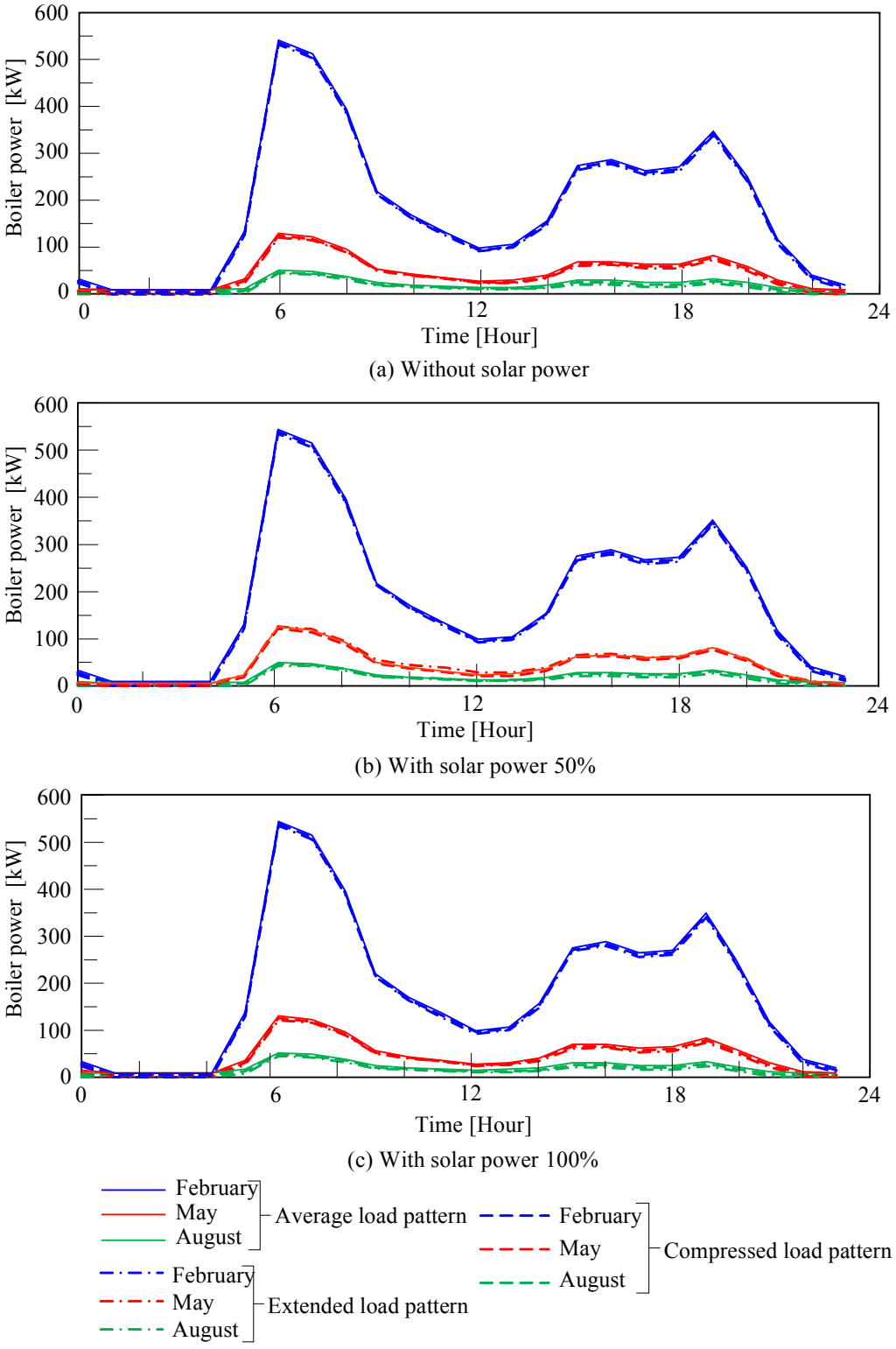

Fig. 3-12 Boiler power supply of the SOFC

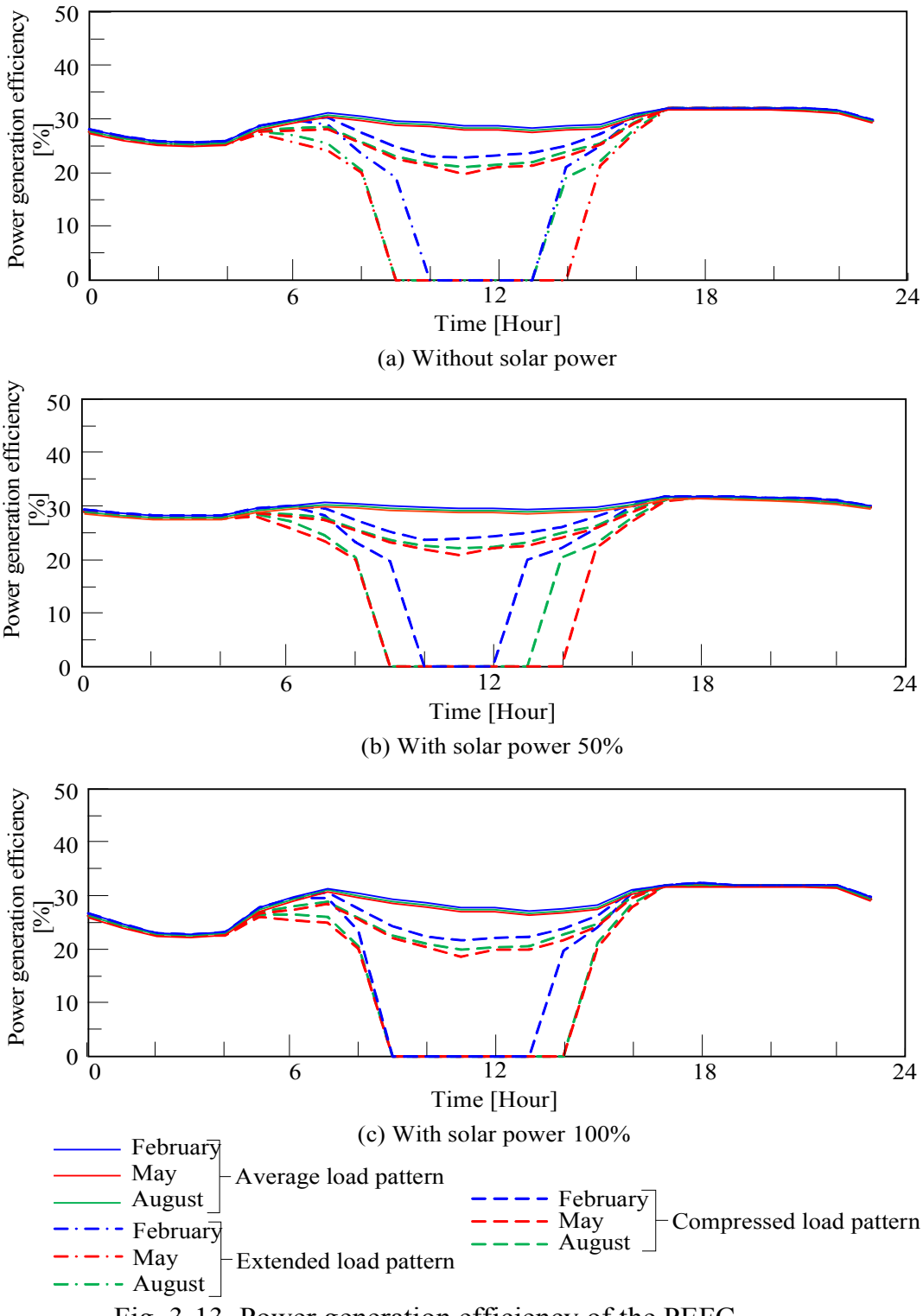

Fig. 3-13 Power generation efficiency of the PEFC

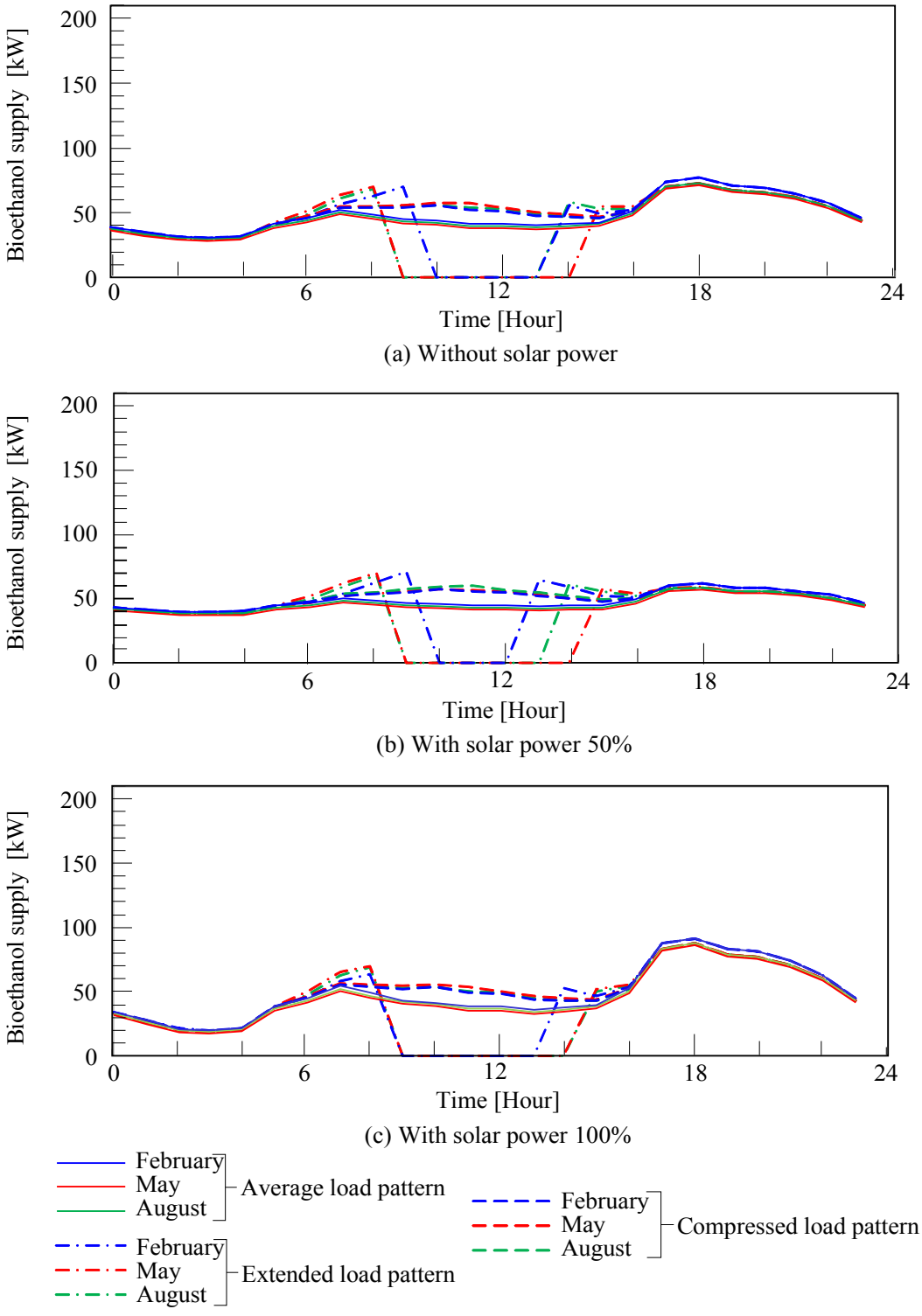

Fig. 3-14 Bioethanol fuel supply of the PEFC

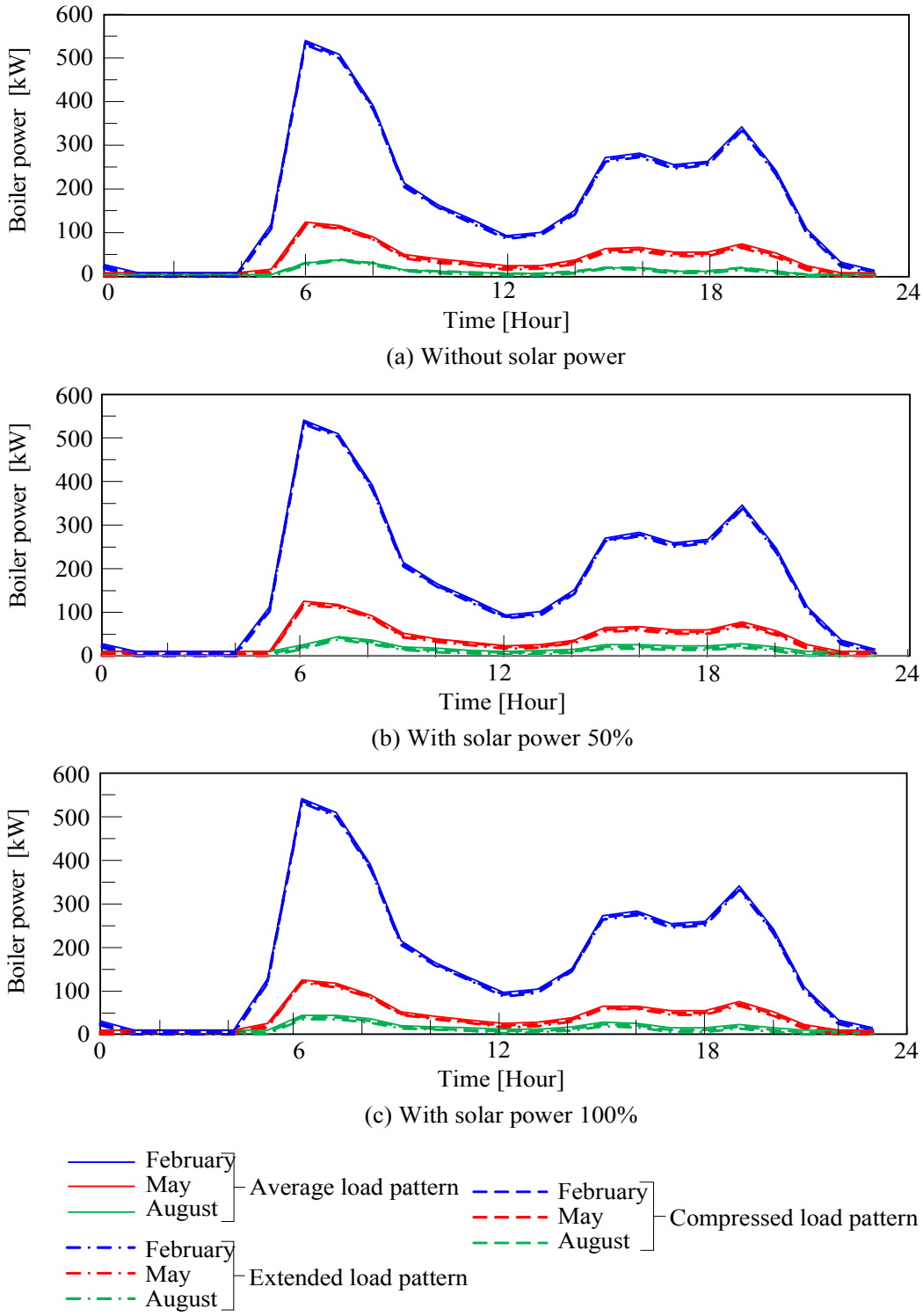

Fig. 3-15 Boiler power supply of the PEFC

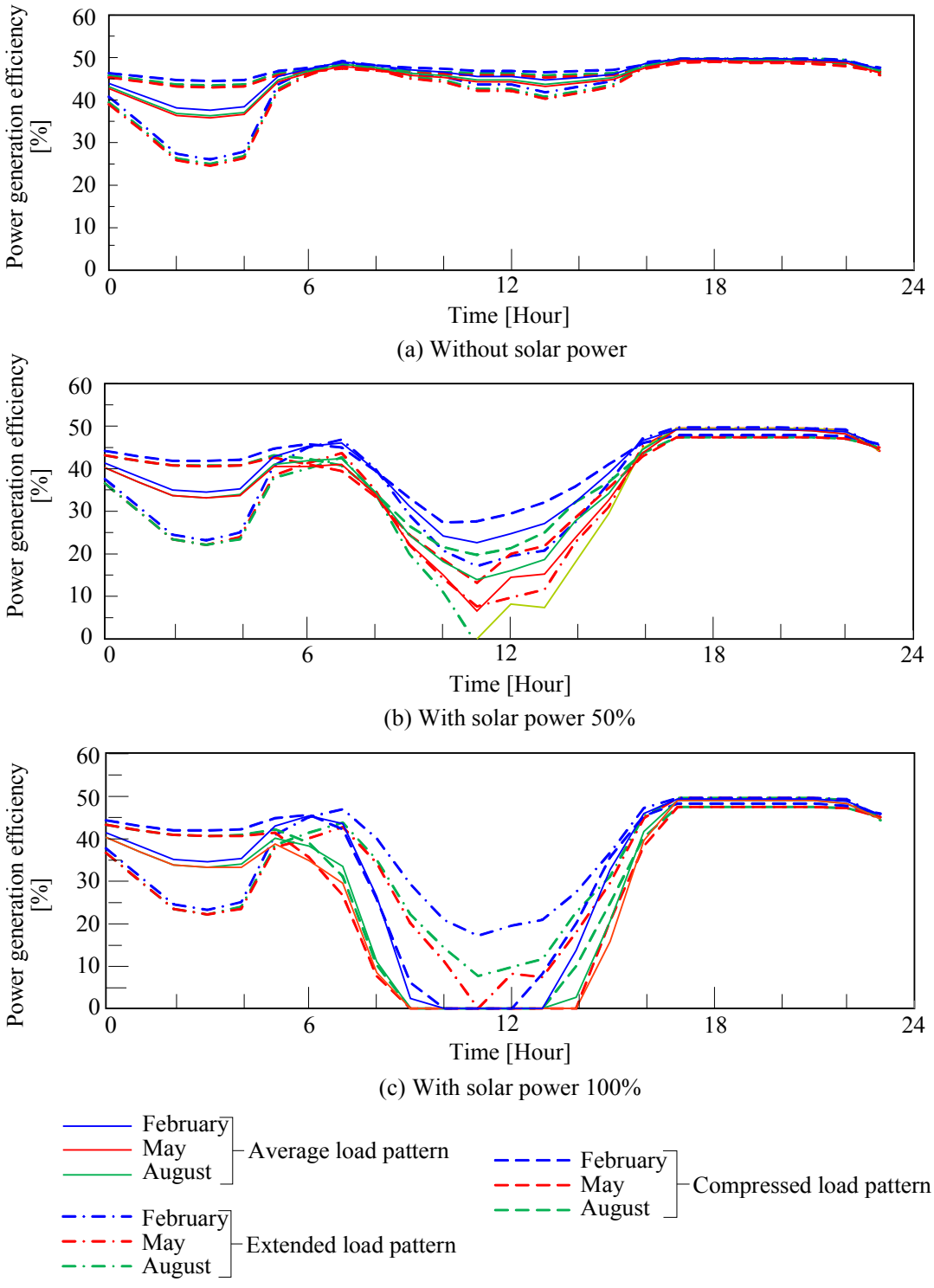

Fig. 3-16 Power generation efficiency of the SOFC-PEFC combined system

The operation plan of the SOFC-PEFC combined system is shown in Figs. 3-16 to 3-19. Figure 3-16 shows the analysis results of the power generation efficiency of the proposed system. When photovoltaic power generation is not introduced (Fig. 3-16 (a)), the change in the power generation efficiency is small. However, the load factor of the system falls when the amount of photovoltaic power generated increases. Therefore, the proposed system differs in performance according to the season and the weather. Figures 3-17 and 3-18 show the analysis results for the consumption of the bio-ethanol supplied to the reformer (R/M) and the natural gas supplied to the SOFC, respectively. From the consumption of natural gas shown in Fig. 3-18, the power load peak at 16:00 to 22:00 shown in Fig. 3-7 (a) is leveled by the operation of the SOFC. On the other hand, if the amount of photovoltaic power generated increases, the amount of daily bio-ethanol supplied to the reformer (R/M) will increase, as shown in Fig. 3-17. Because the load factor of the SOFC will fall if the power supply from photovoltaic power generation increases, the power generation efficiency falls. Therefore, because the amount of exhaust heat from the SOFC increases, the amount of bio-ethanol supplied to the reformer increases. Figure 3-18 shows the analysis results of the boiler operation. These results are the same as the results of Figs. 3-12 and 3-15. Because the heat load (Fig. 3-7 (b)) used in this analysis is large compared with the system exhaust heat (reformer (R/M), the condenser unit (C/U) and the PEFC in Fig. 3-1 (b)), the difference in the boiler

operation between each system is small. Figure 3-20 shows the analysis results for the fuel consumption in each system of a representative day every month. In the SOFC, the PEFC and the SOFC-PEFC combined system, natural gas, bio-ethanol, natural gas and bio-ethanol are consumed. Figure 3-20 (a) shows the results, not including boiler fuel. On the other hand, Fig. 3-20 (b) shows the results including boiler fuel. In Fig. 3-20 (a), the fuel consumption of the SOFC-PEFC combined system is reduced 10 to 35% compared with the SOFC or PEFC independent system. If boiler fuel is added to the fuel consumption of the fuel cell, as shown in Fig. 3-20 (b), the fuel consumption in May and August will decrease greatly. Because the heat load of the winter season in a cold, snowy area is very large compared with the power load, there are few reduction effects of the fuel consumption of the proposed system with boiler fuel. On the other hand, because there is little heat load in mid-term and the summer season, the effect of the fuel reduction of the proposed system is large. Figure 3-21 shows the daily mean power generation efficiency of the SOFC-PEFC combined system. The power generation efficiency considering all load patterns of the proposed system is 27% to 48%. Although the power generation efficiency changes according to the season and load pattern, the photovoltaic power influences the system efficiency most strongly. When introducing photovoltaic power into an independent micro-grid, the improvement of the efficiency decrease due to the partial-load operation of the fuel cells is important.

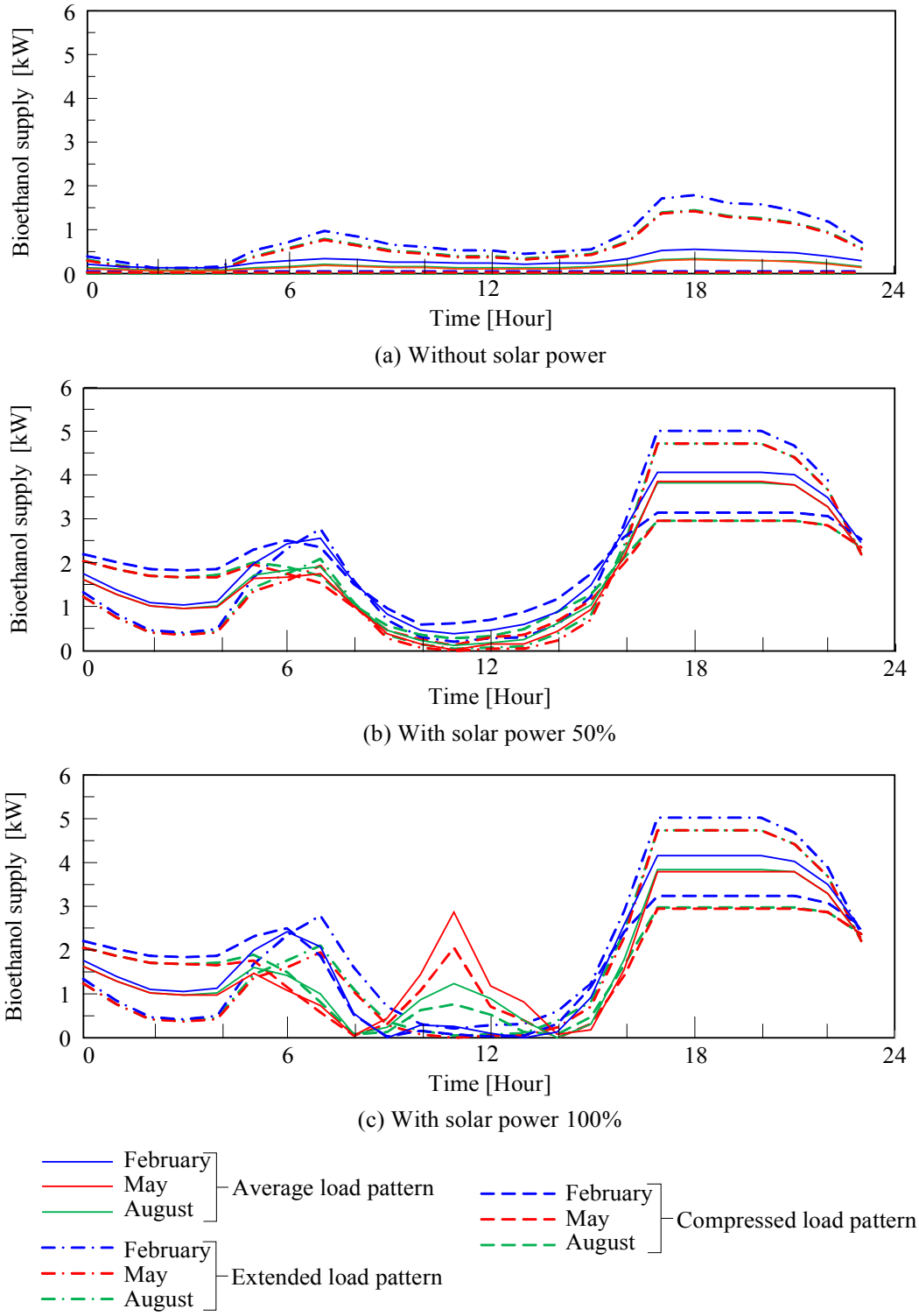

Fig. 3-17 Bio-ethanol supply of the SOFC-PEFC combined system

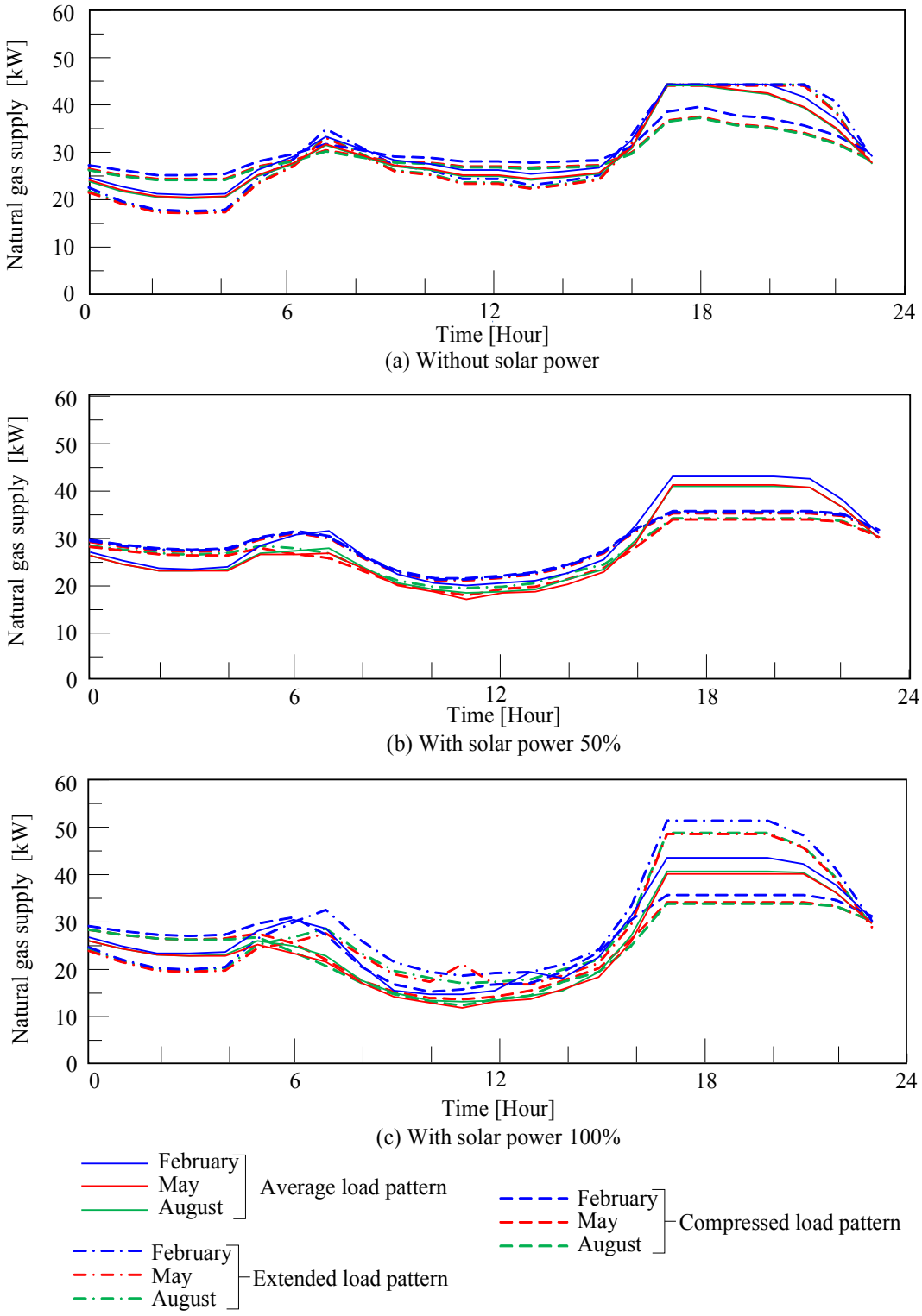

Fig. 3-18 Natural gas supply of the SOFC-PEFC combined system

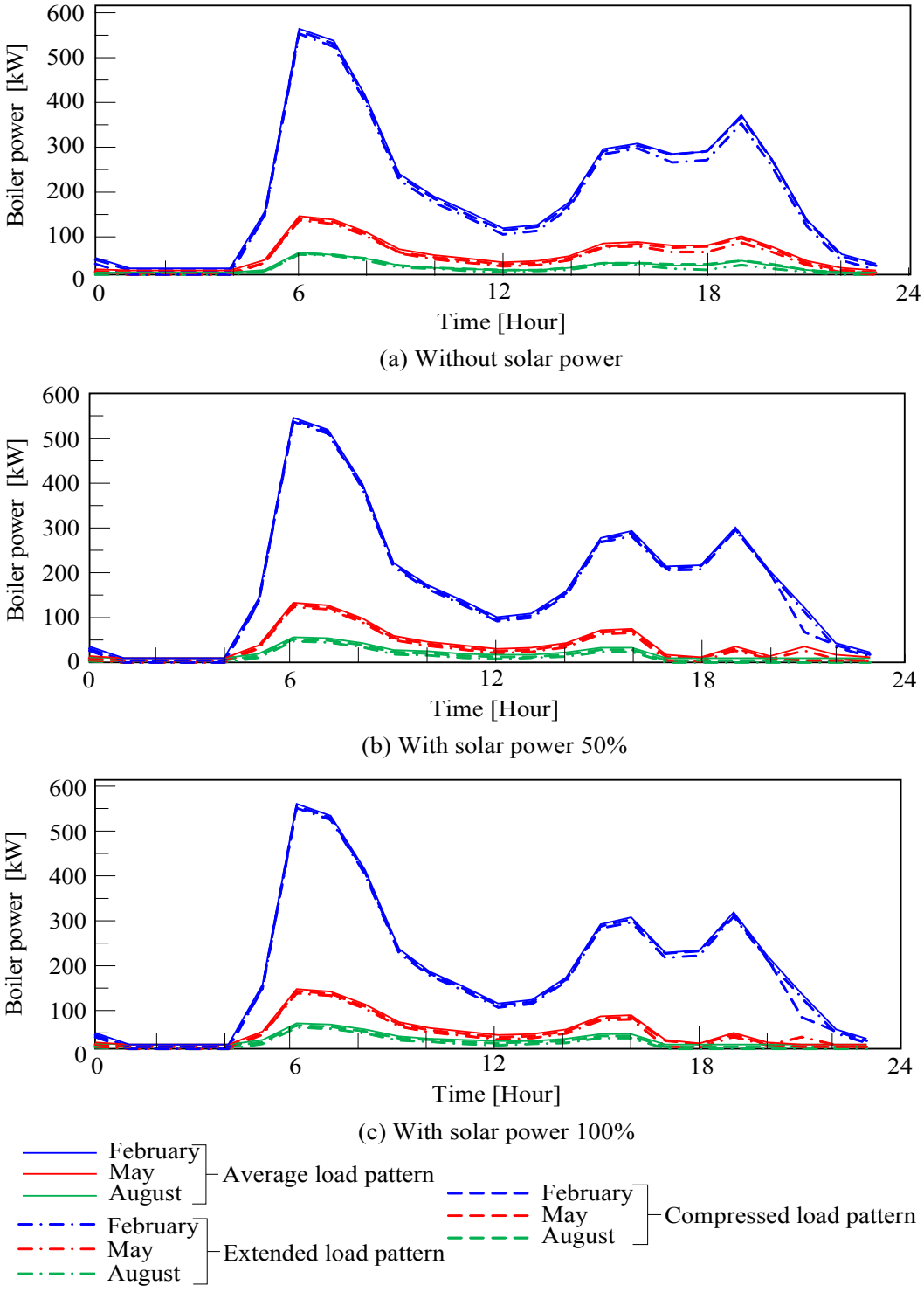

Fig. 3-19 Boiler power supply of the SOFC-PEFC combined system

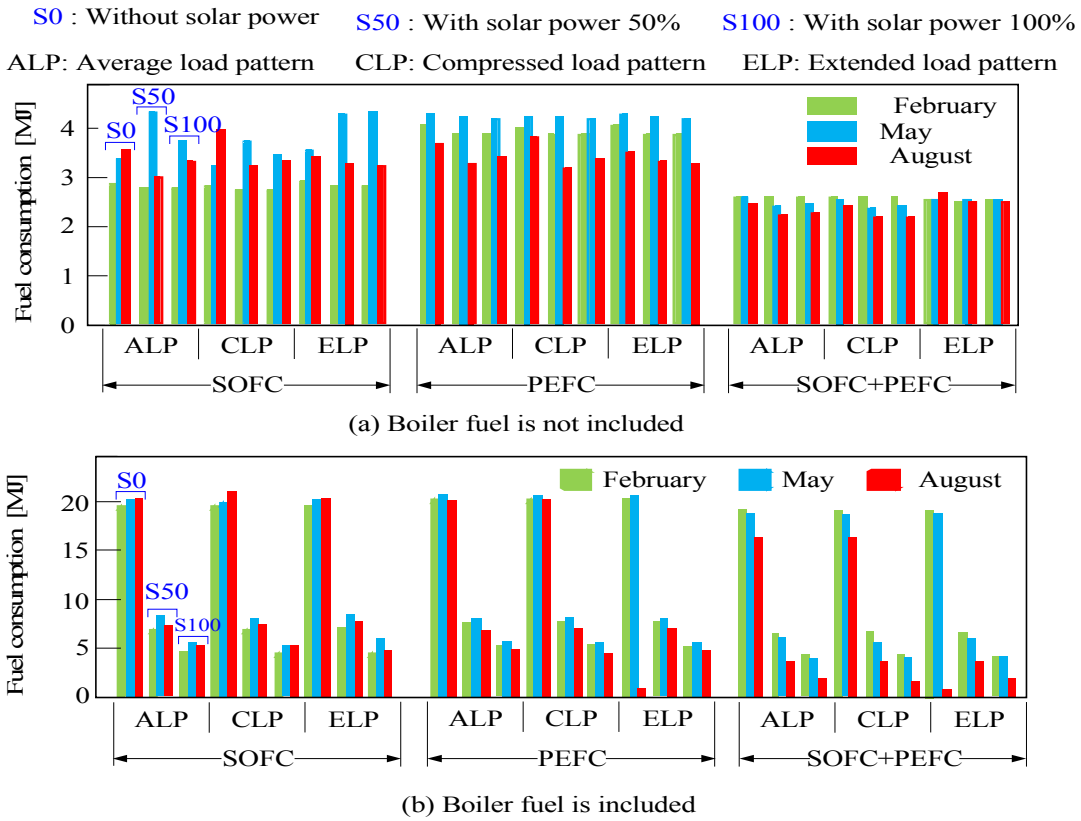

Fig. 3-20 Analysis result of the fuel consumption of a representative day

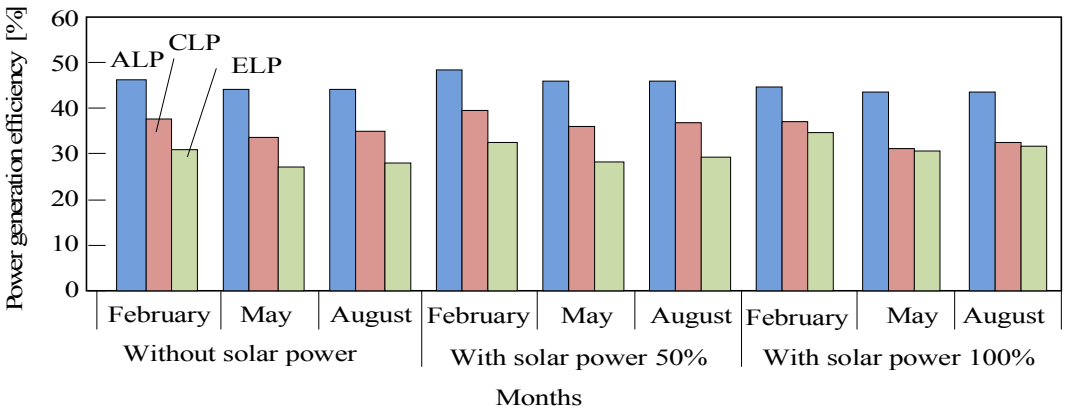

Fig. 3-21 Total power generation efficiency on a representative day of the SOFC-PEFC combined system

4 Conclusion and Future Works

In this thesis, a NN prediction algorithm for photovoltaic power generation is developed. A study on operation optimization of a combined energy system with a photovoltaic power generation is illustrated. Optimizing the operation planning of a photovoltaic system with a diesel engine generator or a SOFC-PEFC combined system is clarified.

In this chapter, the main conclusion obtained from the work carried out in this study will be summarized. Furthermore, the suggestion for the future work will be mentioned.

4.1 Conclusion

Depending on the analysis operation of the photovoltaic system and the diesel engine generator combined system, the following conclusions are reported:

(1) A prediction algorithm using NN for electricity production from a photovoltaic system is developed. When comparing the results of the actual photovoltaic output power with the power production from the NN algorithm, the average values for the prediction error of electricity production from the solar cell are 25%, 29%, 19% and 26% for December, March, June and September, respectively.

(2)The operating period of the engine generator is shortened by introducing the NN

prediction algorithm for the power and heat supplied to the demand side. The engine operating time is reduced by 12.5% in December and 16.7% for March and September. The diesel engine heat characteristics are described, and a back-up boiler operation plan is developed.

Moreover, depending on the analysis operation of the photovoltaic system and a SOFC-PEFC combined system, the following conclusions are obtained:

(1) When photovoltaic generation is not introduced into the SOFC-PEFC combined system, the change in the power generation efficiency is small. However, the load factor of the proposal system falls when the amount of photovoltaic power increases.

(2) On the other hand, if the amount of photovoltaic power generated increases, the amount of daily bio-ethanol supplied to the reformer will increase. Because the load factor of the SOFC decreases if the power supply due to photovoltaic power increases, power generation efficiency decreases. Therefore, because the amount of exhaust heat from the SOFC increases, the amount of bio-ethanol supplied to the reformer increases. In other words, the proposed system differs in performance according to the season and the weather.

(3) The fuel consumption of the SOFC-PEFC combined system is reduced 10 to 35% compared with the SOFC or PEFC systems independently. If boiler fuel is added to the fuel consumption of the fuel cell, the fuel consumption in May and August will decrease greatly. Because the heat load of the winter season in a cold, snowy area is very large compared with the power load, there are few reduction effects on the fuel

consumption of the proposed system.

(4) The power generation efficiency considering three load patterns (average load pattern, compressed load pattern and extended load pattern) of the proposed system is 27% to 48%. However, because the heat load is very large compared with the power load, the difference between the SOFC independent system and the PEFC independent system is small.

4.2 Future Works

In this thesis, an independent micro-grid of photovoltaic and diesel engine generator or SOFC-PEFC combined systems are proposed. The suggested operating methods of both systems are mentioned and tested. The results are good, especially in case of the photovoltaic and the diesel engine generator combined system. Furthermore, a good performance of a photovoltaic system and a SOFC-PEFC combined system to supply energy to a micro-grid of 30 residences without any external source. Although the power generation efficiency changes according to the season and load pattern in case of the photovoltaic and the SOFC-PEFC combined system, the photovoltaic power influences the system efficiency most strongly. When introducing photovoltaic power into an independent micro-grid of photovoltaic and SOFC-PEFC combined system, the improvement of the efficiency decrease due to the partial-load operation of the fuel cells is required.

Acknowledgment

It is my honor to be accepted as a Ph.D. student in the power engineering laboratory of Kitami Institute of Technology, Kitami, Japan. All praises and thanks to my Cod (Allah) for guidance me in my life. I am wondering if I can take an opportunity to thank all those who help me during my stay in Japan.

First of all, I am extremely grateful to my advisor, Professor Shin'ya OBARA who supports and helps me, I thanks him too much for helping me in my study. I shall ever remain grateful to him for his co-operation, financial support and amiable demeanor in accomplishing this work. Professor Shin'ya OBARA has kindly reviewed this thesis, provided me with many helpful suggestions and also conducted the review panel. Moreover, I expect to express my sincere thanks to the associated prof. Takao Ueda and the assistant prof. Koichi Nakamura in power engineering laboratory. I wish to express my gratefulness to Egyptian scholarship mission to give me this opportunity to augment my engineering knowledge as well as has given me financial support during my study and stay in Japan.

Lastly, I address my special thanks to my parents, my brothers, my sisters, my daughters (Fagr & Doha) and my husband Dr. Mahmoud Khatiri for their emotional support and abundant love. This doctoral thesis is dedicated to them with love.

References

[1] Varun, Ravi Prakash, and Inder Krishnan Bhat:"Energy, Economics and Environmental Impacts of Renewable Energy Systems", Renewable and Sustainable Energy Reviews, Vol. 13, pp. 2716-2721, (2009).

[2] Annika Skoglund, Mats Leijon, Alf Rehn, Marcus Lindahl and Rafael Waters:"On the Physics of Power, Energy and Economics of Renewable Electric Energy Sources- Part II", Renewable Energy, Vol. 34, pp. 1735–1740, (2010).

[3] A.K. Akella, M.P. Sharma, and R.P. Saini:"Optimum Utilization of Renewable Energy Sources in a Remote Area", Renewable and Sustainable Energy Reviews, Vol. 11, pp. 894-908, (2007).

[4] AK. Akella, RP. Saini, and MP. Sharma:"Social, Economical and Environmental Impacts of Renewable Energy Systems", Renewable Energy, Vol. 34, pp. 390–396, (2009).

[5] F. Trieb, O. Langnib, and H. Klaib:" Solar Electricity Generation-Comparative View of Technologies, Costs and Environmental Impact", Solar Energy, Vol. 59, pp. 89-99, (1997).

[6] C.Kalaitzakis and G.J.Vachtsevanos: "On the Control and Stability of Gird Connected Photovoltaic sources", IEEE Trans. Energy Conversion, EC-2, No. 4, pp. 556-562, (1987).

[7] S.P.S. Badwal, Giddey, P. Bandopadhayay, H.A. Al-Thani, and A. Helal:" Hydrogen Renewable Energy Storage System for Remote Area Power

Generation", 17th World Hydrogen Energy Conference, Brisbane, Australian Institute of Energy and the International Association for Hydrogen Energy, pp. 15-19 (2008).

[8] Shin'ya OBARA and Abeer Galal El-Sayed: "Developments of Residential-Energy Supply System Using a Plant Shoot Solar Cell and Water Electrolyzer", Proceedings of the Sustainable Energy and Environmental Protection (SEEP 2010), PC057, pp.1-11, Bari, Italy, (2010).

[9] Chemmangot, V. Nayer, Mochamad Ashari and W.W.L. Keerthipala:"a Gird – Interactive Photovoltaic Uninterrupted Power Supply System Using Battery Storage and a Back up Diesel generator", IEEE Trans. Energy Conversion, Vol. 15, No. 3, pp. 348-353, (2000).

[10] Y. Sukamongkol, S. Chungpaibulpatana, and W. Ongsakul :"a Simulation Model for Predicting the Performance of a Solar Photovoltaic System with Alternating Current Loads", Renewable Energy, Vol. 27, pp. 237– 258, (2002).

[11] H. Matsuda: "Interconnecting Dispersed Photovoltaic Power Generation Systems with Existing Utility Grid", A Study at ROKKO Inland Test Facility, Japan", Int. Journal of Solar Energy, Vol. 13, pp. 1-10, (1992).

[12] H. Schaefer and G. Hagedorn: "Hidden Energy and Correlated Environmental Characteristics of PV Power Generation", Renewable Energy, Vol. 2, No. 2, pp. 159-166, (1992).

[13] M. Muselli, G. Notton and A. Louche: "Design of Hybrid-Photovoltaic Power Generator with Optimization of Energy Management", Solar Energy, Vol. 65, No. 3, pp. 143-157, (1999).

[14] J.W. Hurwitch and C.A. Carpenter: “Technology and Application Options for Future Battery Power Regulation”, IEEE Transactions on Energy Conversion, Vol. 6, No. 1, pp. 216-223, March (1991).

[15] Th.F. El-Shatter, M.N. Eskandar, and M.T. El-Hagry:”Hybrid PV/Fuel Cell System Design and Simulation”, Renewable Energy, Vol. 27, NO. 3, pp. 479–485, (2002).

[16] D. Kottick, M. Blau and D. Edelstein: “Battery Energy Storage for Frequency Regulation in an Island Power System”, IEEE Transactions on Energy Conversion, Vol. 8, No. 3, pp. 455-458, September (1993).

[17] H.J. Kunisch, K.G. Kramer and H. Dominik: “Battery Energy Storage: Another Option for Load-Frequency-Control and Instantaneous Reserve”, IEEE Transactions on Energy Conversion, Vol. EC-1, No. 3, pp. 41-46, September (1986) .

[18] M. Ashari and C.V. Nayar: “An optimum Dispatch Strategy using Set Points for a Photovoltaic (PV)-Diesel-Battery Hybrid Power System”, Solar Energy, Vol. 66, No. 1, pp. 1-9, (1999).

[19] B.S. Richards, D.P.S. Cap~ao, A.I. Schafer :” the effect of Energy Fluctuations on Performance of a Photovoltaic Hybrid Membrane System”, Environmental Science & Technology, Vol. 42, pp. 4563-4569, (2008) .

[20] A.I. Schafer, A. Broeckmann, B.S. Richards :” Development and Characterization of a Photovoltaic Hybrid Membrane System”, Environmental Science & Technology, Vol. 41, pp. 998-1003, (2007).

[21] Y. Ismail, Y. Kemmoku, H. Takikawa, and T. Sakakibara: “An Operating

Method for Fuel Saving in a Stand-Alone Wing/Diesel/Battery System", Journal of Japan Solar Energy Society , Vol. 28, No. 2, pp. 31-38, (2002).

[22] Shigehiro Yamamoto, Kazuyoshi Sumi, Eiichi Nishikawa and Takeshi Hashimoto: " An Operating Method Using Prediction of Photovoltaic Power for a Photovoltaic-Diesel Hybrid Power Generation System", Transactions of the Institute of Electrical Engineering of Japan, B, Power and Energy, Vol. 124, No. 4, pp. 521-530, (2004).

[23] Shin'ya Obara, et al., "Study on Small-Scale Co-generation System for Domestic House Considering Partial Load and Load Fluctuation", Journal of the Japan Society of Mechanical Engineers, Vol. 71, No.704, pp.1169-1176, (2005).

[24] SM. Shaahid, and MA. Elhadidy:"Economic Analysis of Hybrid Photovoltaic - Diesel - Battery Power Systems for Residential Load in hot Regions a Step to Clean Future", Renewable and Sustainable Energy Reviews, Vol. 12, pp. 488-503, (2008).

[25] ES. Hrayshat:"Techno-Economic Analysis of Autonomous Hybrid Photo voltaice – Diesel - Battery System", Energy for Sustainable Development, Vol. 13, pp. 143-150, (2009).

[26] Tsunoda, A. et al.:"Newly-Developed Diesel Engines for Generator Set", Mitsubishi Juko Giho Vol.40 No.4 (2003).

[27] Sakaguchi, K. et al.:"Environmental Friendly Diesel Engine "UEC Eco-Engine"", Mitsubishi Heavy Industries Technical Review, Vol. 41, No.1, (2004).

[28] R. Benelmir R, and M. Feidt:" Energy Cogeneration Systems and Energy Management Strategy", Energy Conversion Management, Vol. 39, pp. 1791–

802, (1998).

[29] A. Parlak, H. Yasar, and B. Sahin:" Performance and Exhaust Emission Characteristics of a Lower Compression Ratio LHR Diesel Engine", Energy Conversion Management, Vol. 44, pp. 163–75, (2003).

[30] G. Bidini, U. Desideri, S. Saetta, PP. Bacchini:" Internal Combustion Engine Combined Heat and Power Plants", Case Study of the University of Perugia Power Plant, Appl Thermal Engineering, Vol. 18, pp. 401–12, (1998).

[31] Y. Huangfu, Wu JY, RZ Wang, and ZZ Xiz: " Development of an Experimental Prototype of an Integrated Thermal Management Controller for Internal Combustion Engine-Based Cogeneration Systems", Appl Energy, Vol. 84, No. 12, pp. 1356–73,(2007).

[32] D. Leung D, Y. Lou, and TL. Chan:" Optimization of Exhaust Emissions of a Diesel Engine Fuelled with Biodiesel", Energy Fuels, Vol. 20, pp. 1015–23, (2006).

[33] Mehmet Kanog, Leyman Kazım Isık, Aysegu and Abusog:"Performance Characteristics of a Diesel Engine Power Plant", Energy Conversion Management, Vol. 46, pp. 1692-1792, (2005).

[34] Abeer Galal El-Sayed and Shin'ya OBARA: "Energy Supply Characteristic of the Solar Cell and Diesel Engine Combined System with a Prediction Algorithm of Solar Power Generation", Journal of Power and Energy Systems, JSME, Vol. 4, No. 1, pp. 27-38, (2010).

[35] Shin'ya Obara: "Fuel Reduction Effect of the Solar Cell and Diesel Engine Hybrid System with a Prediction Algorithm of Solar Power Generation", Journal

of Power and Energy Systems, Vol. 2, No. 4, pp. 1166-1177, (2008).

[36] J.D. Mondol, Y.G Yohanis, and B. Norton: " Comparison of Measured and Predicted Long Term Performance of Gird a Connected Photovoltaic System", Energy Conversion & Management, Vol. 48, No. 4, pp.1065-1080, (2007).

[37] I. Yasuda:" Development of Hydrogen Production Technology for Fuel Cell, Energy Synthesis Engineering, Vol. 28, No.2, (2005).

[38] Shin'ya Obara and K. Kudo:" Installation Planning of small Scale Fuel Cell Cogeneration in Consideration of Load Response Characteristics", Transaction Japan Society of Mechanical Engineering Series B, Vol. 71, No. 706, pp. 1678-1685, (2005).

[39] Shin'ya Obara:" Dynamic Characteristics of a PEM Fuel Cell System for Individual Houses", International Journal of Energy Res , Vol. (30), No. 15, pp. 1278-1294, (2006).

[40] K. Sedghisigarchi:" Dynamic and Transient analysis of Power Distribution System with Fuel Cells", Part 1: Fuel -Cell Dynamic Model, IEEE Transaction of Energy Conversions, Vol. 19, No. 2, pp. 432-428. (2004).

[41] G. Gigliucci, L. Petruzzi, E. Cerelli, A. Garzisi, and AL. Mendola:" Demonstration of a Residential CHP system Based on PEM Fuel Cells", Journal of Power Sources , Vol. 62, pp. 131-138, (2004).

[42] A. Kazim:" Economical and Environmental Assessments of Proton Exchange Membrane Fuel Cells in Public Buildings", Energy Conversion Management , Vol. 42, pp. 763–772, (2001).

[43] Vittorio Verda, and Michele Cali Quaglia:"Solid Oxide Fuel Cell Systems for

Distributed Power Generation and Co-generation", International Journal of Hydrogen Energy, Vol. 33, pp. 2087-2096, (2008).

[44] Shin'ya OBARA and Abeer Galal El-Sayed: "Analysis of the Overall Efficiency of a PEFC with a Bio-ethanol-Solar-Reforming System for Individual Houses", Proceedings of the 3rd International Conference on Sustainable Energy and Environmental Protection (SEEP09), Part 2, pp. 325-330, Dublin, Ireland. (2009)

[45] Shin'ya Obara and Abeer Galal El-Sayed: "Compound Micro-grid Installation Operation Planning of PEFC and Photovoltaics with Prediction of Electricity Production using GA and Numerical Weather Information", International Journal of Hydrogen Energy, Vol. 34, No. 19, pp. 8213-8222, (2009).

[46] Shin'ya Obara:" Equipment Arrangement Planning of a Fuel cell Energy Network optimized for Cost Minimization", Renewable Energy, Vol. 32, pp. 382-406,(2007).

[47] Naim H. Afgan, Maria G. Carvalho:" Sustainability Assessment of Hydrogen Energy Systems", International Journal of Hydrogen Energy, Vol. 29, No. 13, , pp. 1327-1342, (2004).

[48] Muhsin Tunay Gencoglu, and Zehra Ural:"Design of a PEM Fuel Cell System for Residential Application", International Journal of Hydrogen Energy, Vol. 34, No. 12, pp. 5242-5248, (2009)

[49] Georg Erdmann:" Future Economics of the Fuel Cell Housing Market", International Journal of Hydrogen Energy, Vol. 28, No. 7, pp. 685-694, (2003)

[50] S. Obara:"Effective-use Method of Exhaust Heat for Distributed Fuel Cells", International Journal of Hydrogen Energy, Vol. 31, pp. 981-993, (2006).

[51] S. Ibe et al:" Development of Fuel Processor for Residential Fuel Cell Cogeneration System", Proceedings of 21st annual meeting of Japan Society of Energy and Resources. Osaka, pp. 493–6, (2002).

[52] Tak-Hyoung Lim, Rak-Hyun Song, Dong-Ryul Shin, Jung-Il Yang, Heon Jung, I.C. Vinke, and Soo-Seok Yang:" Operating Characteristics of a 5 kW Class Anode-Supported Planar SOFC Stack for a Fuel Cell/Gas Turbine Hybrid System", International Journal of Hydrogen Energy, Vol. 33, No. 3, pp. 1076-1083, (2008).

[53] S. H. Chan, H. K. Ho, and Y. Tian:" Multi-Level Modeling of SOFC–Gas Turbine Hybrid System", International Journal of Hydrogen Energy, Vol. 28, No. 8, pp. 889-900, (2003)

[54] Ali Volkan Akkaya, Bahri Sahin, and Hasan Huseyin Erdem:" An analysis of SOFC/GT CHP System Based on Exegetic Performance Criteria", International Journal of Hydrogen Energy, Vol. 33, No. 10, pp. 2566-2577, (2008).

[55] Sadegh Motahar, and Ali Akbar Alemrajabi:" Energy Based Performance Analysis of a Solid Oxide Fuel Cell and Steam Injected Gas Turbine Hybrid Power System", International Journal of Hydrogen Energy, Vol. 34, No. 5, pp. 2396-2407, (2009).

[56] Y. Haseli, I. Dincer, and G.F. Naterer:"Thermodynamic Modeling of a Gas Turbine Cycle Combined with a Solid Oxide Fuel Cell", International Journal of Hydrogen Energy, Vol. 33, No. 20, pp. 5811-5822, (2008).

[57] W. Winkler, and H. Lorenz:" The design of Stationary and Mobile solid oxide Fuel cell — Gas Turbine Systems", Journal of Power Sources, Vol. 105, pp.

222–229, (2002).

[58] Abeer Galal El-Sayed and Shin'ya OBARA: “Power Generation Efficiency of Photovoltaics and a SOFC-PEFC Combined Micro-grid with Time Shift Utilization of the SOFC Exhaust Heat”, Journal of Power and Energy Systems, JSME,Vol. 4, No. 2, pp. 274-289 , (2010).

[59] S. Hayhkin, Neural Networks, A comprehensive foundation, Ed. Macmillan, New York, (1994).

[60] H. Adeli and S. L. Hung:“An adaptive Conjugate Gradient Learning Algorithm for Effective Training of Multilayer Neural Networks” Applied Mathematics and Computation, Vol. 62, No 1, pp. 81-102, (1994).

[61] H. Adeli, and X. Jiang: ”Neuro-Fuzzy Logic Model for Freeway Work Zone Capacity Estimation”, Journal of Transportation Engineering, Vol. 129, No. 5, pp. 484-493, (2003).

[62] H. Adeli, and X. Jiang:” Dynamic Fuzzy Wavelet Neural Network Model for Structural System Identification”, Journal of Structural Engineering, Vol. 132, No. 1, pp. 102-111, (2006).

[63] A. M. Schaefer and H. G. Zimmermann:” Recurrent Neural Networks are Universal Approximators”, International Journal of Neural Systems, Vol. 17, No. 4, pp. 253-263, (2007).

[64] D. E. Rumelhart, G. E. Hinton, and R. J Williams:” Learning Internal Resentations by Error Propagation”, In D. E. Rumelhart, & J. L. Mc Clelland (Eds.), Parallel Distributed Processing, Vol. 1, pp. 318-362, (1986).

[65] J.F. Kreider, and X.A . Wang: ”Improved Artificial Neural Networks for

Commercial Building Energy Use Prediction", Solar Engineering, Vol. 1, pp. 361-366, (1992).

[66] J. Yang, H. Rivard, and R.Zmeureanu:" On-line Building Energy Prediction Using Adaptive Artificial Neural Network", Energy and Buildings, Vol. 37, No. 12, pp. 1250-1259, (2005).

[67] B.P. Feuston and J.H. Thurtell:" Generalized Nonlinear Regression with Ensemble of Neural Nets, the great Energy Predictor Shootout", ASHRAE Transactions, Vol. (100), No. 2, pp. 1075-1080, (1994).

[68] E. Entchev and L.Yang:"Application of Adaptive Neuro-Fuzzy Inference System Techniques and Artificial Neural Networks to Predict Solid Oxide Fuel Cell Performance in Residential Micro generation Installation", Journal of Power Sources, Vol. 170, No. 1, pp. 122-129, (2007).

[69] R.R.A. Issa, I. Flood and M. Asmus:" Development of a Neural Network to Predict Energy Consumption", Proceedings of the Sixth International Conference on the Application of Artificial Intelligence to Civil & Structural Engineering Computing, pp. 65-66, (2001).

[70] S.A Kalogirou:"Application of Artificial Neural Networks for Energy Systems", Applied Energy, Vol. 67, No. (1-2), pp. 17-35, (2000).

[71] A.S Alfuhaid, M.A. El-Sayed, and M.S Mahmoud:"Cascaded Artificial Neural Network for Short Term Load Forecasting", IEEE Transactions on Power Systems, Vol. 12, No. 8, pp. 649-661, (1999).

[72] M. Aydinalp Koksal, and V.I Ugursal:"Comparison of Neural Network, Conditional Demand analysis and Engineering Approaches for Modeling End-

use Energy Consumption in the Residential Sector", Applied Energy, Vol. 85, No. 4, pp. 271-296, (2008).

[73] Z. Alibhai, R. Lum, A. Huster, W.A, and D.B. Kotak:"Coordination of Distributed Energy Resources, Systems, Man, and Cybernetics", IEEE International Conference , H.G. Stassen, ed., Hague, Netherlands, Vol. 2, pp. 1990-1995, (2004).

[74] A. Carlos, and A. Hernandz:"Fuel Consumption of a Microgrid", IEEE Transaction Ind. Appl., Vol. 41, No. 3, pp. 673-681, (2005).

[75] S. Abu-Sharkh, R.J Arnold, T. Markavart, Ross, K. Streemers, P. Wilson, and R. Yao:"Can Microgrids Make a Major Contribution to UK Energy Supply?", Renewable Energy, Vol. 10, No. 2, pp. 78-127, (2006).

[76] Shin'ya Obara:" Operating Schedule of a Combined Energy Network System with Fuel Cell", International Journal of Energy Research, Vol. 30, No. 13, pp. 1055-1073, (2006).

[77] H. Robert:"Microgrid: A Conceptual Solution", Proceedings of the 35th Annual IEEE power Electronics Specifications Conference, Aachen, Vol. 6, pp. 4285-4290, (2004).

[78] M. Tranrioven:" Reliability and Cost – Benefits of Adding Alternate Power Sources to an Independent Micro-grid Community", Journal of Power Sources, Vol. 150, pp. 136-149, (2005).

[79] T. Gouda, et al., Microgrid, p. 74, Denki Shimbun, (2004).(in Japanese)

[80] Shin'ya OBARA and Abeer Galal El-Sayed: "Power Generation Efficiency of Photovoltaics and a SOFC-PEFC Combined Micro-grid with Time Shift

Utilization of the SOFC Exhaust Heat“, Proceedings of the Going Green Care Innovation Conference, No. 069, pp. 1-11, Vienna, Austria, (2010).

[81] SANYO Nickel-Metal Hydride Production Information, http://www.sanyo.co.jp.

[82] Shin'ya Obara:“Improvement of Power Generation Efficiency of an Independent Micro Grid Composed of Distributed Engine Generators”, ASME Transl. Journal of Energy Resources Technology, Vol. 129, Issue 3, pp. 190-199, (September 2007).

[83] Shin'ya Obara: ”Energy Cost of an Independent Micro-grid with Control of Power Output Sharing of a Distributed Engine Generator”, Journal of Thermal Science and Technology, Vol. 2, No. 1, pp. 42-53, (2007).

[84] Solar Energy Utilization Handbook, Japan Solar Energy Society, Ohmsha, Ltd, pp. 10-88, (1985).

[85] NEDO Technical information database, Standard meteorology and Solar radiation data (METPV-3), http://www..nedo.co.jp.

[86] Online data service, GPV/GSM (Grid Point Value / GSM (Global Spectral Model)), http://www.jmbsc.or.jp/hp/online/f-online0a.html, Japan meteorological business support center, (2009).

[87] Data of Japan Meteorological Agency, http://database.rish.kyoto-u.ac.jp/arch/jmadata/gpv-original.html, Kyoto University, (2009).

[88] Abeer Galal El-Sayed and Shin'ya OBARA: “ Operation Plan of the Micro grid Linked to a Photovoltaic with the Power Prediction Method by a Neural Network Using the Numerical Information”, Proceedings of the 7th International Symposium on Environmentally Conscious Design & Inverse Manufacturing

(Eco Design), pp. 1021 – 1026, Sapporo, Japan. (2009)

[89] Shin'ya OBARA and Abeer Galal El-Sayed:"Energy Supply Characteristic of the Solar Cell and Diesel Engine Combined System with a Prediction Algorithm of Solar Power Generation", Proceedings of the 13th International Middle East Power System Conference, (MEPCON'09), Renewable Energy (II), pp. 1-6, Assiut, Egypt, (2009).

[90] R.M. Kil and Y. Song: "Random Search Based on Genetic Operators, "Lecture Notes in Artificial Intelligence", Spring-Verlag , Vol. 1285, pp. 196-205, (1997).

[91] Haykin, S., Neural Networks: A Comprehensive Foundation (Prentice Hall International Edition), Prentice-Hall, Uper Saddle River, NJ, (1998).

[92] Fumihiko Yoshiba, Yoshiyuki Izaki, Takao Watanabe, Wide range load controllable MCFC cycle with pressure swing operation, Journal of Power Sources, Vol. 137, pp. 196–205, (2004).

[93] Shin'ya Obara: "Power Generation Efficiency of an SOFC-PEFC combined System with time shift Utilization of SOFC exhaust heat", International Journal of Hydrogen Energy, Vol. 35, No. 2, pp. 757-767, (2010).

[94] T. Nakamura and M. Sei., Energy Related Technology. High-Efficiency Fuel Processor for Fuel Cell System, Technical Report, Matsushita Electric Works, Ltd, Vol. 77, pp. 4-9, (2002).

[95] K. Oda, A Small-scale Reformer for Fuel Cell Application, Sanyo technical review, Vol. 31, No.2, pp. 99-106, (1999).

[96] Development of a several 10kW class circular-flat-type low-temperature operation SOFC system, Result report symposium 2007, New Energy and

Industrial Technology Development Organization in Japan, http://www.nedo.go.jp/informations/events/200623/26_7.pdf, (in Japanese).

[97] Takeda, Y. et al., Development of Fuel Processor for Rapid Start-up, Proc. 20th Energy System Economic and Environment Conference, Tokyo, pp. 343-344, (2004).

[98] Mikkola, M., Experimental Studies on Polymer Electrolyte Membrane Fuel Cell Stacks, Master's thesis submitted in partial fulfillment of the requirements for the degree of Master of Science in Technology, Helsinki University of Technology, pp. 58-79, (2001).

[99] Feitelbergy Alan S, Rohr Jr Donald F:" Operating line Analysis of Fuel Processors for PEM fuel cell Systems", International Journal of Hydrogen Energy, Vol. 30, No. 11, pp. 1251-1257, (2005).

[100] Narita k. Research on unused energy of cold region cities and utilization for district heat and cooling. Ph.D thesis, Dep. Sociology-Environmental Engineering Faculty of Engineering, Hokkaido University Sapporo, Japan, (1996).

Research List

Publishing of scientific papers in the Journals

1. **Abeer Galal El-Sayed** and Shin'ya OBARA: "Energy Supply Characteristic of the Solar Cell and Diesel Engine Combined System with a Prediction Algorithm of Solar Power Generation", Journal of Power and Energy Systems, JSME, Vol. 4, No. 1, pp. 27-38, (2010).

2. **Abeer Galal El-Sayed** and Shin'ya OBARA: "Power Generation Efficiency of Photovoltaics and a SOFC-PEFC Combined Micro-grid with Time Shift Utilization of the SOFC Exhaust Heat", Journal of Power and Energy Systems, JSME,Vol. 4, No. 2, pp. 274-289 , (2010).

3. Shin'ya OBARA and **Abeer Galal El-Sayed**: " Compound Micro grid Installation Operation Planning of a PEFC and Photovoltaics with Prediction of Electricity Production Using GA and Numerical Weather Information", International Journal of Hydrogen Energy, Vol. 34, Issue 19, pp. 8213-8222, (2009).

4. Shin'ya OBARA and **Abeer Galal El-Sayed**:" Study on a Bioethanol Solar Reforming System with the Solar Insulation Fluctuation in Consideration of Heat Chemical Reaction", Journal of Power and Energy Systems, JSME, Vol. 3, No. 2, pp. 321-332, (2009).

5. Shin'ya OBARA and **Abeer Galal El-Sayed**: "Analysis of the Overall Efficiency

of a PEFC with a Bioethanol-Solar-Reforming System for Individual Houses", Simulation modeling Practice and Theory, (SEEP09 Special Issue), (2010).

Conferences

1. **Abeer Galal El-Sayed** and Shin'ya OBARA: " Operation Plan of the Micro grid Linked to a Photovoltaic with the Power Prediction Method by a Neural Network Using the Numerical Information", Proceedings of the 7th International Symposium on Environmentally Conscious Design & Inverse Manufacturing (Eco Design), pp. 1021 – 1026, Sapporo, Japan, December (2009).

2. **Abeer Galal El-Sayed** and Shin'ya OBARA: "Power Generation Efficiency of Photovoltaics and a SOFC-PEFC Combined Micro-grid with Time Shift Utilization of the SOFC Exhaust Heat", International Power Electronics Conference (IPEC), pp. 2629 -2636, Sapporo, Japan, June (2010).

3. Shin'ya OBARA and **Abeer Galal El-Sayed**: "Analysis of the Overall Efficiency of a PEFC with a Bioethanol-Solar-Reforming System for Individual Houses", Proceedings of the 3rd International Conference on Sustainable Energy and Environmental Protection (SEEP09), Part 2, pp. 325-330, Dublin, Ireland, (2009).

4. Shin'ya OBARA and **Abeer Galal El-Sayed**:"Energy Supply Characteristic of the Solar Cell and Diesel Engine Combined System with a Prediction Algorithm of Solar Power Generation", Proceedings of the 13th International Middle East Power System Conference, (MEPCON'09), Renewable Energy (II), pp. 1-6, Assiut, Egypt,

(2009).

5. Shin'ya OBARA and **Abeer Galal El-Sayed**: "Developments of Residential-Energy Supply System Using a Plant Shoot Solar Cell and Water Electrolyzer", Proceedings of the Sustainable Energy and Environmental Protection (SEEP 2010), PC057, pp.1-11, Bari, Italy, (2010).

6. Shin'ya OBARA and **Abeer Galal El-Sayed**: "Study on a Bioethanol Solar Reforming System with the Solar Insolation Fluctuation in Consideration of Heat Chemical Reaction", Proceedings of the 5th Dubrovnik Conference on Sustainable Development of Energy, Water and Environment Systems (SDEWES09), pp. 1-10, Dubrovnik, Croatia, (2009).

7. Shin'ya OBARA and **Abeer Galal El-Sayed**: "Power Generation Efficiency of Photovoltaics and a SOFC-PEFC Combined Micro-grid with Time Shift Utilization of the SOFC Exhaust Heat", Proceedings of the Going Green Care Innovation Conference, No. 069, pp. 1-11, Vienna, Austria, (2010).

8. **Abeer Galal El-Sayed** and Shin'ya OBARA: "Energy Supply Characteristic of the Solar Cell and Diesel Engine Combined System with a Neural Network Prediction Algorithm of Solar Power Generation", IEE Japan, Published in The Hokkaido Chapters of the Institutes of Electrical and Information Engineers, Conference CD, No. 71, pp. 1-2, Kitami, Japan, October (2009).

9. **Abeer Galal El-Sayed** and Shin'ya OBARA: "Voltage Control of Photovoltaic Generator in Distribution Network", IEE Japan, Published in The Hokkaido Chapters of

the Institutes of Electrical and Information Engineers, Conference CD, No. 67, pp. 1-2, Kitami, Japan, October (2009).

Appendix

1- C++ program of the NN in the training process:

```
//---------------------------------------------------------------------------
 #include <vcl.h>
 #pragma hdrstop
#include <stdio.h>
 #include <fstream.h>
#include <math.h>
#include "Unit1.h"
 using namespace std;
//---------------------------------------------------------------------------
 #pragma package(smart_init)
#pragma resource "*.dfm"
 TForm1 *Form1;
 //.....................
 fstream stream_r2;fstream stream_r3;
 fstream stream_w0;fstream stream_w1;fstream stream_r4;
 fstream stream_r5;ifstream stream_r1;
```

```
 fstream stream_w2;fstream stream_w3;
 float Data[97];
float Teach[96];
 float R_learn=0.1;
 float R_stabi=0.1;
 float w01[97][97];
 float w12[96][97];
float dw_o[96][97];
float dw_m[97][97];
 float y[97];
  float y1[97];
 float y_teach[96];
 float x01[97][97];
 float x12[97][97];
float y_out[97];
 //---------------------------------------------------------------------------
 __fastcall TForm1::TForm1(TComponent* Owner)
        : TForm(Owner)
 {
 }
```

```
//---------------------------------------------------------------------------
void __fastcall TForm1::FormCreate(TObject *Sender)
{
   int tim;
  srand( (unsigned)time( NULL ) );
   for(int k=0;k<=95;k++)for(int j=0;j<=96;j++)dw_o[k][j]=0.0;
    for(int j=0;j<=96;j++)for(int i=0;i<=96;i++)dw_m[j][i]=0.0;
    stream_r1.open("data.txt");
   stream_r5.open("teach.txt");
    stream_w0.open("result0.txt" );
 stream_w1.open("result1.txt");
  stream_w2.open("weight01.txt");
  stream_w3.open("weight12.txt");
    for(int i=0;i<=96;i++){
            stream_r1 >> i  >> Data[i];
  }
 for(int i=0;i<=96;i++)y[i]=Data[i];
   for(int t=0;t<=95;t++){
            stream_r5 >> t >> Teach[t];
  }
```

```
for(int t=0;t<=95;t++)y_teach[t]=Teach[t];
  for(int i=0;i<=96;i++){
          for(int j=0;j<=96;j++){
               w01[j][i]=-0.1+(0.1*(((rand()%100)/100.0+(rand()%100)/10000.0
                                    +(rand()%100)/1000000.0)));
              if(j==0)w01[j][i]=0.0;
           }
}


          for(int j=0;j<=96;j++){
            for(int k=0;k<=95;k++){
              w12[k][j]=-0.5+(1.0*(((rand()%100)/100.0+(rand()%100)/10000.0
                                    +(rand()%100)/1000000.0)));
           }
}
  for(int j=0;j<=96;j++){
          for(int i=0;i<=96;i++){
              stream_w0 << j <<'\t' << i <<'\t'<< w01[j][i]<<endl;
           }
}
```

```
 for(int k=0;k<=95;k++){
          for(int j=0;j<=96;j++){
              stream_w0 << "k" << k<< '\t' <<"j" << j <<'\t' << "w12[k][j]" <<
w12[k][j] <<endl;
           }
 }
          for(int l=0;l<=10000;l++){
            for(int j=0;j<=96;j++){
              for(int i=0;i<=96;i++){
                  x01[j][i]=w01[j][i]*y[i];
               }
           }
           float add_y1;
          for(int j=0;j<=96;j++){
               add_y1=0.0;
              for(int i=0;i<=96;i++){
                   add_y1=add_y1+x01[j][i];
               }
              y1[j]=add_y1;
           }
```

```
 for(int j=0;j<=96;j++)y1[j]=1.0/(1.0+exp(-y1[j]));
y1[0]=1.0;
   for(int j=0;j<=95;j++){
     for(int i=0;i<=96;i++){
          x12[j][i]=w12[j][i]*y1[i];
      }
}

 float add_y2;
 for(int k=0;k<=95;k++){
      add_y2=0.0;
    for(int j=0;j<=96;j++){
         add_y2=add_y2+x12[k][j];
      }
     y_out[k]=add_y2;
}

  for(int k=0;k<=95;k++){
    y_out[k]=1.0/(1.0+exp(-y_out[k]));
      stream_w1 << k << y_out[k];
```

```
            }
            float err=0.0;
            for(int k=0;k<=95;k++){
                 err=err+(y_teach[k]-y_out[k])*(y_teach[k]-y_out[k]);
                stream_w0 << "k" << "y_teach[k]" << "y_out[k]"<< k << '\t'<<
y_teach[k] <<'\t'<< y_out[k]<< endl;
            }
           err=1/2.0*err;
            stream_w0 << "l" << l << '\t' <<"err" << err << endl;
            for(int k=0;k<=95;k++){
               for(int j=0;j<=96;j++){
                    dw_o[k][j]=R_learn*(y_teach[k]-y_out[k])*y_out[k]*(1.0-
 y_out[k])*y1[j]+R_stabi*dw_o[k][j];
               }
            }

            for(int k=0;k<=95;k++){
               for(int j=0;j<=96;j++){
                    w12[k][j]=w12[k][j]+dw_o[k][j];
               }
```

```
            }


             float add_k;
            for(int j=0;j<=96;j++){
                add_k=0.0;
                 for(int k=0;k<=95;k++)add_k=(y_teach[k]-y_out[k])*y_out[k]*(1.0-
 y_out[k])*w12[k][j];
                 for(int i=0;i<=96;i++){
                     dw_m[j][i]=R_learn*y1[j]*(1.0-
y1[j])*y[i]*add_k+R_stabi*dw_m[j][i];
                  }
            }


            for(int j=0;j<=96;j++){
                 for(int i=0;i<=96;i++){
                     w01[j][i]=w01[j][i]+dw_m[j][i];
                      w01[0][i]=0.0;
                  }
            }
 }
```

```
   for(int j=0;j<=96;j++){
            for(int i=0;i<=96;i++){
                 stream_w2 << j <<'\t'<< i <<'\t'<< w01[j][i]<<endl;
             }
  }
   for(int k=0;k<=95;k++){
            for(int j=0;j<=96;j++){
                 stream_w3 <<k <<'\t'<< j <<'\t'<< w12[k][j]<<endl;
             }
  }

 stream_r1.close();stream_r2.close();stream_r3.close();stream_r4.close();
  stream_w0.close();stream_w1.close();
 }
 //---------------------------------------------------------------------------
```

2- C++ program of the NN in the analysis process:

```
 //---------------------------------------------------------------------------
  #include <vcl.h>
  #pragma hdrstop
```

```
#include <stdio.h>
 #include <fstream.h>
#include <math.h>
#include "Unit1.h"
 using namespace std;
//---------------------------------------------------------------------------
 #pragma package(smart_init)
#pragma resource "*.dfm"
 TForm1 *Form1;
 fstream stream_r2;fstream stream_r3;
fstream stream_w0;fstream stream_w1;
fstream stream_r1;
float Data[97];
float Teach[96];
 float R_learn=0.1;
 float R_stabi=0.1;
 float w01[97][97];
 float w12[96][97];
float dw_o[96][97];
float dw_m[97][97];
```

```
float y[97];
  float y1[97];
 float y_teach[96];
 float x01[97][97];
 float x12[97][97];
float y_out[97];
 //---------------------------------------------------------------------------
 __fastcall TForm1::TForm1(TComponent* Owner)
    : TForm(Owner)
 {
 }
 void __fastcall TForm1::FormCreate(TObject *Sender)
 {
    int tim;
   srand( (unsigned)time( NULL ) );
    for(int k=0;k<=95;k++)for(int j=0;j<=96;j++)dw_o[k][j]=0.0;
     for(int j=0;j<=96;j++)for(int i=0;i<=96;i++)dw_m[j][i]=0.0;
     stream_r1.open("data.txt");
     stream_w0.open("result0.txt" );
  stream_w1.open("result1.txt");
```

```
 stream_r2.open("weight01.txt");
 stream_r3.open("weight12.txt");
  for(int i=0;i<=96;i++){
          stream_r1 >> i >> Data[i];
}
for(int i=0;i<=96;i++)y[i]=Data[i];
  for(int j=0;j<=96;j++){
   for(int i=0;i<=96;i++){
               stream_r2 >> j >> i >> w01[j][i];
    }
}
 for(int k=0;k<=95;k++){
   for(int j=0;j<=96;j++){
               stream_r3 >> k >> j >> w12[k][j];
    }
}
   for(int j=0;j<=96;j++){
    for(int i=0;i<=96;i++){
       x01[j][i]=w01[j][i]*y[i];
     }
```

```
  }
   float add_y1;
 for(int j=0;j<=96;j++){
    add_y1=0.0;
   for(int i=0;i<=96;i++){
        add_y1=add_y1+x01[j][i];
    }
   y1[j]=add_y1;
         }
for(int j=0;j<=96;j++)y1[j]=1.0/(1.0+exp(-y1[j]));
 y1[0]=1.0;
 for(int j=0;j<=95;j++){
   for(int i=0;i<=96;i++){
        x12[j][i]=w12[j][i]*y1[i];
    }
   }
   float add_y2;
for(int k=0;k<=95;k++){
    add_y2=0.0;
   for(int j=0;j<=96;j++){
```

```
            add_y2=add_y2+x12[k][j];
          }
         y_out[k]=add_y2;
        }
     for(int k=0;k<=95;k++){
                  y_out[k]=1.0/(1.0+exp(-y_out[k]));
                  stream_w0 << k << '\t' << y_out[k]<< endl;
        }
   stream_r1.close();stream_r2.close();stream_r3.close();
   stream_w0.close();stream_w1.close();
}
//---------------------------------------------------------------------------
```